Chapter 4

Synthesis of Novel Quinoline-Isoxazole Hybrid Molecules Containing Amine Side Chain, *In Vitro* Anti-Microbial Evaluation and Their *In Silico* Studies

4.1 Introduction

Isoxazole is an electron-dense azole featuring an oxygen atom next to the nitrogen. It is moreover the category of compounds that encompass this ring. Isoxazolyl is the monovalent functional group originating from isoxazole. Isoxazole rings are present in certain natural compounds, including ibotenic acid (**I**) and muscimol (**II**) (**Figure 1**).[110] The structural characteristics of isoxazole facilitate many non-covalent interactions, including hydrogen bonding (with nitrogen and oxygen as hydrogen bond acceptors), π- π stacking (due to the unsaturated five-membered ring), and hydrophilic interactions (exhibiting an overall hydrophilic profile with a CLogP of 0.121).[111] A common characteristic of organic compounds created in recent decades is that most of them may have a heterocyclic ring.[112] The incorporation of isoxazole may enhance efficacy, reduce toxicity, and optimize pharmacokinetic characteristics.[113,114]

Ibotenic acid (I) **Muscimol (II)**

Figure 1: Natural compounds containing isoxazole ring.

Isoxazoles can be produced using many methods utilizing both homogeneous and heterogeneous catalysts.[115] Nonetheless, the most extensively studied and documented synthesis of isoxazole derivatives occurs via the (3+2) cycloaddition reaction, wherein an alkyne functions as the dienophile and nitrile oxide serves as the diene.[115] Two proposed methods for the 1,3-dipolar cycloaddition reaction have been documented: first, a pericyclic cycloaddition reaction via a concerted mechanism,[116] and second, a stepwise mechanism involving the creation of a diradical intermediate.[117] Consequently, the first proposed concept

has been approved, namely, a coordinated pathway, through the interaction of the diene and the dienophile (**Figure 2**).[116]

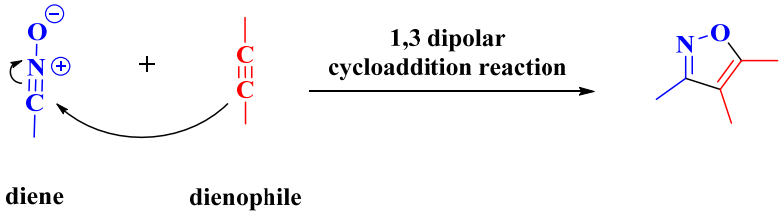

Figure 2: Mechanism of the 1,3-dipolar cycloaddition process.

On the other hand, it is widely known that isoxazole is linked to a variety of biological activities as a result of the variety of non-bonding interactions it can engage in.[118] Numerous natural products[119] and functional materials contain the biologically active isoxazole.[120] In biological systems, the isoxazole entities could easily connect with several enzymes and receptors, as evidenced by the wide range of biological functions they possess[121] including anti-bacterial,[122] anti-fungal,[123] anti-viral,[124] anti-tubercular,[125] anti-cancer,[126] and anti-inflammatory[127] activities. In addition, quinoline and its derivatives are part of several medical compounds, which include moxifloxacin (**1,** antibacterial),[128] grepafloxacin (**2,** antibacterial),[129] enoxacin (**3,** antibacterial),[130] mefloquine (**4,** anti-inflammatory),[131] chloroquine (**5,** antimalarial)[132], ciprofloxacin (**6,** antituberculosis),[133] and nedocromil (**7,** anticonvulsant)[134] Isoxazole and its derivatives are also found in several drug molecules like cloxacillin (**8**, antibacterial),[135] NVP-AUY922 (**9**, anticancer),[136] valdecoxib (**10**, anti-inflammatory),[137] sulfamethoxazole (**11**, antibacterial)[138] and leflunamide (**12,** anti-inflammatory).[137] In the previous reports bioactive, and selective quinoline-isoxazole hybrids heterocycles were created[139] and tested for their in vitro cytotoxic activity against various cancer molecular targets, such as tyrosine kinase EGFR inhibition (**13**),[140] breast cancer (**14**, MCF-7),[141] melanoma cancer (**15)**[142] (**Figure 3**). Keeping this in mind and to continue our search for new antimicrobial agents,[143,144] we have designed and developed new quinoline-containing isoxazole derivatives **(6a-o)** and anticipated that these new hybrid derivatives may demonstrate potent activity.

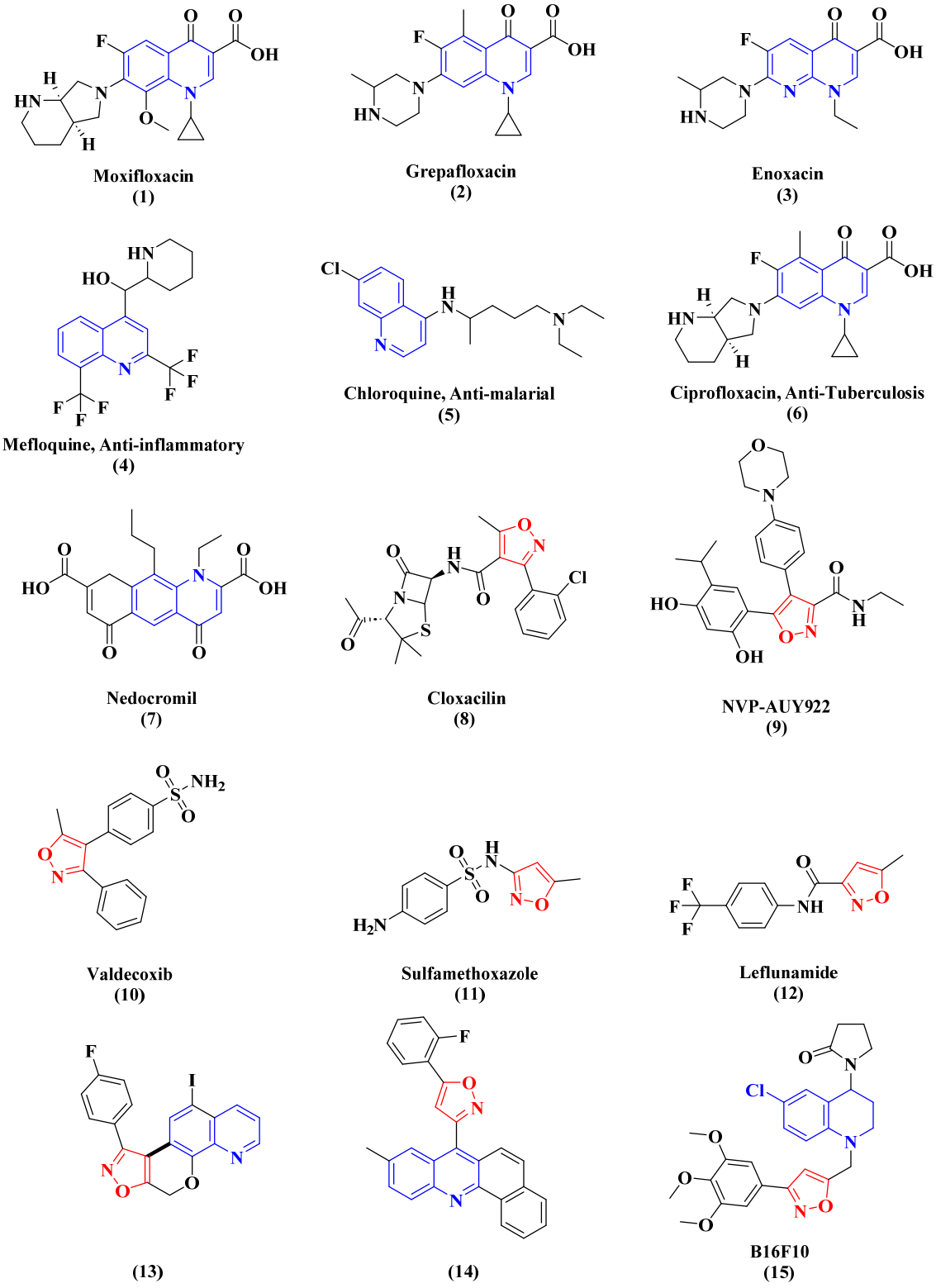

Figure 3. Structures of Marketed drugs and active compounds having quinoline and isoxazole moieties.

4.1.1 Synthetic methodologies for the substituted quinoline-isoxazole hybrids and its biological significance

The subsequent step entailed the production of polymer-bound enamino ketones **2** through the reaction of polymer conjugates **1** with *N*,*N*-dimethylformamide dimethyl acetal (DMF-DMA). To achieve optimal results, dry DMF served as the solvent under microwave irradiation at 120 °C for 1 h, resulting in quantifiable yields. In the last phase, five-membered hetero cyclization was performed by reacting intermediate **2** with hydroxylamine hydrochloride in a solvent mixture (DMF/i-PrOH, 4:1) under microwave irradiation at 90°C for 30 min, followed by cleavage. The five-membered isoxazoles **3** were ultimately acquired with a yield of 50–70% (**Figure 4.1**).[145]

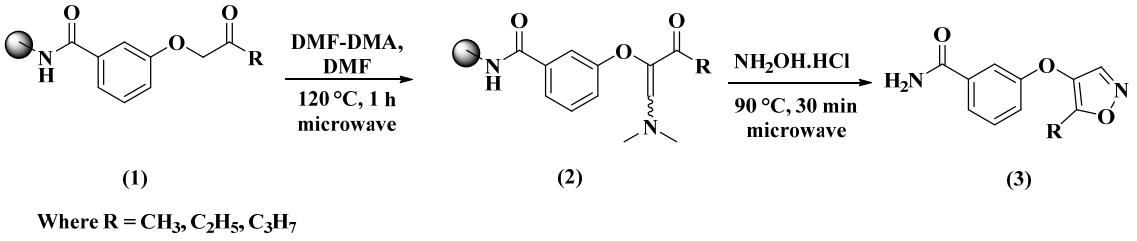

Figure 4.1

Lee et al. initiated the synthesis by formylating 4-ethylresorcinol (**4**) using $POCl_3$ and DMF. Subsequently, 5-ethyl-2-hydroxy-4-methoxybenzaldehyde (**5**) was synthesized through methylation using methyl iodide and potassium carbonate. An intermediate chemical was synthesized by reacting 5-ethyl-2-hydroxy-4-methoxybenzaldehyde with benzyl bromide and potassium carbonate. 4-methoxybenzylmagnesium chloride was added, followed by tetra propylammonium perruthenate (TPAP) oxidation, resulting in the formation of the intermediate ketone (**6**) from the aldehyde. The treatment of dimethylformamide dimethyl acetal (DMF/DMA) in refluxing toluene yielded enamino ketone (**7**) from diaryl-ethanone. Finally, diaryl isoxazole was synthesized through the heterocyclization of the intermediate molecule (**8**) with hydroxylamine in saturated methanolic acetic acid, utilizing sodium carbonate as a base, and $KRIBB_3$ was acquired via debenzylation (**9**) (**Figure 4.2**).[146]

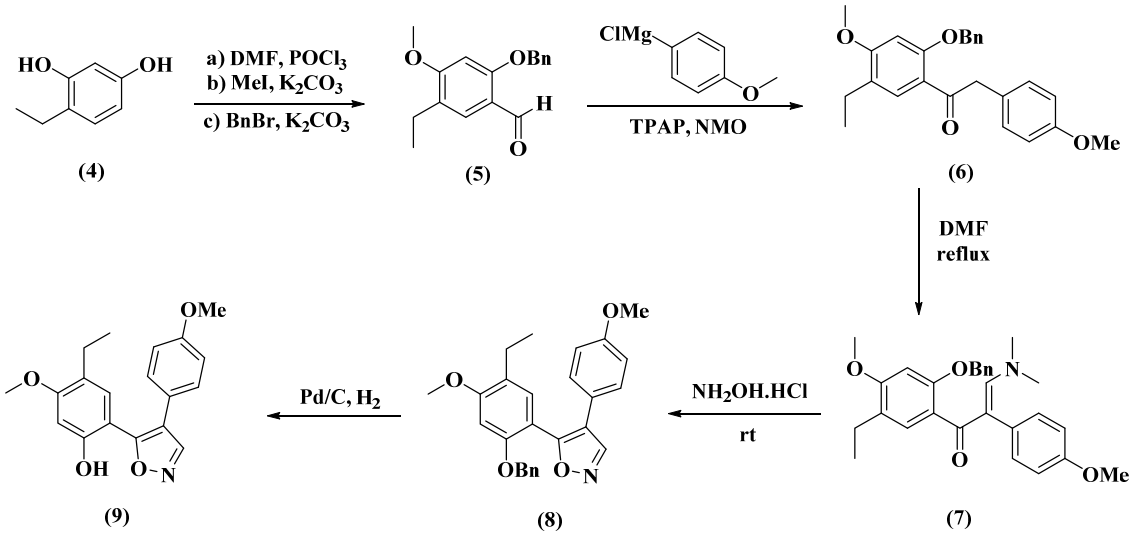

Figure 4.2

Reddy et al. documented the synthesis of regioselective 3,5-disubstituted isoxazoles (**12**) utilizing aldoximes (**10**), propargyl bromide (**11**), and *N*-chlorosuccinimide (NCS) in aqueous conditions by a 1,3-dipolar cycloaddition process. This approach is significant due to its convenient conditions, facilitating user-friendly solvents and straightforward manipulation of the reaction to yield the necessary isoxazoles. Compound **12** was showing promising cytotoxic activity against MCF-7 breast cancer cell line (**Figure 4.3**).[147]

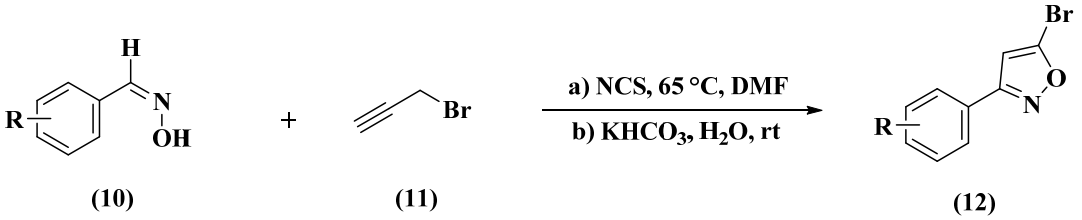

Where R = Cl, Br, NO_2, OMe, OTs, OBz

Figure 4.3

In 2016, Tanyeli et al. has developed an innovative approach for the synthesis of isoxazole derivatives by a one-pot cascade reaction utilizing ultrasonication. To manufacture isoxazole derivatives (**15**), aromatic aldehydes (**13**) and ethyl nitro acetate (**14**) were reacted in water

with 20 mol% 1,4-diazabicyclo[2.2.2]octane (DABCO) as the catalyst at 80 °C for 24 hours under ultrasonication (**Figure 4.4**).[148]

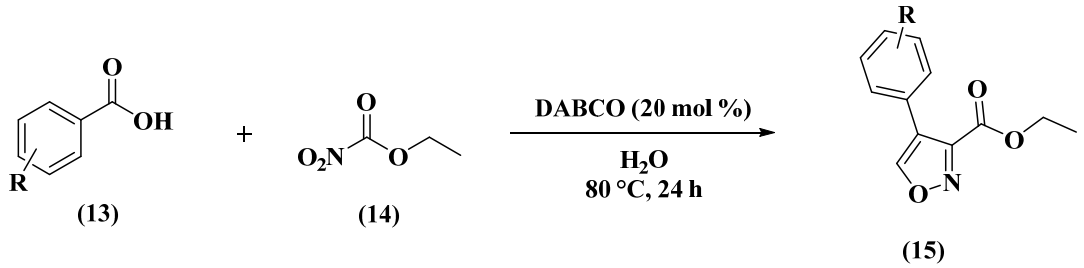

Where, R = H, 4-Cl, 4-Br, 4-NO_2, 4-OCH_3, 3-Cl, 4-Me

Figure 4.4

Cinnoline scaffolds (**16**) were reacted with produced oxime derivatives (**17**) in the presence of aqueous sodium hypochlorite and DIPEA in dichloromethane solvent at ambient temperature for 8–16 h, resulting in the formation of corresponding cinnoline-isoxazole scaffolds (**18**) with excellent yield (**Figure 4.5**), which exhibited remarkable inhibitory effect against gram-positive bacteria such as *Staphylococcus aureus* and *Bacillus subtilis*, and gram-negative bacteria such as *Pseudomonas aeruginosa* and *Escherichia coli* (**Figure 4.4**). [149]

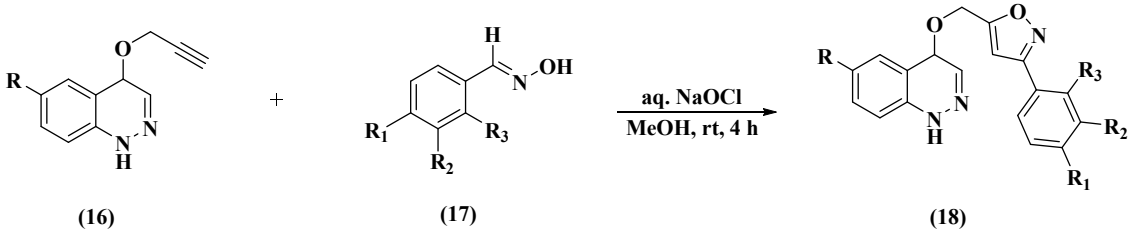

Where, R = $C_8H_5N_2$, 4-Br$C_8H_5N_2$
R_1 = H, Cl, F, OCH_3
R_2 = H, Cl, F, OCH_3
R_3 = H, Cl, F, OCH_3

Figure 4.5

4.2 Results and Discussion

4.2.1 Chemistry

This was done in an effort to develop novel quinoline-isoxazole hybrids containing amide side chain derivatives which showing promissing anti-microbial activity. Fifteen synthesized molecules having quinoline and isoxazole in their primary structure are reported here.

The synthetic route of quinoline containing isoxazole hybrid molecules (**6a-o**) is depicted in Scheme 1. Compound **4** already synthesised and depicted in chapter-1. Further, by using the hetero Diels-Alder approach, a solution of (*Z*)-2-chloro-*N*-hydroxyquinoline-3-carbimidoyl chloride (**4**) and $KHCO_3$ in DMF was treated with propargyl bromide at room temperature to produce intermediate (**5**).[150] At last, compound **5** was treated with $NaHCO_3$ and substituted aniline using THF:H_2O (1:1) as a solvent at 60 °C to yield the novel quinoline containing isoxazole derivatives (**6a-o**).[44] By examining their spectroscopic data, such as ^{1}H-NMR, ^{13}C-NMR, IR and mass spectroscopy, the compounds **6a-o** were characterized. For instance, the ^{1}H spectrum of compound **6a** presented that 4-methoxy (OCH_3) protons were detected at 3.64 δppm as a singlet and aliphatic methyl was detected at 4.52 δppm as a singlet. The aromatic region of quinoline ring protons was detected between 8.80 to 7.74 δppm and the isoxazole proton appeared as a singlet at 6.89 δppm. Substituted aniline doublet peaks were detected between 6.75 to 6.67 δppm. At 5.99 δppm a singlet peak was detected of amine (NH). A position of amine singlet peak was confirmed by D_2O.

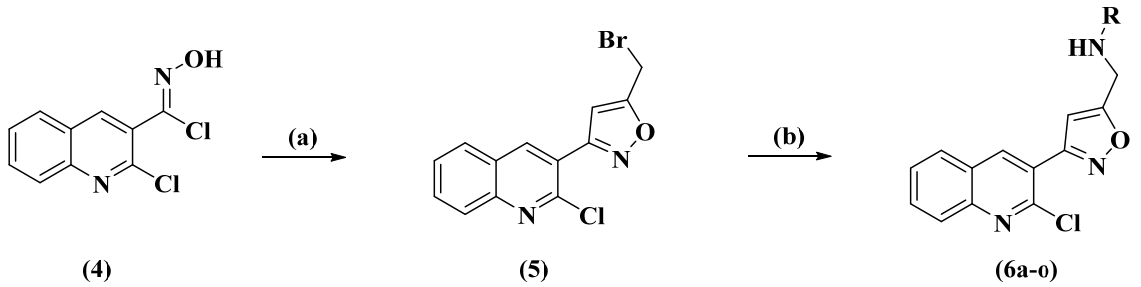

(4) (5) (6a-o)

Reaction condition: a) Propargyl bromide, $KHCO_3$, DMF, rt; b) R-NH_2, $NaHCO_3$, THF:H_2O (1:1), 60°C, 4h.

Scheme 1: Synthesis of the novel quinoline-isoxazole hybrids containing amide side chain derivatives.

Table 1: Physicochemical characteristics of the novel quinoline-isoxazole hybrids containing amide side chain derivatives **6a-o**.

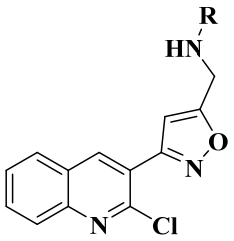

Compound	R	Molecular Weight	Molecular Formula	Yield (%)	Melting Point (°C)
6a	4-OCH_3-C_6H_4-	365.82	$C_{20}H_{16}ClN_3O_2$	94	90-92
6b	C_6H_5-	335.79	$C_{19}H_{14}ClN_3O$	92	102-104
6c	4-Br-C_6H_4-	414.69	$C_{19}H_{13}BrClN_3O$	96	123-125
6d	4-CH_3-C_6H_4-	349.82	$C_{20}H_{16}ClN_3O$	92	82-84
6e	4-Cl-C_6H_4-	370.23	$C_{19}H_{13}Cl_2N_3O$	95	118-120
6f	2-OCH_3-C_6H_4-	365.82	$C_{20}H_{16}ClN_3O_2$	95	89-91
6g	2-$C_{10}H_8$-	385.86	$C_{23}H_{16}ClN_3O$	91	110-112
6h	4-F-C_6H_4-	353.78	$C_{19}H_{13}ClFN_3O$	80	121-123
6i	3-Cl-C_6H_4-	370.23	$C_{19}H_{13}Cl_2N_3O$	92	117-119
6j	1-$C_{10}H_8$-	385.86	$C_{23}H_{16}ClN_3O$	98	110-112
6k	2,4-CH_3-C_6H_3-	363.85	$C_{21}H_{18}ClN_3O$	96	85-87
6l	2,6-CH_3-C_6H_3-	363.85	$C_{21}H_{18}ClN_3O$	97	88-90
6m	2,3-CH_3-C_6H_3-	363.85	$C_{21}H_{18}ClN_3O$	98	96-98
6n	2-CH_3-C_6H_4-	349.82	$C_{20}H_{16}ClN_3O$	96	118-120
6o	2,5-CH_3-C_6H_3-	363.85	$C_{21}H_{18}ClN_3O$	99	98-100

4.3 Biological Activity:

All the newly synthesized hybrid quinoline derivatives containing substituted isoxazole **(6a-o)** were tested for their potential activity against two fungal strains: *Aspergillus niger* (ATCC 16888) and *Candida albicans* (ATCC 10231), two gram positive bacteria: *Bacillus subtilis* (ATCC 6051) and *Staphylococcus aureus* (ATCC 23235) and two gram negative bacteria: *Escherichia coli* (ATCC 25922) and *Salmonella typhi* (ATCC 19430). The inhibition zone (mm) was tested against ampicillin & gentamycin as a positive control for antibacterial activity

and nystatin as a positive control for antifungal activity. The test's outcomes shows that the compounds underwent significant action against every type of bacterial and fungal species tested, with an inhibition zone ranging from 5 to 24 mm. In comparison with the reference drugs ampicillin, gentamycin and nystatin, the synthesized molecules demonstrated moderate to higher inhibition. The tested compounds antimicrobial activity was determined by using a 100 µg/ml concentration in the dimethyl sulfoxide (DMSO) as a solvent. Figure **1** provides a graphical representation of the antibacterial activity data. A graphical representation of the antifungal activity data is shown in Figure **2**.

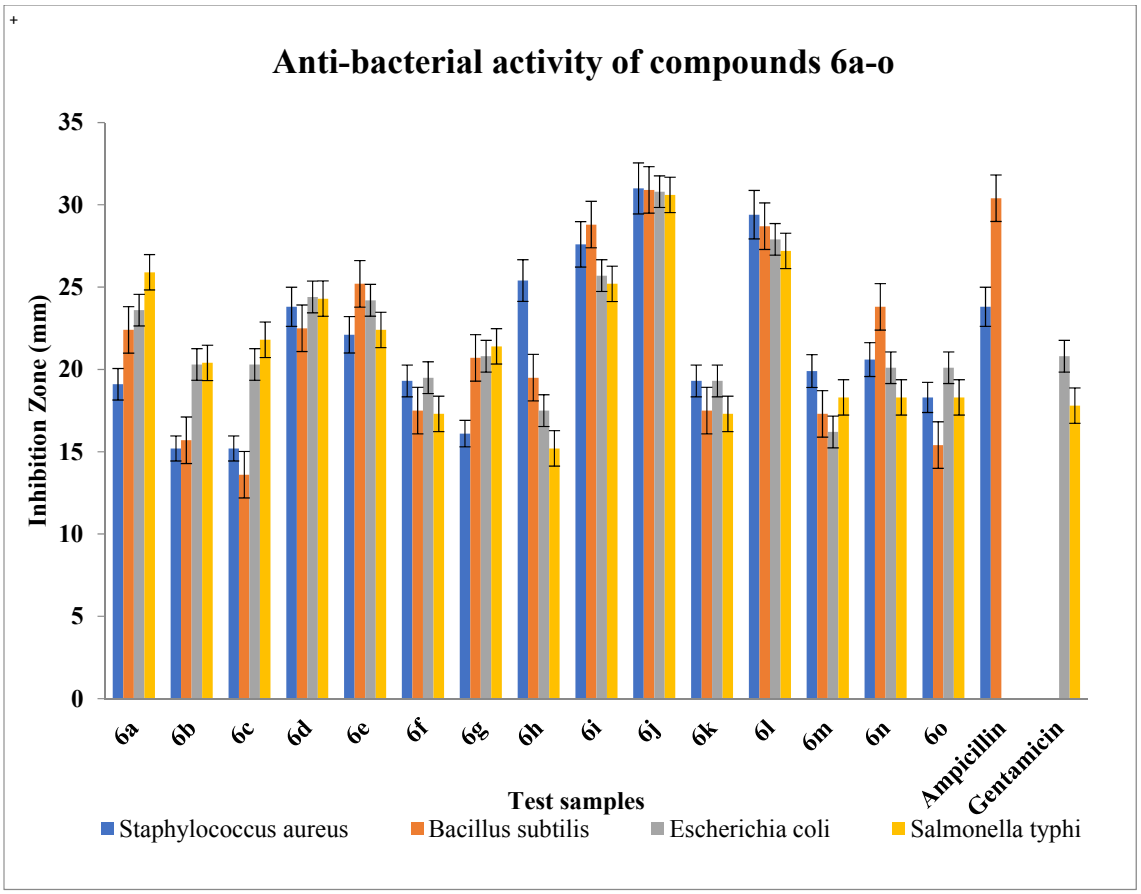

Figure 1: Graphical presentation of anti-bacterial activity for compounds **6a-o**.

The highest anti-bacterial activity is calculated against the highest values shown by the compounds **6j** and **6l** for the bacterial strains of *Bacillus subtilis, Staphylococcus aureus* and *Escherichia coli*, and Salmonella typhi for compound **6j** and **6l**.

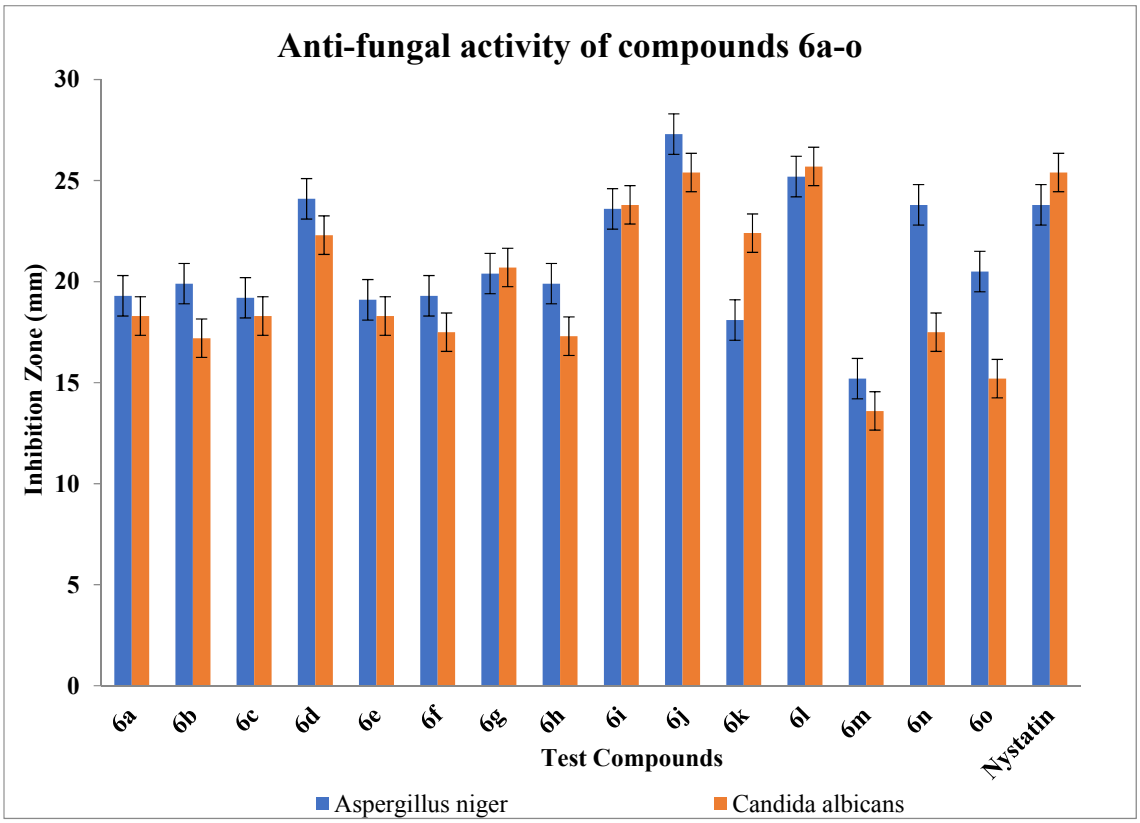

Figure 2: Graphical presentation of anti-fungal activity for compounds **6a-o**.

Compound **6d**, **6j** and **6l** were observed to be having quite inhibition against fungal species *Aspergillus niger* and *Candida albicans* respectively.

4.4 Structure-Activity Relationship (SAR):

The Structure-Activity Relationship (SAR) study revealed interesting insights into the antimicrobial properties of the synthesized compounds. Compound **6a**, with a methoxy group at the para position, showed strong antibacterial activity against gram-negative pathogens like *Escherichia coli* (**23.6 ± 1.2 mm**) and *Salmonella typhi* (**25.9 ± 0.63 mm**), surpassing the standard drug gentamicin, which exhibited zones of inhibition of **20.8 ± 0.68** mm and **17.8 ± 0.33** mm, respectively. In contrast, compounds **6b** and **6c**, featuring a phenyl ring and a halogen (*p*-Br) substitution, showed reduced activity against *Salmonella typhi*, with inhibition zones of **20.4 ± 0.63 mm** and **21.8 ± 0.63 mm.** Adding a methyl group (CH_3) as an electron-donating group at the para position in compound **6d** enhanced antibacterial activity (**23.8 mm ± 0.2 mm**), while a chlorine (*p*-Cl) group as an electron-withdrawing substituent in compound **6e** also displayed good activity (**24.2 mm ± 0.72 mm**) against both gram-negative pathogens. However, compound **6f**, with a methoxy group at the ortho position, had the weakest activity.

The introduction of a β-naphthyl ring in compound **6g** led to moderate antibacterial effects on gram-negative bacteria and boosted antifungal activity (**20.5 mm± 2.05 mm**). Compounds **6h** and **6i**, which contain fluorine and chlorine as electron-withdrawing groups at para and meta positions, showed notable differences. Compound **6h** demonstrated excellent antibacterial activity against gram-positive pathogens like *S. aureus* (**25.4 ± 0.58 mm**) and *B. subtilis* (**19.5 ± 0.58 mm**), while **6i** showed improved activity against both bacteria and fungi. Compound **6j** with an α-naphthyl substitution, was the most effective overall, showing strong inhibition against all pathogens tested. Compound **6k**, with two methyl groups at ortho and para positions, exhibited moderate antifungal activity against *Candida albicans* (**22.4 ± 0.58 mm**). Meanwhile, compound **6l**, which had methyl groups at two ortho positions (2,6), demonstrated outstanding efficacy against all pathogens, with a zone of inhibition (**26 mm± 2.1 mm**) exceeding the standards. Conversely, compound **6m**, with methyl substitutions at ortho and meta positions, had minimal antifungal activity but showed moderate antibacterial effects on *Salmonella typhi* (**18.3 ± 2.1 mm**). Finally, compounds **6n** and **6o**, with methyl substitutions at ortho-ortho and ortho-meta positions, showed moderate activity against *Salmonella typhi* (**18.3 ± 0.58 mm** and **18.3 ± 1.2 mm**) respectively. Comparable to gentamicin (**17.8 ± 0.33 mm**). Overall, the synthesized compounds exhibited a range of moderate to high *in-vitro* antimicrobial activities, with compounds **6j** and **6l** standing out as particularly promising.

4.5 Molecular Docking with *E. coli* DNA gyrase:

In silico studies, especially molecular modeling an important technique for the identification of the putative binding mode of the compounds with the target protein. Hence, a molecular docking study using AutoDock Vina was carried out on the crystal structure of the 24 kDa domain of *E. coli* DNA gyrase as a target for docking studies is driven by its biological significance, its potential as a drug target, the availability of structural data, and the utility of computational methods in drug discovery efforts.[98] After the energy minimization, the generated three-dimensional molecular structures were subjected to docking investigations within the binding pocket of DNA gyrase The docking study results of synthesized hybrids **6a-o** are summarized in Table **2**. As evident, many amino acid residues were found in the interaction of ligands including Arg A:20, Glu B:58, Lys B:162, Asp A:17, and Arg B:204. Further, all prepared molecules exhibited good binding energy with the target varying from -7.0 to -8.3 $kJmol^{-1}$. Especially compound **6j** exhibited the highest docking score of –8.3 $kJmol^{-1}$ having two conventional hydrogen bonds with Asp A:17, and Lys B:162.

Table 2: *In silico* docking results of the newly synthesized quinoline containing isoxazole compounds **6a-o** and gentamicin with the binding site of DNA gyrase.

Compounds	Docking score (kJ mol^{-1})	Interacting residues	Number of H-Bonds
6a	-7.6	Arg A:20, Glu B:58	2
6b	-7.0	Lys B:162	1
6c	-7.6	Glu B:58	1
6d	-7.7	Arg A:20, Glu B:58	2
6e	-7.6	Lys B:162, Glu B:58	2
6f	-7.2	Asp A:17, Lys B:162	2
6g	-7.8	Lys B:162, Glu B:58	2
6h	-7.6	Lys B:162, Glu B:58	2
6i	-7.7	Asp A:17, Lys B:162	2
6j	-8.3	Asp A:17, Lys B:162	2
6k	-7.5	Arg A:20	1
6l	-7.9	Lys B:162	1
6m	-7.8	Arg A:20, Glu B:58	2
6n	-7.4	Arg B:204	1
6o	-7.6	Arg A:20	1
Gentamicin	-6.9	Glu A:174, Arg A:20	2

The docking studies portrayed that for compound **6a** isoxazole's nitrogen atom formed H-bonding with Arg A:20, and its -NH formed H-bindings with Glu B:58. While in the case of compound **6b** H-bonding formed with Lys B:162. In the case of compound **6c**, the halogen atom formed H-bond with Glu B:58. Compound **6d** has the same symmetrical bonding as compound **6a** oxazole's nitrogen atom and its -NH formed two H-bonding with Arg A:20 and Glu B:58. In compound **6e** the nitrogen atom of quinoline and -NH generated two H-bonding respectively with Lys B:162 and Glu B:58. Compound **6f** formed two conventional hydrogen bonds with Asp A:17 and Lys B:162. Both compounds **6g** and **6h** showed two H-bonding with Lys B:162 and Glu B:58, out of which compound **6g** has a good docking score of -7.8 kJ mol^{-1} as mentioned in (**Table 2**). Compound **6i** formed two conventional hydrogen bonds with Asp A:17 and Lys B:162. Compound **6j** also interacted with two strong H-bonding with Asp A:17 and Lys B:162, as displayed in (**Figure 1**), with the highest docking score of -8.3 kJ/mol, shown in (**Table 2**). Compound **6k** made a single hydrogen bond with Arg A:20. Also, compound **6l**

made a single hydrogen bond with Lys B:162, with a good docking score of -7.9 kJ mol^{-1}, as mentioned in (**Table 1**). Compound **6m** has two conventional hydrogen bonds with Arg A:20 and Glu B:58, with a docking score of -7.8 kJ mol^{-1}, as mentioned in (**Table 2**). Further, compounds **6n** and **6o** formed single H-bonding with Arg B:204 and Arg A:20 respectively. At last, a reference molecule gentamicin also interacted with two strong H-bonding with Arg A:20 and Glu A:174, as displayed in (**Figure 2**) with a lowest docking score -6.6 kJ mol^{-1} shown in (**Table 2**).

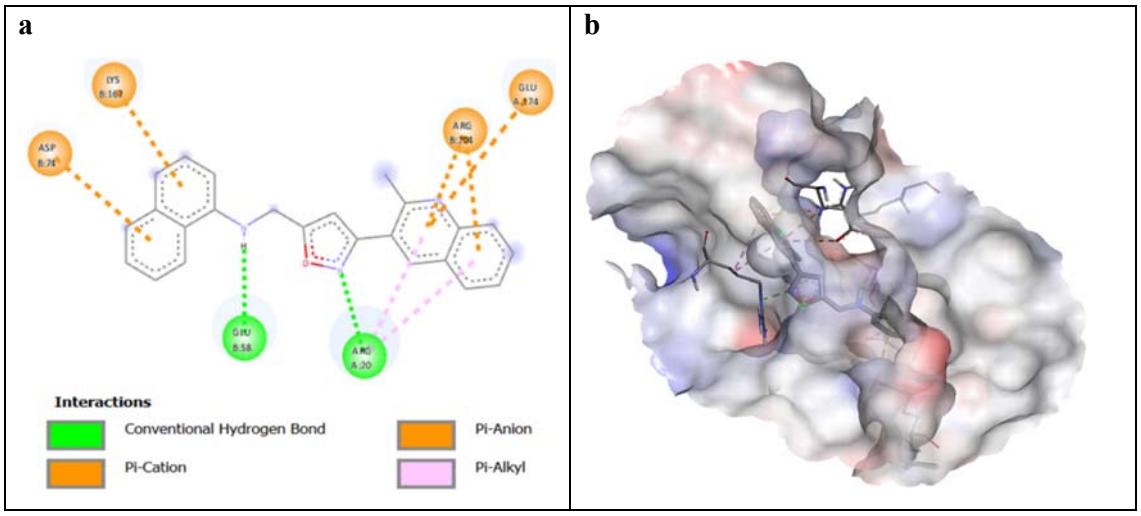

Figure 1. Docking pose of compound **6j** with 24 kDa domain of *E. coli* DNA gyrase. (**a**) Receptor-ligand interaction on a 2-D diagram; (**b**) Receptor-ligand interaction on a 3-D diagram.

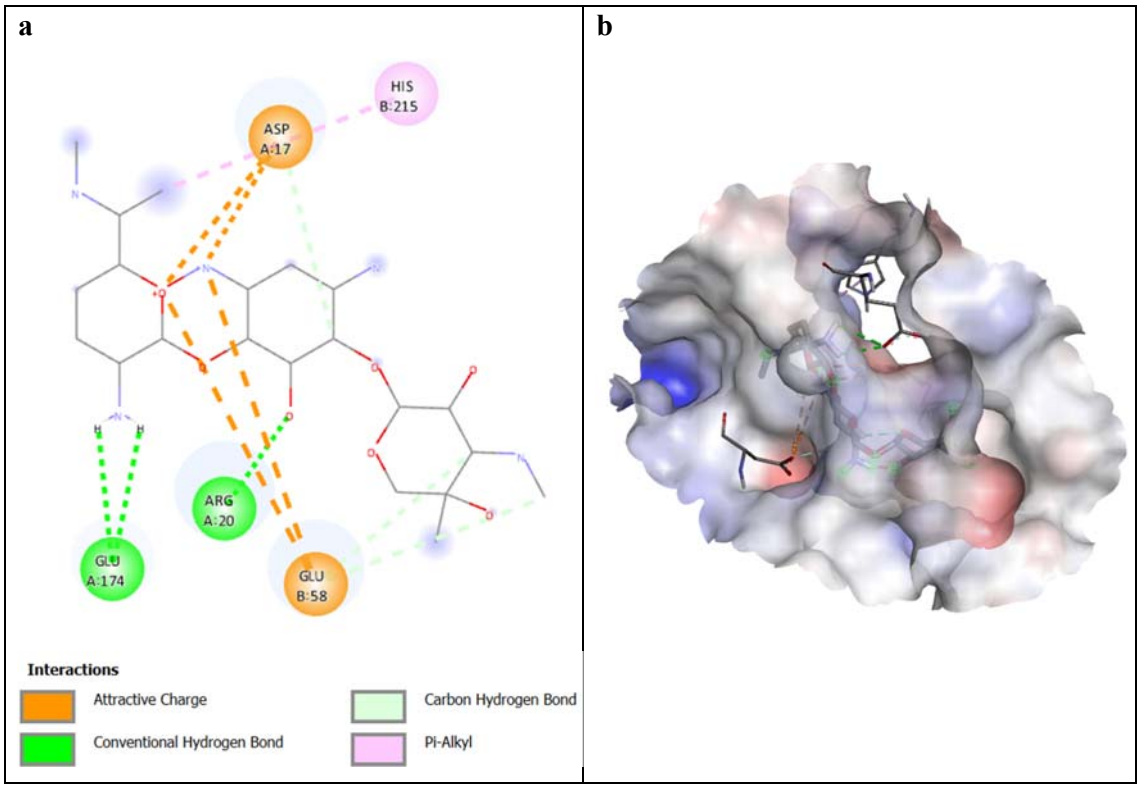

Figure 2. Docking pose of gentamicin with 24 kDa domain of *E. coli* DNA gyrase. (**a**) Receptor-ligand interaction on a 2-D diagram; (**b**) Receptor-ligand interaction on a 3-D diagram.

4.5.1 Molecular Dynamics Simulation analysis

The molecular dynamics technique is used to investigate the stability and conformational changes of the molecules in the simulated protein.[151] In the current work, the 24 kDa domain of *E. coli* DNA gyrase with the most potent compound **6j** was chosen for molecular dynamics modeling. The stability of the complexes was assessed using potential energy throughout a 100-ns simulation time with a 2-ns time interval. This study examined the relationships between Root Mean Square Deviation (RMSD) and Root Mean Square Fluctuations (RMSF).

4.5.2 Root Mean Square Deviation

RMSD is a measure of how far atoms move from one frame to another. The structural conformation of the protein and the stability of the ligand regarding the protein and its binding site can be inferred from the monitoring of their RMSDs, whereas the stability of the ligand

can be revealed from the monitoring of the protein. Changes of 1-3 Å are acceptable for small and globular proteins. Compound **6j** and protein achieved stability with slight fluctuations during the first 12 ns of MD simulation (**Figure 3**). After that, it stayed linked to the protein for the remainder of the simulation session. Furthermore, the difference in RMSD values between compound **6j** and protein average value was 1.3 Å, which demonstrates that the **6j**-protein complex (Crystal structure of the 24 kDa domain of *E. coli* DNA gyrase, PDB ID: 4DUH) is stable.

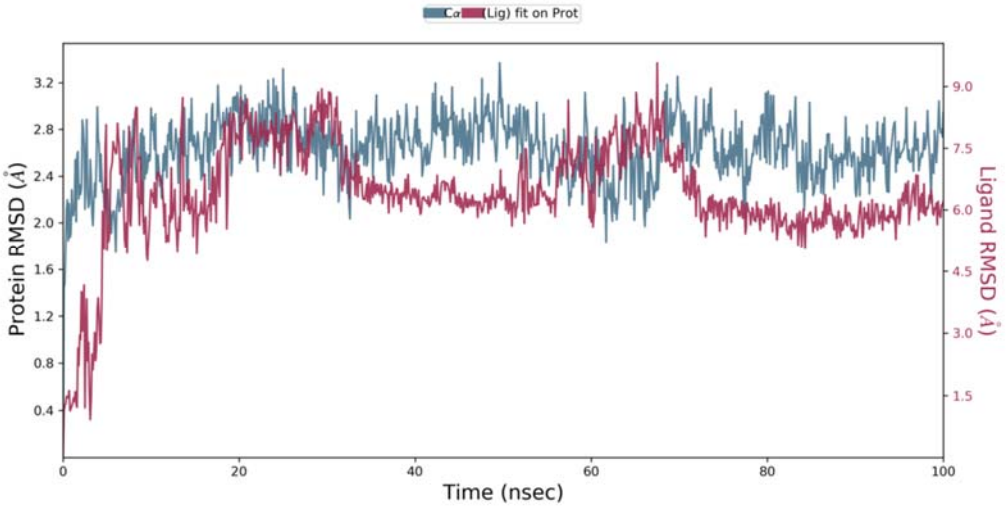

Figure 3. Root Mean Square Deviation (RMSD) plot of compound **6j-protein** complex.

4.5.3 Root Mean Square Fluctuations

The root mean square fluctuations (RMSF) show the fluctuations of each protein amino acid residue across the simulation time period. Lower RMSF values for compounds **6j** (**Figure 4**) in the system imply minor structural reorganizations and conformational changes at the binding site residues during the course of the simulation. The study indicated that the structure and organization of the protein do not deviate significantly from their original conformation after interacting with the compound.

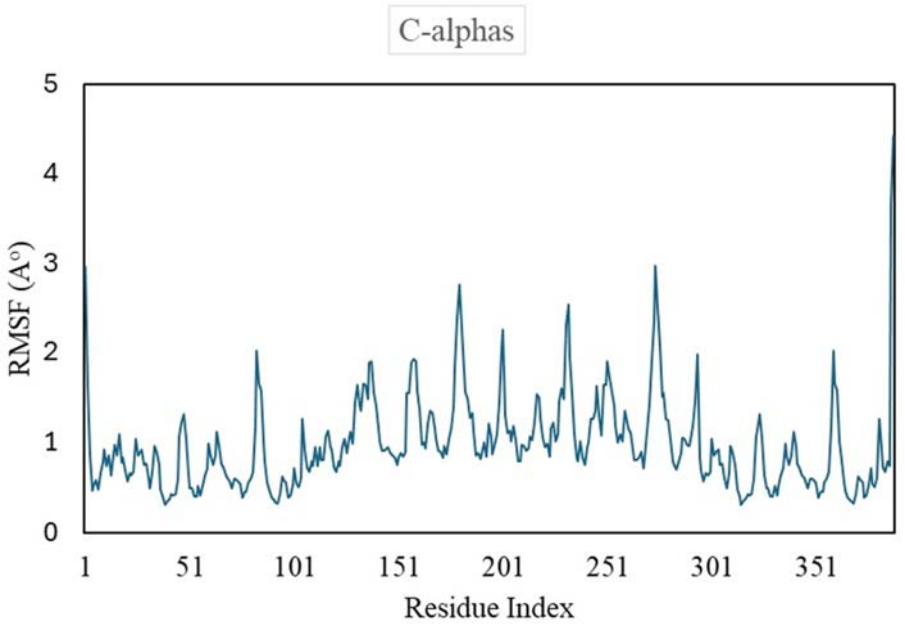

Figure 4. Root Mean Square Fluctuations (RMSF) plot of compound **6j-protein** complex.

The ligand-protein contacts show the specific residues of the protein that interact with the ligand (**Figure 5**). The ALA 18 forms several contacts with the ligand, suggesting its significant role in ligand binding. Whereas ARG 168 forms hydrogen bonds or ionic interactions with the ligand, indicated by the dashed lines connecting the nitrogen atom of ARG 168 to the ligand. The GLU 193 also forms an interaction with the ligand, likely contributing to the overall binding affinity. The protein-ligand contacts in the bar chart represent the interaction frequency of different residues with the ligand over a MDS (**Figure 6**). The different colours in the bars likely represent different types of interactions, such as hydrogen bonds, hydrophobic interactions, or electrostatic interactions. Overall, the varying interaction fractions suggest that certain residues like ARG 168 are consistently involved in ligand binding, while others may have more transient interactions.

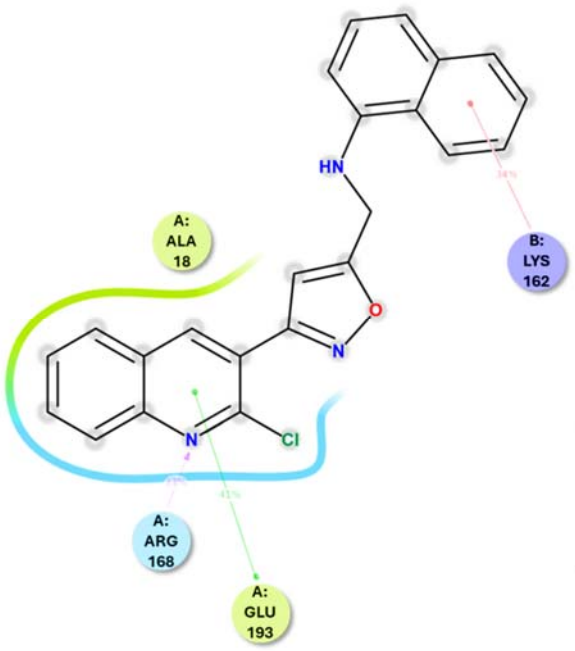

Figure 5. Interaction diagram of compound **6j**-protein contacts.

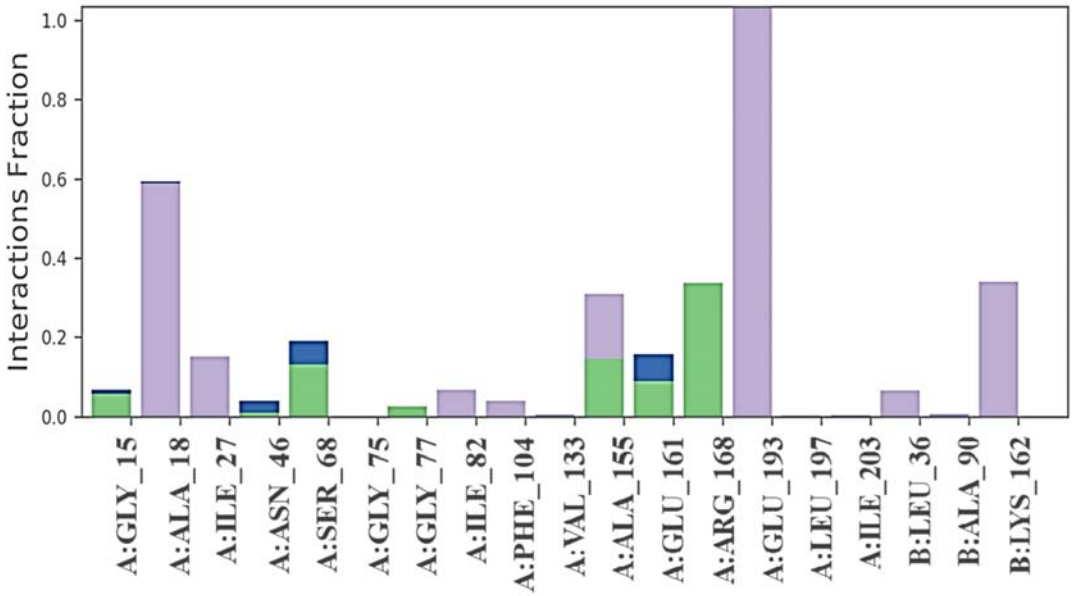

Figure 6. Interaction graph of protein-**6j** contacts.

4.6 Conclusion:

A novel series of hybrid molecules of quinoline derivatives containing substituted isoxazole was synthesized and characterized using NMR, Mass spectral and IR analysis. All the synthesized molecules were evaluated for their antibacterial and antifungal properties. Most of the newly synthesized compounds showed excellent antibacterial efficacy against both pathogens. Out of all the synthesized compounds, two compounds **6j** and **6l** showed promising results in antimicrobial activity with the highest docking score of -8.3 kJ/mol and -7.9 kJ/mol. While compound **6d** showing promising antifungal activity and compounds **6e,** and **6h-i** were able to show good or moderate antibacterial and antifungal activity. Furthermore, docking and MD analysis revealed that compound **6j** may have exhibited antimicrobial potency through inhibition of *E. coli* DNA gyrase.

4.7 Experimental Section:

4.7.1 Chemistry

The open-capillary method was used to determine the melting points on an electrothermal device (SUNTEK), and the results are uncorrected. Compounds were detected on precoated silica gel 60 F254 (Merck) thin-layer chromatography with UV light at 254 nm, 365 nm and/or with iodine vapour. A Bruker AVANCE III (400 MHz) spectrometer was used to capture ^{1}H and ^{13}C NMR spectra in DMSO-d_6, D_2O and $CDCl_3$ using tetramethyl silane (TMS) as an internal standard, and chemical shifts are represented in ppm. Shimadzu GCMS QP2010 Ultra mass spectrometer was used to record mass spectra utilising a direct intake probe. All the reagents purchased from Sigma-Aldrich, Spectrochem and TCI and used without further purification.

Synthesis of 5-(bromomethyl)-3-(2-chloroquinolin-3-yl)isoxazole (5):[150]

A mixture of (*Z*)-2-chloro-*N*-hydroxyquinoline-3-carbimidoyl chloride (**4,** 0.32 g, 1 mmol) and $KHCO_3$ (0.20 g, 2 mmol) in DMF (4 mL) was stirred for 30 minutes at rt. To the resulting mixture propargyl bromide (0.24 g, 2 mmol) was added and the reaction was continued for completion at rt for 4 h. After completion of the reaction (monitored by TLC), the reaction mixture was poured onto ice-cold water. The precipitate thus appeared was collected by filtration with suction and washed with water, and dried. The obtained residue was slurry

washed with diethyl ether to give title compound **5** which was sufficiently pure to use in the next step.

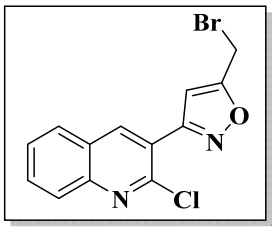

An off-white solid, Yield: 0.26 g, 80%, mp: 120-122 °C. IR (KBr) ν_{max}/cm^{-1}: 3294, 2956 (Ar-C-H), 2358 (C=N), 1741 (Ar-CH=CH), 1587 (Aromatic ring), 1371 (C-N), 1028 (C-O), 874 (C-Cl), 754 (C-Br) cm^{-1}. ^1H NMR (400 MHz, DMSO-d_6) δppm: 8.86 (s, 1H, Ar-H), 8.17 (d, *J* = 8.2 Hz, 1H, Ar-H), 8.05 (d, *J* = 8.5 Hz, 1H, Ar-H), 7.94 (d, *J* = 1.8 Hz, 1H, Ar-H), 7.76 (t, *J* = 7.6 Hz, 1H, Ar-H), 7.17 (s, 1H, Ar-H), 4.97 (s, 2H, CH_2), ppm. ^{13}C NMR (101 MHz, $CDCl_3$) δppm: 167.40, 159.78, 147.44, 147.35, 139.44, 131.34, 127.96, 127.65, 127.38, 126.20, 121.77, 104.81, 17.91. Mass spectrum: 324 *m/z* (M^+). Anal. Calcd. $C_{13}H_8BrClN_2O$ (323.57): C, 48.26; H, 2.49; N, 8.66%. Found: C, 48.23; H, 2.53; N, 8.73%.

General procedure for the synthesis of compounds (6a-o):

To a well stirred mixture of 5-(bromomethyl)-3-(2-chloroquinolin-3-yl)isoxazole (**5**, 0.80 mmol) and different substituted aniline (0.80 mmol) in a H_2O:THF (1:1, 12 mL), $NaHCO_3$ (0.96 mmol) was added in portions and the mixture was stirred at 60 °C for 4 h. After completion of the reaction (monitored by TLC), the reaction mixture was then poured onto crushed ice. The precipitate thus appeared was collected by filtration with suction and washed with water, and dried. The obtained residue was purified by giving wash of diethyl ether to give title compounds **(6a-o)**, which are analytically pure.

By using the same general synthetic procedure for **6a-o**, the following compounds were prepared:

***N*-((3-(2-chloroquinolin-3-yl)isoxazol-5-yl)methyl)-4-methoxyaniline (6a):**

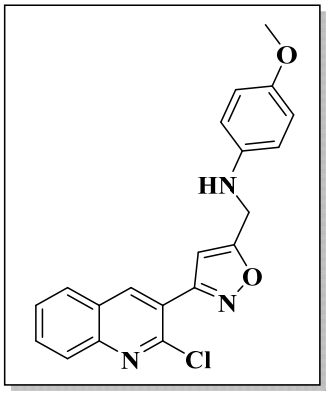

Compound **6a** was prepared from **5** (0.20 g, 0.62 mmol) and p-methoxy aniline (0.08 g, 0.62 mmol) in H_2O:THF (1:1, 12 mL), $NaHCO_3$ (0.06 g, 0.74 mmol). An off-white solid (0.19 g, 94% yield); mp: 90-92 °C. IR (KBr) ν_{max}/cm^{-1}: 3367 (NH), 2989 (Ar-C-H), 1606 (Ar-CH=CH), 1513 (Aromatic ring), 1328 (C-N), 1237 (C-O), 779 (C-Cl), 752 (C-OCH_3 Mono Substitution) cm^{-1}. ^1H NMR (400 MHz, DMSO-d_6) δppm: 8.80 (s, 1H, Ar-H), 8.16 (d, *J* = 7.9 Hz, 1H, Ar-H), 8.04 (d, *J* = 8.4 Hz, 1H, Ar-H), 7.93 (t, *J* = 7.7 Hz, 1H, Ar-H), 7.74 (t, *J* = 7.5 Hz, 1H, Ar-H), 6.89 (s, 1H, Ar-H), 6.75 (d, *J* = 8.3 Hz, 2H, 2 × Ar-H), 6.67 (d, *J* = 8.6 Hz, 2H, 2 × Ar-H), 5.99 (s, 1H, NH, exchangeable in D_2O), 4.51 (d, *J* = 6.4 Hz, 2H, CH_2), 3.64 (s, 3H, OCH_3). ^{13}C NMR (101 MHz, DMSO-d_6) δppm: 170.97, 159.49, 152.55, 147.56, 147.34, 140.23, 139.32, 131.16, 127.93, 127.59, 127.26, 126.20, 122.25, 114.50, 114.24, 103.05, 55.24, 40.97. MS *m/z* (%): 366 (M^+); Anal. Calcd. $C_{20}H_{16}ClN_3O_2$ (365.82): C, 65.67; H, 4.41; N, 11.49%. Found C, 65.71; H, 4.39; N, 11.55%.

***N*-((3-(2-chloroquinolin-3-yl)isoxazol-5-yl)methyl)aniline (6b):**

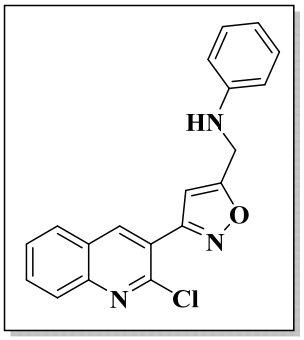

Compound **6b** was prepared from **5** (0.20 g, 0.62 mmol) and aniline (0.06 g, 0.62 mmol) in H_2O:THF (1:1, 12 mL), $NaHCO_3$ (0.06 g, 0.74 mmol). An off-white solid (0.18 g, 92% yield); mp: 102-104 °C. IR (KBr) ν_{max}/cm^{-1}: 3391 (NH), 2868 (Ar-C-H), 1603 (Ar-CH=CH), 1488

(Aromatic ring), 1417 (C-N), 1029 (C-O), 690 (C-Cl) cm^{-1}. ^1H NMR (400 MHz, DMSO-d_6) δppm: 8.78 (s, 1H, Ar-H), 8.14 (d, *J* = 8.3 Hz, 1H, Ar-H), 8.02 (d, *J* = 8.5 Hz, 1H, Ar-H), 7.90 (t, *J* = 7.8 Hz, 1H, Ar-H), 7.72 (t, *J* = 7.8 Hz, 1H, Ar-H), 7.11 (t, *J* = 7.7 Hz, 2H, 2 × Ar-H), 6.90 (s, 1H, NH), 6.71 (d, *J* = 8.1 Hz, 2H, 2 × Ar-H), 6.60 (t, *J* = 7.5 Hz, 1H, Ar-H), 4.57 (s, 2H, , CH_2). ^{13}C NMR (101 MHz, DMSO-d_6) δppm: 172.21, 159.44, 147.78, 147.21, 146.99, 140.37, 132.07, 128.94, 128.56, 127.97, 127.63, 126.37, 122.30, 116.64, 112.44, 103.54, 38.79. Mass spectrum: 336 *m/z* (M^+). Anal. Calcd. $C_{19}H_{14}ClN_3O$ (335.79): C, 67.96; H, 4.20; N, 12.51%. Found: C, 68.11; H, 4.03; N, 12.39%.

4-Bromo-*N*-((3-(2-chloroquinolin-3-yl)isoxazol-5-yl)methyl)aniline (6c):

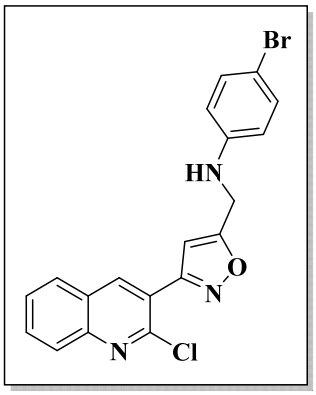

Compound **6c** was prepared from **5** (0.20 g, 0.62 mmol) and 4-bromo aniline (0.11 g, 0.62 mmol) in H_2O: THF (1:1, 12 mL), $NaHCO_3$ (0.06 g, 0.74 mmol). An off-white solid (0.19 g, 96% yield); mp: 123-125 °C. IR (KBr) ν_{max}/cm^{-1}: 3327 (NH), 2944 (Ar-C-H), 2361 (C=N), 1618 (Ar-CH=CH), 1595 (Aromatic ring), 1327 (C-N), 1029 (C-O), 779 (C-Cl), 760 (C-Br) cm^{-1}. ^1H NMR (400 MHz, DMSO-d_6) δppm: 8.80 (s, 1H, Ar-H), 8.16-7.75 (m, 4H, 4 × Ar-H), 7.26 (d, *J* = 7.8 Hz, 2H, 2 × Ar-H), 6.92 (s, 1H, Ar-H), 6.71 – 6.64 (m, 3H, NH, 2 × Ar-H), 4.58 (s, 2H, CH_2). ^{13}C NMR (101 MHz, DMSO-d_6) δppm: 171.70, 159.48, 147.21, 147.08, 147.01, 140.43, 132.12, 131.46, 128.59, 128.01, 127.64, 126.38, 122.27, 114.43, 107.37, 103.66, 38.62. Mass spectrum: 414 *m/z* (M^+). Anal. Calcd. $C_{19}H_{13}BrClN_3O$ (414.69): C, 55.03; H, 3.16; N, 10.13%. Found: C, 55.14; H, 3.05; N, 9.98%.

_N_-((3-(2-chloroquinolin-3-yl)isoxazol-5-yl)methyl)-4-methylaniline (6d):

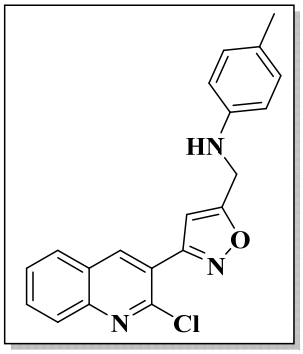

Compound **6d** was prepared from **5** (0.20 g, 0.62 mmol) and 4-methyl aniline (0.07 g, 0.62 mmol) in H_2O: THF (1:1, 12 mL), $NaHCO_3$ (0.06 g, 0.74 mmol). A gray solid (0.18 g, 92% yield); mp: 82-84 °C. IR (KBr) ν_{max}/cm^{-1}: 3018, (Ar-C-H), 2330 (C=N), 1638 (Ar-CH=CH), 1574 (Aromatic ring), 1027 (C-O), 748 (C-Cl), 601 (C-CH_3, Mono substitution) cm^{-1}. ^1H NMR (400 MHz, DMSO-d_6) δppm: 8.78 (s, 1H, Ar-H), 8.15 (d, J = 8.2 Hz, 1H, Ar-H), 8.02 (d, J = 8.5 Hz, 1H, Ar-H), 7.91 (t, J = 7.7 Hz, 1H, Ar-H), 7.73 (t, J = 7.6 Hz, 1H, Ar-H), 6.92 (d, J = 8.0 Hz, 2H, 2 × Ar-H), 6.88 (s, 1H, Ar-H), 6.61 (d, J = 7.9 Hz, 2H, 2 × Ar-H), 6.19 (s, 1H, NH), 4.53 (d, J = 6.4 Hz, 2H, CH_2), 2.14 (s, 3H, CH_3). ^{13}C NMR (101 MHz, DMSO-d_6) δppm: 172.41, 159.41, 147.21, 146.99, 145.48, 140.38, 132.09, 129.37, 128.57, 127.99, 127.63, 126.38, 125.07, 122.32, 112.59, 103.48, 38.62, 20.03. Mass spectrum: 350 *m/z* (M^+). Anal. Calcd. $C_{20}H_{16}ClN_3O$ (349.82): C, 68.67; H, 4.61; N, 12.01%. Found: C, 68.55; H, 4.69; N, 11.87%.

4-Chloro-_N_-((3-(2-chloroquinolin-3-yl)isoxazol-5-yl)methyl)aniline (6e):

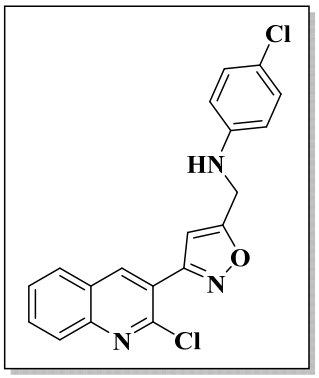

Compound **6e** was prepared from **5** (0.20 g, 0.62 mmol) and 4-chloro aniline (0.09 g, 0.62 mmol) in H_2O: THF (1:1, 12 mL), $NaHCO_3$ (0.06 g, 0.74 mmol). A brown solid (0.19 g, 95% yield); mp: 118-120 °C. IR (KBr) ν_{max}/cm^{-1}: 3335 (NH), 3037 (Ar-C-H), 2361 (C=N), 1596

(Ar-CH=CH), 1490 (Aromatic ring), 1327 (C-N), 1029 (C-O), 778 (C-Cl) cm^{-1}. ^1H NMR (400 MHz, DMSO-d_6) δppm: 8.78 (s, 1H, Ar-H), 8.15 (d, *J* = 8.2 Hz, 1H, Ar-H), 8.02 (d, *J* = 8.4 Hz, 1H, Ar-H), 7.91 (t, *J* = 7.7 Hz, 1H, Ar-H), 7.73 (t, *J* = 7.6 Hz, 1H, Ar-H), 7.13 (d, *J* = 8.3 Hz, 2H, Ar-H), 6.90 (s, 1H, Ar-H), 6.72 (d, *J* = 8.4 Hz, 2H), 4.57 (s, 2H, CH_2). ^{13}C NMR (101 MHz, DMSO-d_6) δppm: 171.75, 159.47, 147.20, 147.00, 146.72, 140.40, 132.10, 129.37, 128.64, 128.57, 127.63, 126.37, 123.34, 122.27, 119.96, 113.87, 103.64, 40.10. Mass spectrum: 370 *m/z* (M^+). Anal. Calcd. $C_{19}H_{13}Cl_2N_3O$ (370.23): C, 61.64; H, 3.54; N, 11.35%. Found: C, 61.77; H, 3.41; N, 11.49%.

***N*-((3-(2-chloroquinolin-3-yl)isoxazol-5-yl)methyl)-2-methoxyaniline (6f):**

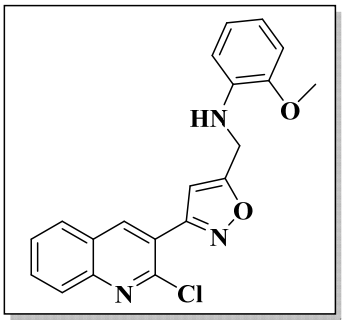

Compound **6f** was prepared from **5** (0.20 g, 0.62 mmol) and 2-methoxy aniline (0.08 g, 0.62 mmol) in H_2O:THF (1:1, 12 mL), $NaHCO_3$ (0.06 g, 0.74 mmol). An off-white solid (0.19 g, 95% yield); mp: 89-91 °C. IR (KBr) ν_{max}/cm^{-1}: 3367 (NH), 3115, 2988 (Ar-C-H), 2358 (C=N), 1606 (Ar-CH=CH), 1513 (Aromatic ring), 1237 (C-N), 1028 (C-O), 779 (C-Cl), 752 (C-OCH_3 Mono Substitution) cm^{-1}. ^1H NMR (400 MHz, $CDCl_3$) δppm: 8.52 (s, 1H, Ar-H), 8.07 (d, *J* = 8.5 Hz, 1H, Ar-H), 7.97 (d, *J* = 8.2 Hz, 1H, Ar-H), 7.93 (t, *J* = 7.7 Hz, 1H, Ar-H), 7.73 (t, *J* = 7.6 Hz, 1H, Ar-H), 7.33 (d, *J* = 8.3 Hz, 2H, 2 × Ar-H), 7.29 (s, 1H, Ar-H), 7.17 (d, *J* = 8.3 Hz, 2H, 2 × Ar-H), 4.51 (s, 2H, CH_2), 3.72 (s, 3H, OCH_3). ^{13}C NMR (101 MHz, DMSO-d_6) δppm: 157.37, 156.27, 153.58, 147.96, 146.85, 141.23, 132.38, 131.38, 128.88, 128.16, 127.80, 127.61, 125.01, 120.85, 118.85, 117.33, 111.68, 55.05, 40.10. Mass spectrum: 366 *m/z* (M^+). Anal. Calcd. $C_{20}H_{16}ClN_3O_2$ (365.82): C, 65.67; H, 4.41; N, 11.49%. Found: C, 65.79; H, 4.53; N, 11.33%.

***N*-((3-(2-chloroquinolin-3-yl)isoxazol-5-yl)methyl)naphthalen-2-amine (6g):**

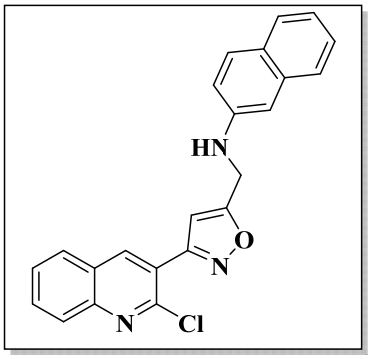

Compound **6g** was prepared from **5** (0.20 g, 0.62 mmol) and 2-napthylamine 0.09 g, 0.62 mmol) in H_2O:THF (1:1, 12 mL), $NaHCO_3$ (0.06 g, 0.74 mmol). An brown solid (0.16 g, 80 % yield); mp: 110-112 °C. IR (KBr) ν_{max}/cm^{-1}: 3385 (NH), 2821 (Ar-C-H), 2361 (C=N), 1621 (Ar-CH=CH), 1576 (Aromatic ring), 751 (C-Cl) cm^{-1}. ^1H NMR (400 MHz, DMSO-d_6) δppm: 9.05 (s, 1H, Ar-H), 8.11 (d, J = 8.2 Hz, 1H, Ar-H), 8.01 (m, 3H, 3 × Ar-H), 7.92 (d, J = 6.1 Hz, 2H, 2 × Ar-H), 7.76 (d, J = 7.2 Hz, 3H, 3 × Ar-H), 7.76 – 7.56 (m, 2H, 2 × Ar-H), 7.50 (t, J = 7.9 Hz, 1H, Ar-H), 7.48 (s, 1H, NH), 4.50 (s, 2H, CH_2). ^{13}C NMR (101 MHz, $CDCl_3$) δppm: 157.32, 156.32, 147.99, 146.87, 141.33, 133.92, 132.53, 130.73, 128.74, 128.32, 128.12, 127.83, 127.65, 127.56, 126.73, 126.52, 126.26, 124.89, 124.58, 121.11, 116.75, 40.50. Mass spectrum: 386 *m/z* (M^+). Anal. Calcd. $C_{23}H_{16}ClN_3O$ (385.85): C, 71.60; H, 4.18; N, 10.89%. Found: C, 71.31; H, 4.33; N, 11.02%.

***N*-((3-(2-chloroquinolin-3-yl)isoxazol-5-yl)methyl)-4-fluoroaniline (6h):**

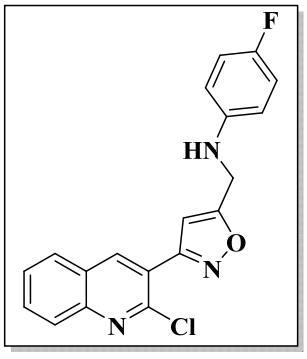

Compound **6h** was prepared from **5** (0.20 g, 0.62 mmol) and 4-fluro aniline (0.07 g, 0.62 mmol) in H_2O:THF (1:1, 12 mL), $NaHCO_3$ (0.06 g, 0.74 mmol). An off-white solid (0.16 g, 80% yield); mp: 121-123 °C. IR (KBr) ν_{max}/cm^{-1}: 3060 (Ar-C-H), 2361 (C=N), 1509 (Aromatic ring), 1026 (C-O), 854 (C-Cl) cm^{-1}. ^1H NMR (400 MHz, DMSO-d_6) δppm: 8.80 (s, 1H, Ar-H),

8.15 – 7.74 (m, 4H, 4 × Ar-H), 6.96 – 6.91 (d, 3H, 3 × Ar-H), 6.71 (s, 2H, 2 × Ar-H), 6.36 (s, 1H, NH), 4.55 (s, 2H, CH_2). ^{13}C NMR (101 MHz, DMSO-d_6) δppm: 172.08, 159.44, 155.91, 147.02, 144.45, 140.73, 140.39, 132.11, 128.58, 128.00, 127.61, 126.39, 123.65, 122.31, 115.43, 115.21, 113.39, 103.58, 40.19. Mass spectrum: 354 *m/z* (M^+). Anal. Calcd. $C_{19}H_{13}ClFN_3O$ (353.78): C, 64.51; H, 3.70; N, 11.88%. Found: C, 64.68; H, 3.55; N, 12.07%.

3-Chloro-*N*-((3-(2-chloroquinolin-3-yl)isoxazol-5-yl)methyl)aniline (6i):

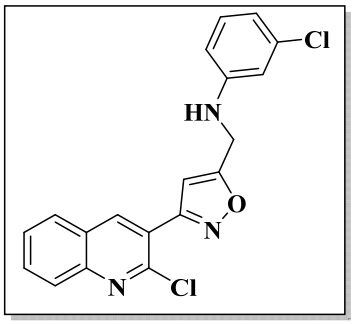

Compound **6i** was prepared from **5** (0.20 g, 0.62 mmol) and 3-chloro aniline 0.09, 0.62 mmol) in H_2O:THF (1:1, 12 mL), $NaHCO_3$ (0.06 g, 0.74 mmol). An off-white solid (0.18 g, 92% yield); mp: 117-119 °C. IR (KBr) ν_{max}/cm^{-1}: 3325 (NH), 3035 (Ar-C-H), 2364 (C=N), 1602 (Ar-CH=CH), 1526 (Aromatic ring), 1327 (C-N), 1030 (C-O), 752 (C-Cl) cm^{-1}. ^1H NMR (400 MHz, DMSO-d_6) δppm: 8.78 (s, 1H, Ar-H), 8.14 (d, J = 8.2 Hz, 1H, Ar-H), 8.02 (d, J = 8.6 Hz, 1H, Ar-H), 7.90 (t, J = 7.7 Hz, 1H, Ar-H), 7.72 (t, J = 7.5 Hz, 1H, Ar-H), 7.11 (t, J = 8.0 Hz, 1H, Ar-H), 6.92 (s, 1H, Ar-H), 6.75 (s, 2H, Ar-H, NH), 6.67 (d, J = 8.3 Hz, 1H, Ar-H), 6.60 (d, J = 7.6 Hz, 1H, Ar-H), 4.61 (s, 2H, CH_2). ^{13}C NMR (101 MHz, DMSO-d_6) δppm: 171.57, 159.49, 149.33, 147.21, 147.00, 140.38, 133.67, 132.08, 130.45, 130.32, 128.57, 127.98, 127.63, 126.37, 122.25, 116.07, 111.70, 103.72, 40.10. Mass spectrum: 370 *m/z* (M^+). Anal. Calcd. $C_{19}H_{13}Cl_2N_3O$ (370.23): C, 61.64; H, 3.54; N, 11.35%. Fouund: C, 61.81; H, 3.69; N, 11.21%.

***N*-((3-(2-chloroquinolin-3-yl)isoxazol-5-yl)methyl)naphthalen-1-amine (6j):**

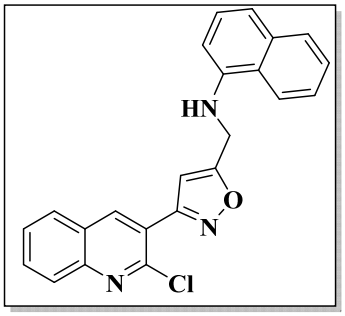

Compound **6j** was prepared from **5** (0.20 g, 0.62 mmol) and 1-napthylamine 0.09 g, 0.62 mmol) in H_2O:THF (1:1, 12 mL), $NaHCO_3$ (0.06 g, 0.74 mmol). An brown solid (0.19 g, 95% yield); mp: 110-112 °C. IR (KBr) ν_{max}/cm^{-1}: 3371 (NH), 2846 (Ar-C-H), 2360 (C=N), 1509 (Aromatic ring), 1329 (C-N), 1158 (C-O), 752 (C-Cl) cm^{-1}. ^1H NMR (400 MHz, $CDCl_3$) δppm: 8.35 (s, 1H, Ar-H), 7.97 (d, *J* = 8.5 Hz, 2H, 2 × Ar-H), 7.94 – 7.77 (m, 5H, 5 × Ar-H), 7.70 – 7.53 (m, 3H, 3 × Ar-H), 7.47 – 7.40 (m, 2H, 2 × Ar-H) 3.92 (s, 2H, CH_2). ^{13}C NMR (101 MHz, $CDCl_3$) δppm: 170.36, 159.37, 147.52, 147.32, 144.64, 141.33, 139.38, 133.83, 131.19, 128.31, 127.91, 127.60, 127.58, 127.28, 126.18, 125.82, 125.56, 124.76, 119.34, 118.52, 104.78, 103.28, 40.23. Mass spectrum: 386 *m/z* (M^+). Anal. Calcd. $C_{23}H_{16}ClN_3O$ (385.85): C, 71.60; H, 4.18; N, 10.89%. Found: C, 71.43; H, 4.31; N, 11.14%.

***N*-((3-(2-chloroquinolin-3-yl)isoxazol-5-yl)methyl)-2,4-dimethylaniline (6k):**

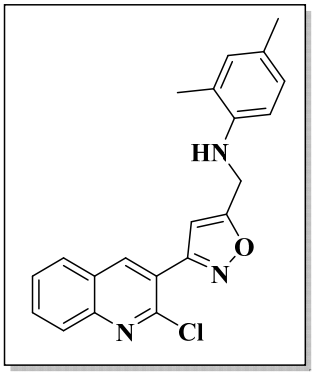

Compound **6k** was prepared from **5** (0.20 g, 0.62 mmol) and 2,4-dimethyl aniline (0.07 g, 0.62 mmol) in H_2O:THF (1:1, 12 mL), $NaHCO_3$ (0.06 g, 0.74 mmol). An off-white solid (0.18 g, 92% yield); mp: 85-87 °C. IR (KBr) ν_{max}/cm^{-1}: 3403 (NH), 3001 (Ar-C-H), 2912, 2364 (C=N), 1671 (Ar-CH=CH), 1562 (Aromatic ring), 1268 (C-N), 1028 (C-O), 757 (C-Cl) cm^{-1}. ^1H NMR (400 MHz, DMSO-d_6) δppm: 8.77 (s, 1H, Ar-H), 8.13 (d, *J* = 8.3 Hz, 1H, Ar-H), 8.01 (d, *J* =

8.5 Hz, 1H, Ar-H), 7.90 (t, *J* = 7.7 Hz, 1H, Ar-H), 7.72 (t, *J* = 7.6 Hz, 1H, Ar-H), 6.84 (s, 1H, Ar-H), 6.80 (d, *J* = 9.9 Hz, 2H, 2 × Ar-H), 6.52 (d, *J* = 8.0 Hz, 1H, Ar-H), 5.57 (s, 1H, NH), 4.59 (s, 2H, CH_2), 2.12 (s, 6H, 2 × CH_3). ^{13}C NMR (101 MHz, DMSO-d_6) δppm: 172.68, 159.41, 147.21, 146.97, 143.11, 140.36, 132.05, 130.75, 128.55, 127.96, 127.62, 126.87, 126.37, 124.96, 122.34, 122.31, 109.71, 103.39, 40.10, 19.98, 17.61. Mass spectrum: 364 *m/z* (M^+). Anal. Calcd. $C_{21}H_{18}ClN_3O$ (363.85): C, 69.32; H, 4.99; N, 11.55%. Found: 69.55; H, 4.77; N, 11.59%.

***N*-((3-(2-chloroquinolin-3-yl)isoxazol-5-yl)methyl)-2,6-dimethylaniline (6l):**

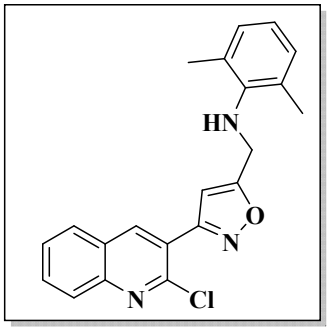

Compound **6l** was prepared from **5** (0.20 g, 0.62 mmol) and 2,6-dimethyl aniline (0.07 g, 0.62 mmol) in H_2O:THF (1:1, 12 mL), $NaHCO_3$ (0.06 g, 0.74 mmol). A gray solid (0.18 g, 92% yield); mp: 88-90 °C. IR (KBr) ν_{max}/cm^{-1}: 3373 (NH), 2942 (Ar-C-H), 2364 (C=N), 1619 (Ar-CH=CH), 1598 (Aromatic ring), 1298 (C-N), 1023(C-O), 853 (C-CH_3 Di substitution), 757 (C-Cl) cm^{-1}. ^{1}H NMR (400 MHz, DMSO-d_6) δppm: 8.77 (s, 1H), 8.17 (d, *J* = 8.1 Hz, 1H), 8.03 (d, *J* = 8.4 Hz, 1H), 7.93 (q, *J* = 8.0 Hz, 1H), 7.75 (q, *J* = 7.5 Hz, 1H), 6.94 (d, *J* = 7.5 Hz, 2H), 6.78 (d, *J* = 8.2 Hz, 2H), 4.38 (s, 2H, CH_2), 2.24 (s, 6H, CH_3). ^{13}C NMR (101 MHz, $CDCl_3$) δppm: 170.58, 159.52, 147.59, 147.36, 139.24, 131.15, 129.81, 128.58, 127.94, 127.57, 127.26, 126.21, 122.92, 122.25, 103.30, 43.21, 17.85. Mass spectrum: 364 *m/z* (M^+). Anal. Calcd. $C_{21}H_{18}ClN_3O$ (363.85): C, 69.17; H, 4.83; N, 11.26%. Found: 69.32; H, 4.99; N, 11.55%.

***N*-((3-(2-chloroquinolin-3-yl)isoxazol-5-yl)methyl)-2,3-dimethylaniline (6m):**

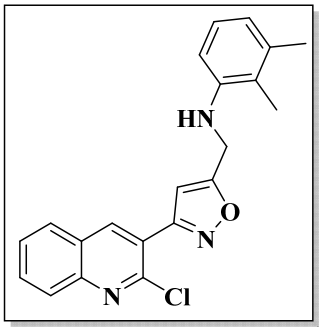

Compound **6m** was prepared from **5** (0.20 g, 0.62 mmol) and 2,3-dimethyl aniline (0.07 g, 0.62 mmol) in H_2O:THF (1:1, 12 mL), $NaHCO_3$ (0.06 g, 0.74 mmol). An off-white solid (0.19 g, 98% yield); mp: 96-98 °C. IR (KBr) ν_{max}/cm^{-1}: 3375 (NH), 2966 (Ar-C-H), 2369 (C=N), 1595 (Ar-CH=CH), 1492 (Aromatic ring), 1238 (C-N), 1027 (C-O), 960 (C-CH_3 Di substitution), 755 (C-Cl) cm^{-1}. ^{1}H NMR (400 MHz, DMSO-d_6) δppm: 9.03 (s, 1H, Ar-H), 8.18 (d, J = 8.2 Hz, 1H, Ar-H), 8.03 – 7.94 (m, 2H, 2 × Ar-H), 7.85 – 7.75 (m, 1H, Ar-H), 7.20 (t, J = 7.5 Hz, 2H, 2 × Ar-H), 7.22 – 7.18 (m, 3H, 3 × Ar-H), 7.04 (t, J = 7.8 Hz, 1H, Ar-H), 6.03 (s, 1H, NH), 4.70 (s, 2H, CH_2), 2.24 (s, 3H, CH_3), 2.18 (s, 3H, CH_3). ^{13}C NMR (101 MHz, $CDCl_3$) δppm: 156.92, 155.83, 148.08, 146.73, 141.45, 136.66, 132.60, 132.31, 131.16, 130.85, 128.92, 128.21, 127.95, 127.83, 127.71, 125.03, 117.02, 40.26 20.16, 16.98. Mass spectrum: 364 *m/z* (M^+). Anal. Calcd. $C_{21}H_{18}ClN_3O$ (363.85): C, 69.32; H, 4.99; N, 11.55%. Found: 69.04; H, 5.18; N, 11.68%.

***N*-((3-(2-chloroquinolin-3-yl)isoxazol-5-yl)methyl)-2-methylaniline (6n)**

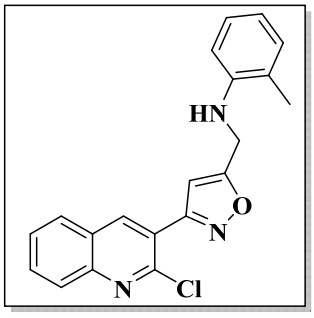

Compound **6n** was prepared from **5** (0.20 g, 0.62 mmol) and 2-methyl aniline (0.07 g, 0.62 mmol) in H_2O:THF (1:1, 12 mL), $NaHCO_3$ (0.06 g, 0.74 mmol). An off-white solid (0.19 g, 96% yield); mp: 118-120 °C. ^{1}H NMR (400 MHz, DMSO-d_6) δppm: 8.72 (s, 1H, Ar-H), 8.10 (d, J = 8.3 Hz, 1H, Ar-H), 8.06-7.89 (m, 2H, 2 ×Ar-H), 7.70 (t, J = 7.6 Hz, 1H, Ar-H), 7.60 (t,

J = 7.4 Hz, 1H, Ar-H), 7.12 (m, 2H, 2 × Ar-H), 6.98 (d, *J* = 8.0 Hz 1H, Ar-H), 6.74 (s, 1H, Ar-H), 6.59 (s, 1H, NH), 4.97 (d, *J* = 6.2 Hz, 2H, CH_2), 2.24 (s, 3H, CH_3). ^{13}C NMR (101 MHz, $CDCl_3$) 171.51, 159.31, 147.23, 146.97, 145.48, 140.38, 132.09, 129.37, 128.57, 127.99, 127.63, 126.38, 125.07, 122.32, 112.59, 103.48, 39.67, 18.04. Mass spectrum: 350 *m/z* (M^+).

_N_-((3-(2-chloroquinolin-3-yl)isoxazol-5-yl)methyl)-2,5-dimethylaniline (6o)

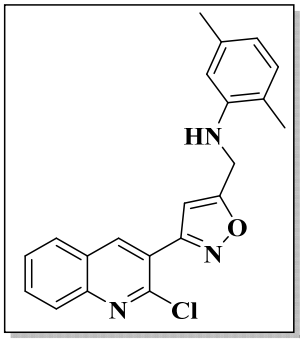

Compound **6o** was prepared from **5** (0.20 g, 0.62 mmol) and 2,6-dimethyl aniline (0.07 g, 0.62 mmol) in H_2O:THF (1:1, 12 mL), $NaHCO_3$ (0.06 g, 0.74 mmol). IR (KBr) ν_{max}/cm^{-1}: 3375 (NH), 2967 (Ar-C-H), 2369 (C=N), 1595 (Ar-CH=CH), 1493 (Aromatic ring), 1238 (C-N), 1028 (C-O), 843 (C-CH_3 Di substitution), 755 (C-Cl) cm^{-1}. ^1H NMR (400 MHz, DMSO-d_6) δppm: 9.04 (s, 1H, Ar-H), 8.18 (d, *J* = 8.2 Hz, 1H, Ar-H), 7.99 (m, 2H, 2 × Ar-H), 7.84 – 7.76 (m, 1H, Ar-H), 7.24 (s, 1H, Ar-H), 7.21 (d, *J* = 6.4 Hz, 2H, 2 × Ar-H), 7.13 (d, *J* = 7.8 Hz, 2H, 2 × Ar-H), 6.03 (s, 1H, NH), 4.65 (s, 2H, CH_2), 2.24 (s, 3H, CH_3), 2.10 (s, 3H, CH_3). ^{13}C NMR (101 MHz, $CDCl_3$) δppm: 167.40, 159.78, 147.44, 147.35, 139.43, 131.33, 127.95, 127.65, 127.37, 126.19, 121.77, 115.82, 104.80, 40.96, 33.87, 17.91. Mass spectrum: 364 *m/z* (M^+). Anal. Calcd. $C_{21}H_{18}ClN_3O$ (363.85): 69.32; H, 4.99; N, 11.55%. Found: C, 69.11; H, 4.76; N, 11.32%

4.7.2 Experiment protocol of anti-microbial activity

The antibacterial and anti-fungal activity was checked against the common fungal pathogens *Aspergillus niger,* and *Candida albicans,* along with the bacterial strains of two gram-positive bacteria (*Bacillus subtilis, Staphylococcus aureus*) and, two gram-negative bacteria (*Escherichia coli* and *Salmonella typhi*). The antibacterial and antifungal standards ampicillin (100 µg/ml), gentamicin (100 µg/ml) and nystatin (100 µg/ml) respectively were used to test the inhibition zone (mm). According to the experimental results, all bacterial strains were significantly inhibited by the tested compounds, which had an inhibition zone ranging from 15

to 33 mm and in the case of fungal species an inhibition zone ranging from 13 to 32 mm was observed. The synthesized compound showed stronger and moderate action compared to reference medicines. The tested compound's antimicrobial activity was determined using a 100 µg/ml attentiveness of a molecule in the solvent DMSO. Figure **3** and **4** provide a graphical representation of the antimicrobial activity data.[107]

4.7.3 Experiment protocol of molecular docking study

The ChemSketch 2021.2.0 software was used for the generation of ligand structures. Furthermore, the docking studies were carried out to find the interacting residues of all compounds, AutoDock Vina 1.1.2 was used and during the docking study the energy minimization of every molecule was performed using Avogadro-1.2.0.[108] The crystal structure of the 24 kDa domain of *E. coli* DNA gyrase was downloaded from the PDB data bank (4DUH). The structural receptor was devoid of all ligands before docking by excluding heteroatoms. Kollaman charge, solvation parameters, and polar hydrogens were added to the protein to complete its processing. For x, y, and z, the appropriate grid box sizes were set to 40, 40, and 40 Å. For each of the variables x, y, and z, the grid centre was set to 29.712, 2.093, and 23.925. The exhaustiveness was 40 and the grid point spacing was 0.375 Å. The most likely binding mechanism was determined using the robust molecular graphics viewer Discovery Studio Visualizer v21.0.[109]

4.7.4 Protocol of molecular dynamic simulation

The DESMOND module (Schrodinger Inc., USA) was used to conduct a molecular dynamics investigation on the best dock protein-ligand combination. The study was conducted using the Berendsen thermostat and barostat procedures for 100 ns. The system was solved, minimized, and put into a TIP3P orthorhombic box measuring 10 Å × 10 Å × 10 Å. Desmond's Protein Preparation, Ligand Preparation, and Epik tools confirmed the chemical structure's precision. The minimized explicit solvation complex of the ligand-receptor complex was simulated for 100 ns using the NPT ensemble (at 300 K and 1.01325 bars). Steepest Descent and Broyden-Fletcher-Goldfarb-Shanno algorithms were used to relax the system. The dynamics simulation approach used the Nose-Hoover thermostat algorithm and the Martyna-Tobias-Klein barostat algorithm at 300 K temperature and 1 atm pressure and OPLS_2005 force field. To mimic physiological conditions counterions and 0.15M sodium chloride were introduced to neutralize

the models. The models underwent relaxation before stimulation and trajectories were stored for inspections at intervals of 100ps and frames selected from MD trajectories at intervals of 100ns post completions of the MDS run. The smooth particle mesh Ewald technique was used to manage both long-range and short-range coulombic interactions, with endpoint values of 9.0 Å. MD simulations were run for 100 ns, and trajectory information was acquired in the remaining 2.0 ns. It is a classical technique used to efficiently calculate long-range coulombic interactions by splitting the interaction into short-range (real space) and long-range (reciprocal space) components. The real-space component is computed directly, while the reciprocal space component is computed using Fourier transforms. This method is highly accurate for calculating columbic interactions. The stability of the docked complexes, **4DUH-6j** was assessed by monitoring, root mean square deviation (RMSD), and root mean square fluctuations (RMSF).[152]

4.8 Spectral data

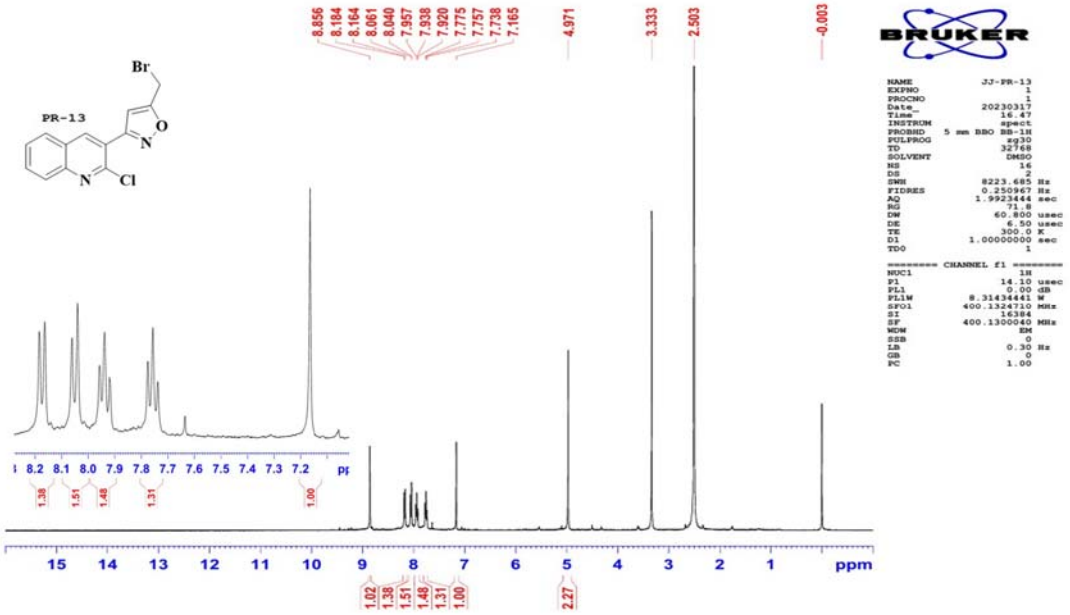

Figure 1: [1]H NMR of compound **5**

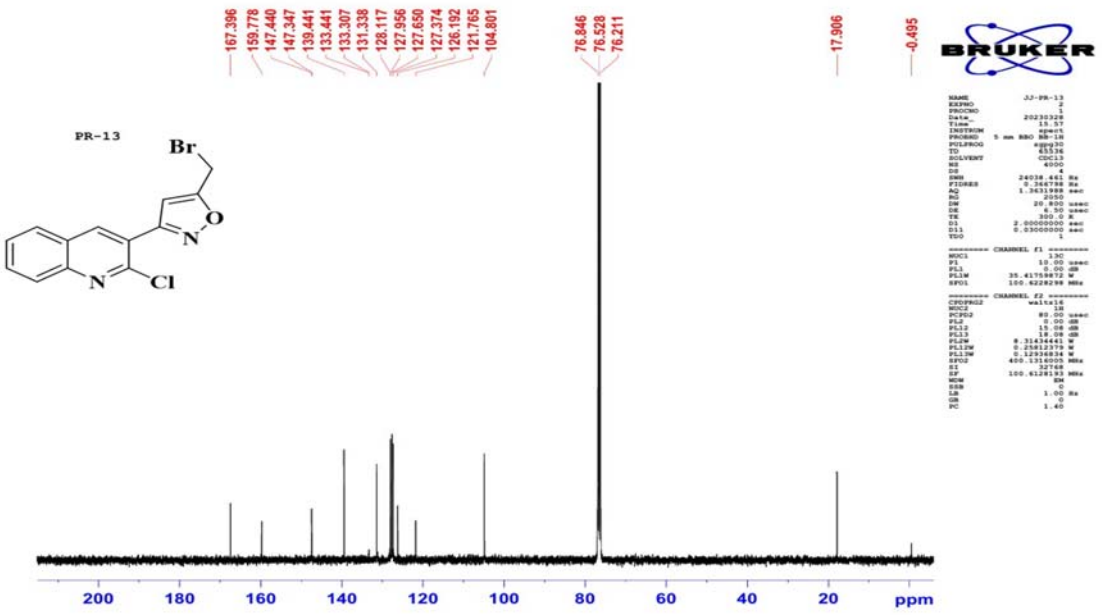

Figure 2: ^{13}C NMR of compound **5**

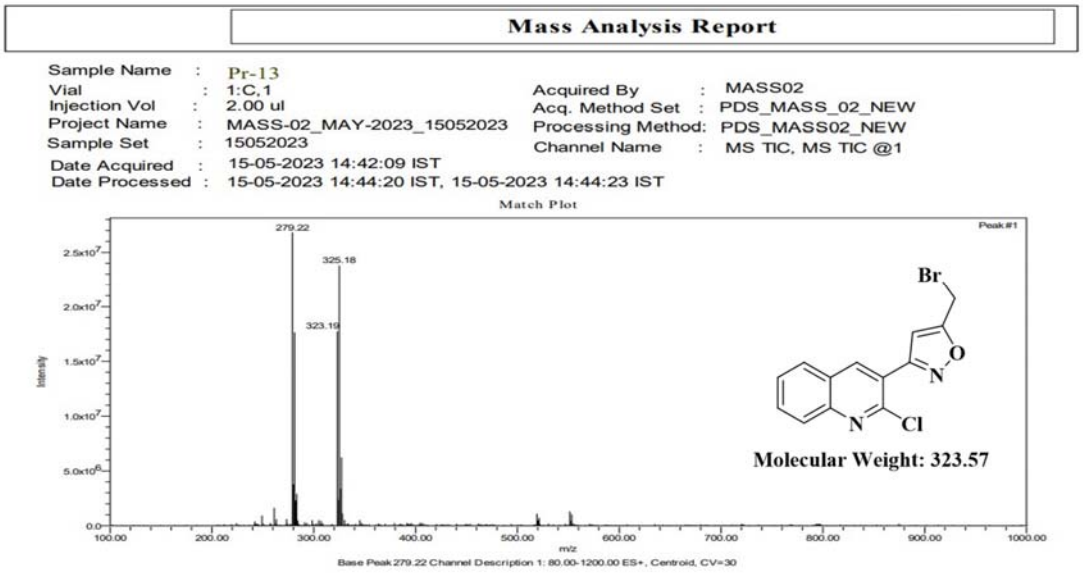

Figure 3: Mass spectra of compound **5**

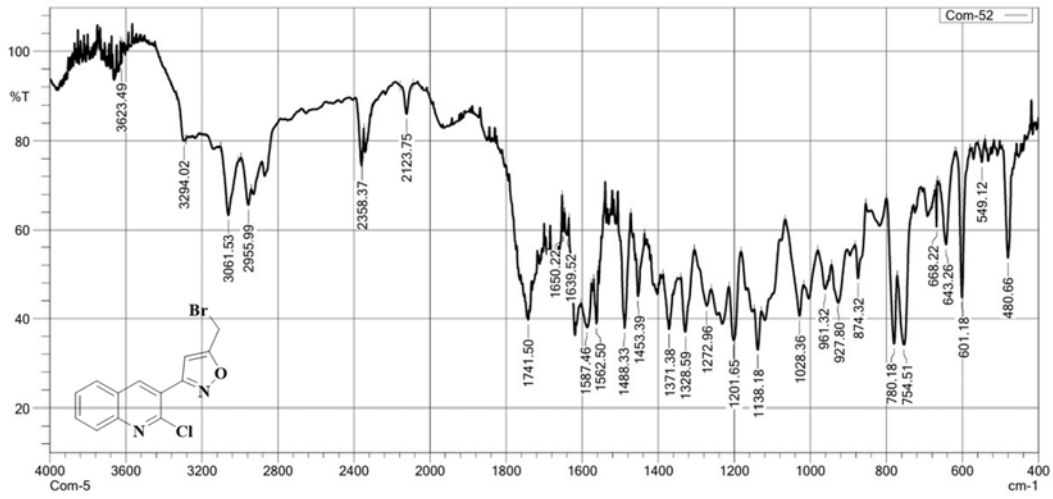

Figure 4: IR spectra of compound **5**

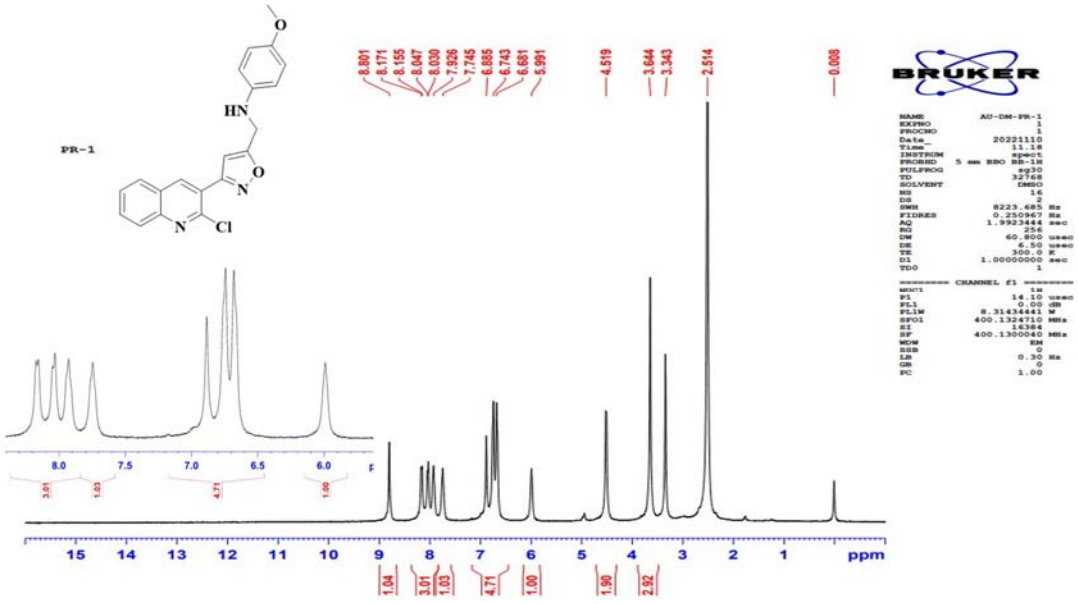

Figure 5: ^{1}H NMR of compound **6a**

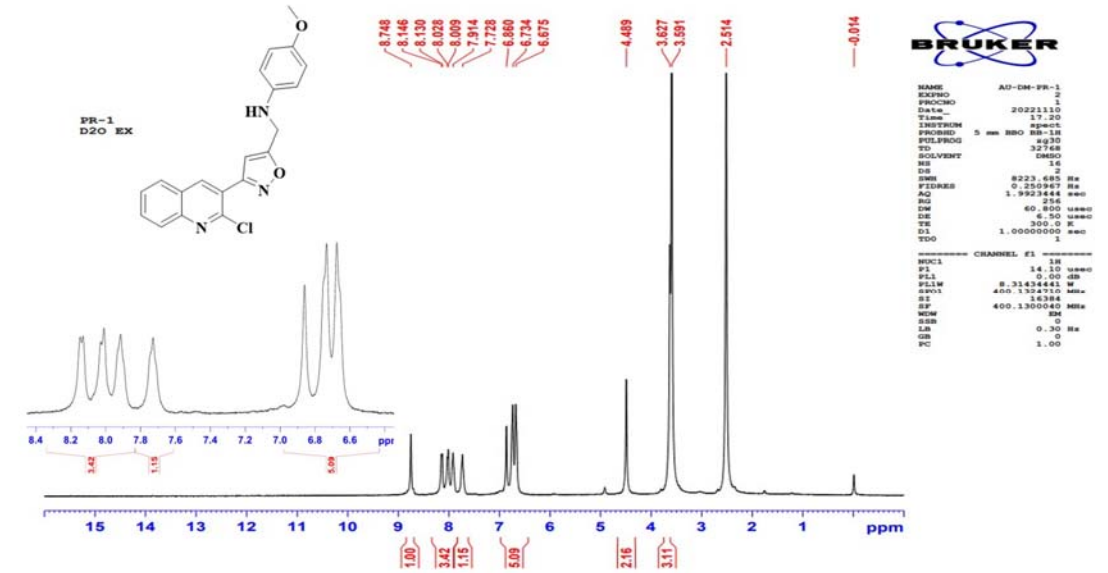

Figure 6: ^{1}H NMR of compound **6a** (D_2O exchange)

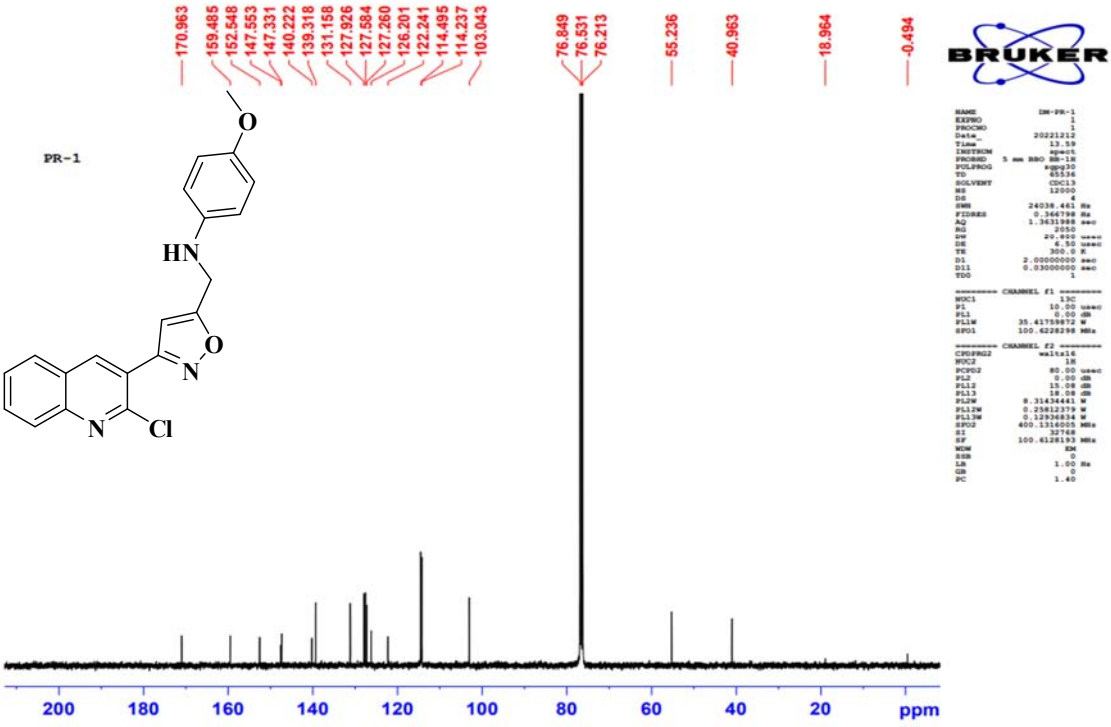

Figure 7: ^{13}C NMR of compound **6a**

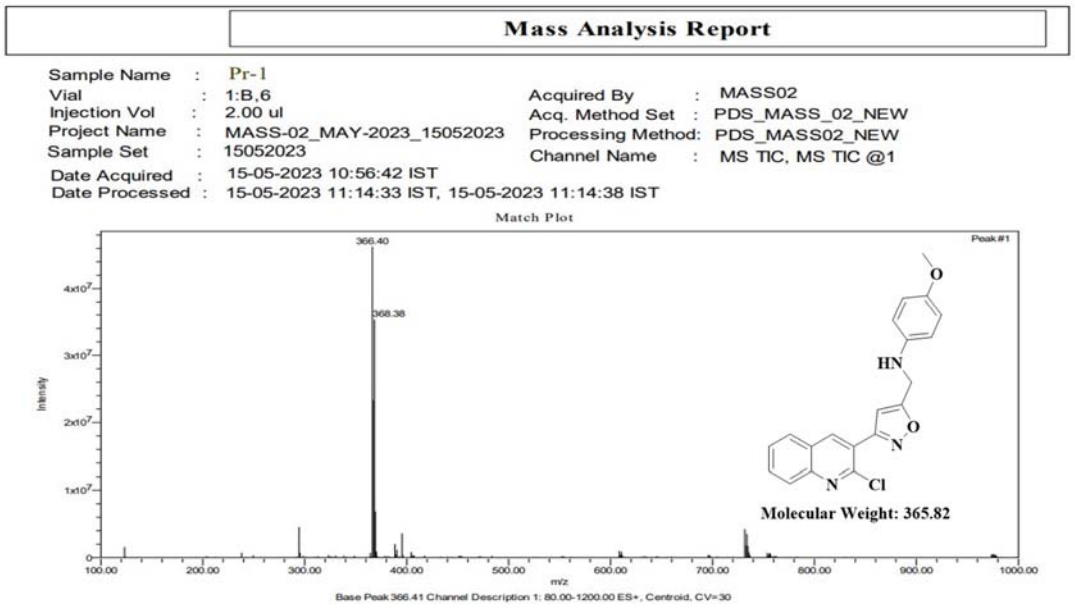

Figure 8: Mass spectra of compound **6a**

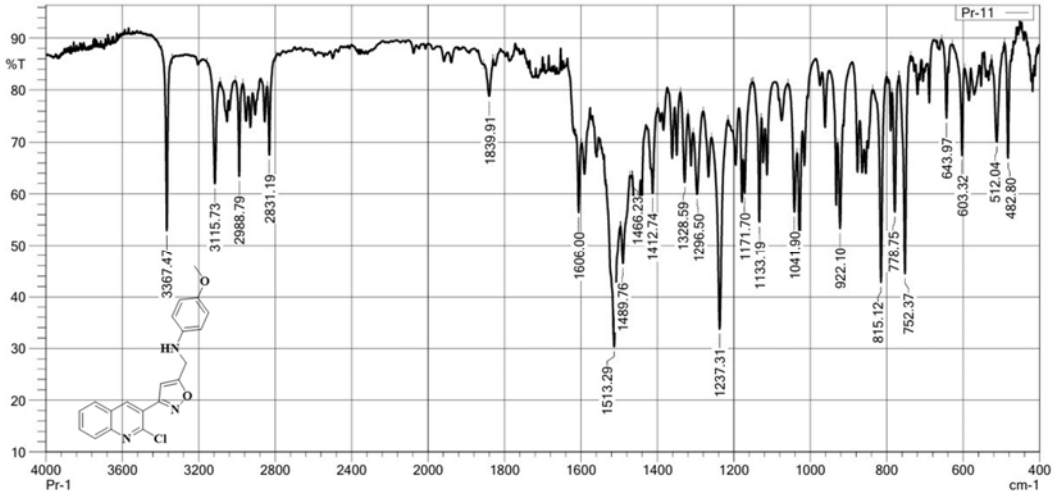

Figure 9: IR spectra of compound **6a**

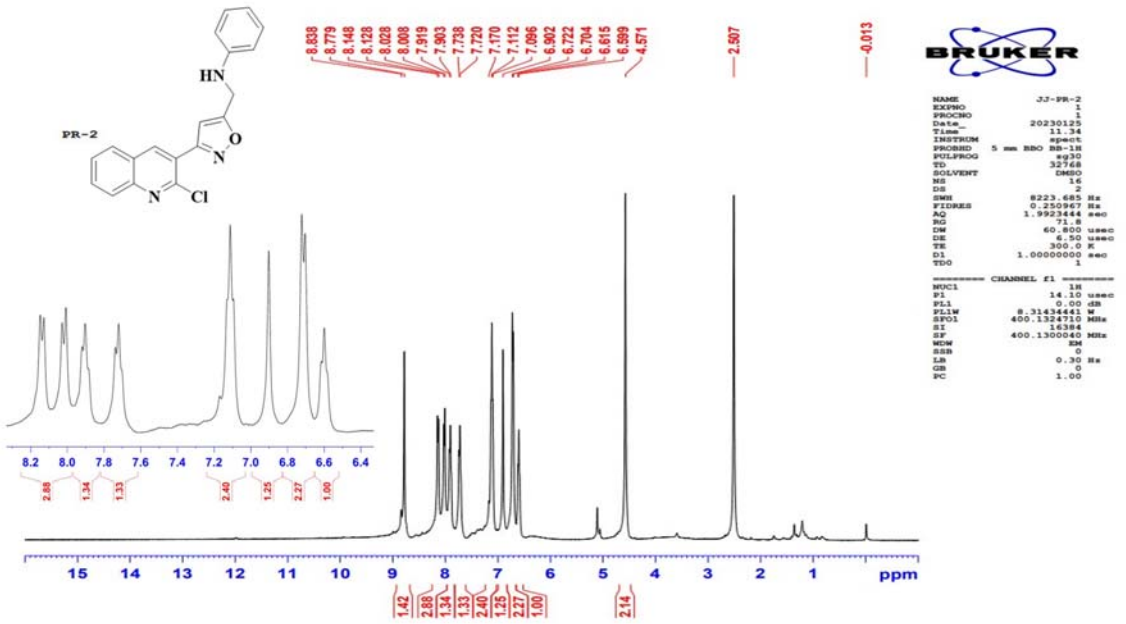

Figure 10: ^{1}H NMR of compound **6b**

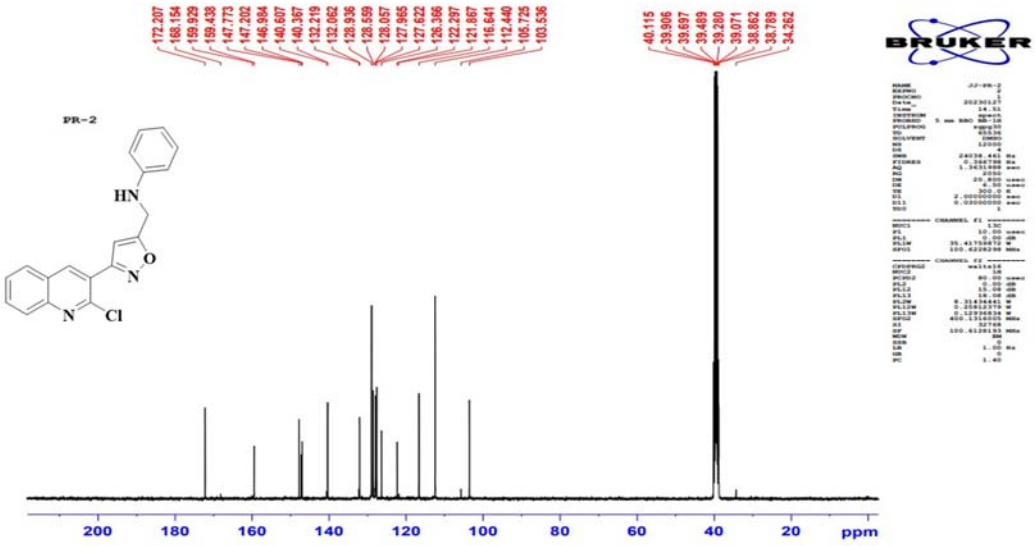

Figure 11: ^{13}C NMR of compound **6b**

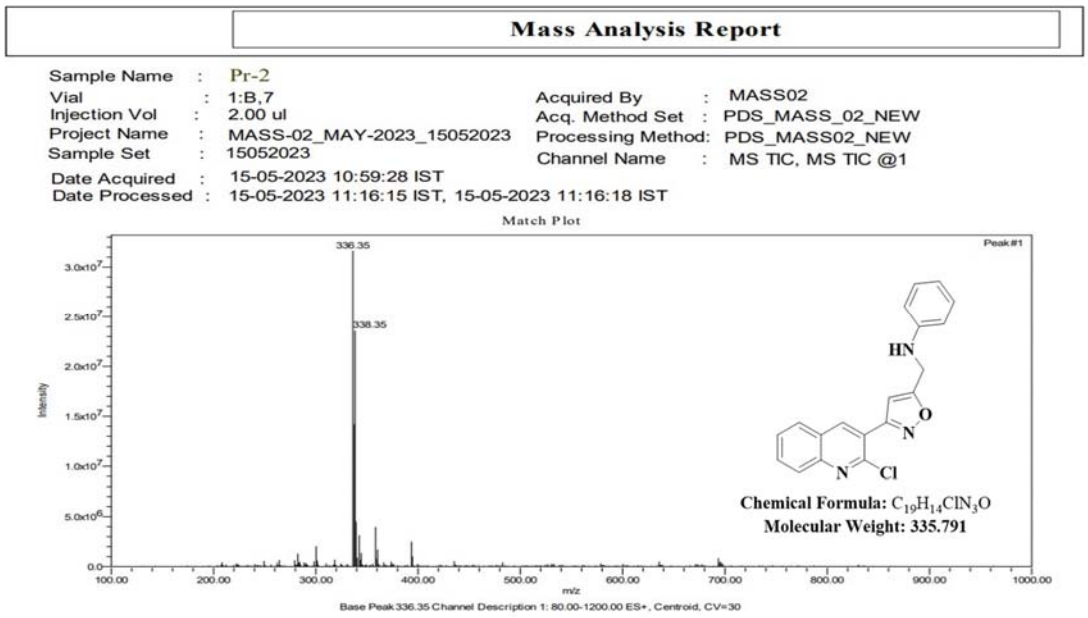

Figure 12: Mass spectra of compound **6b**

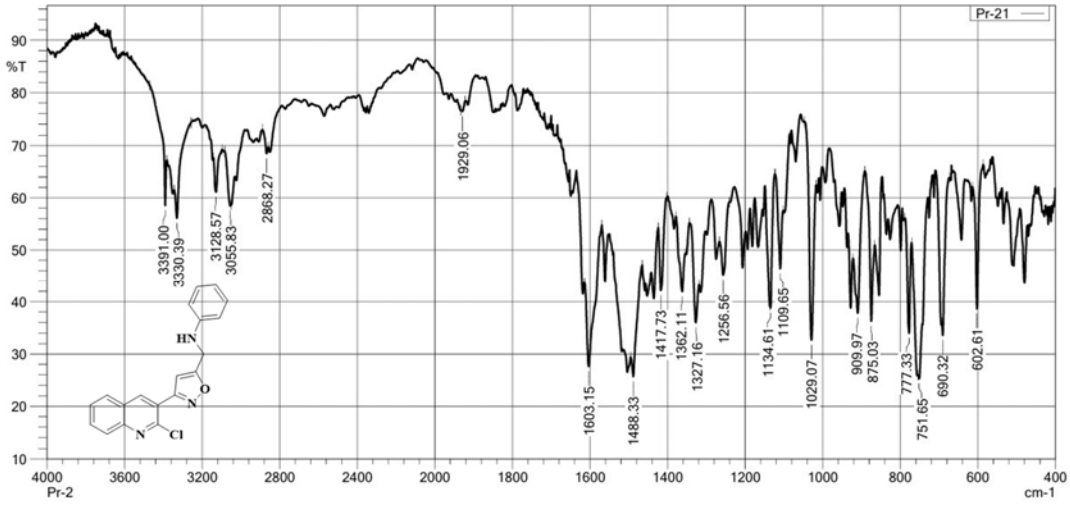

Figure 13: IR spectra of compound **6b**

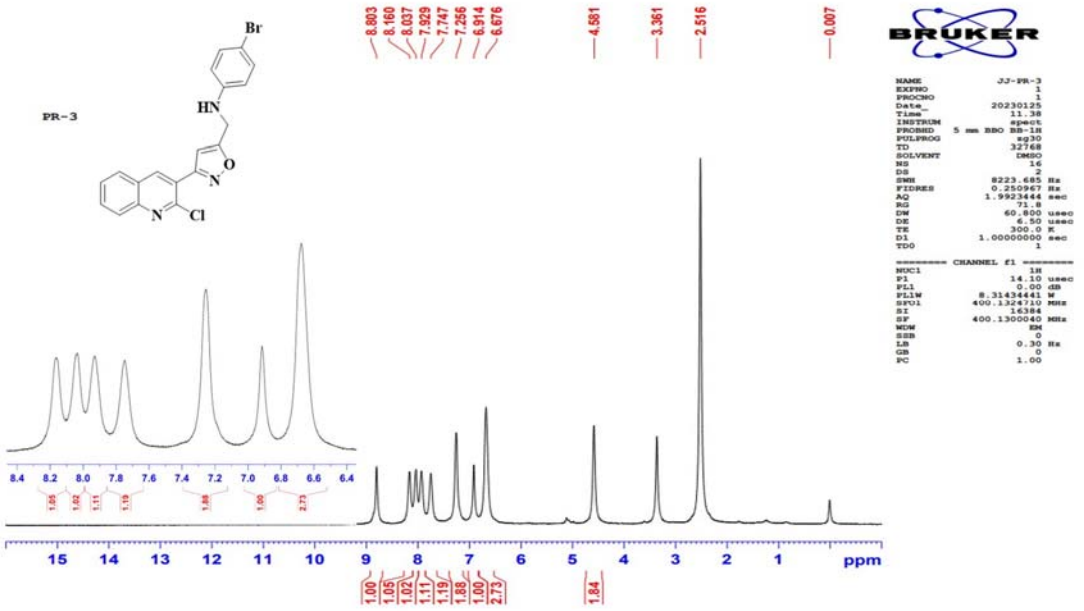

Figure 14: [1]H NMR of compound **6c**

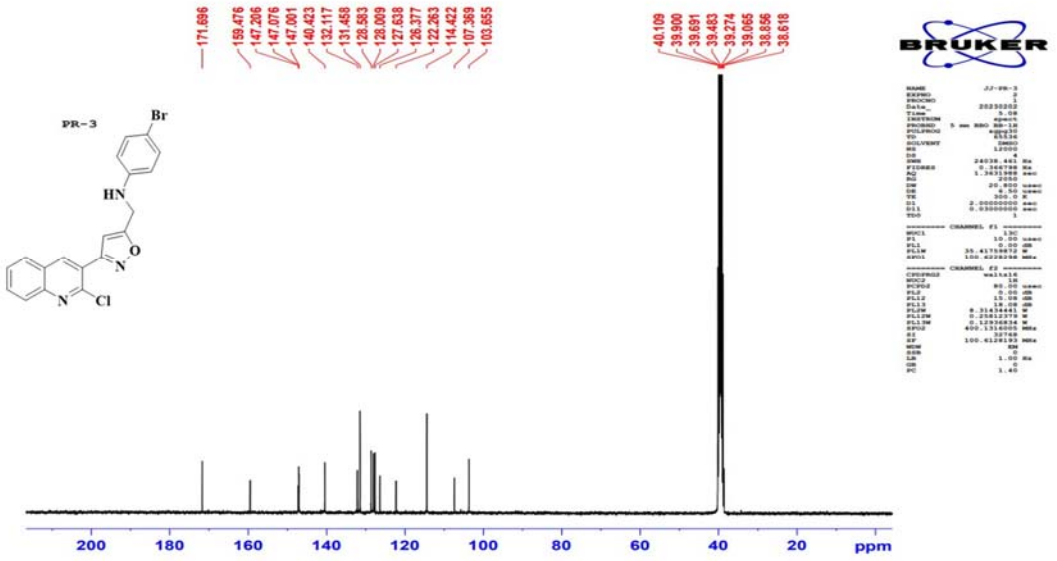

Figure 15: [13]C NMR of compound **6c**

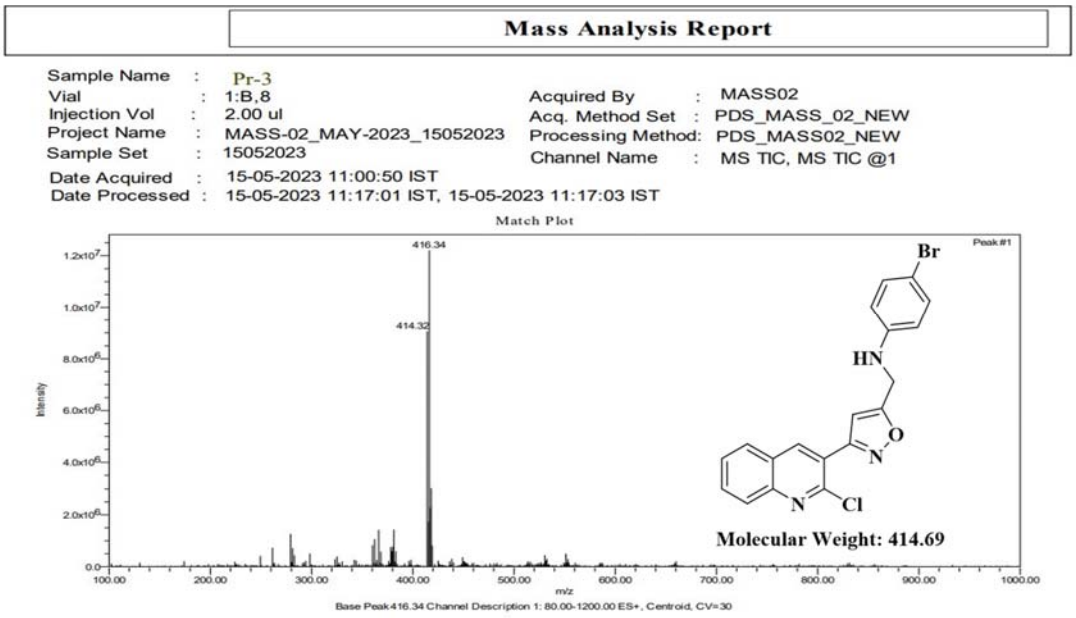

Figure 16: Mass spectra of compound **6c**

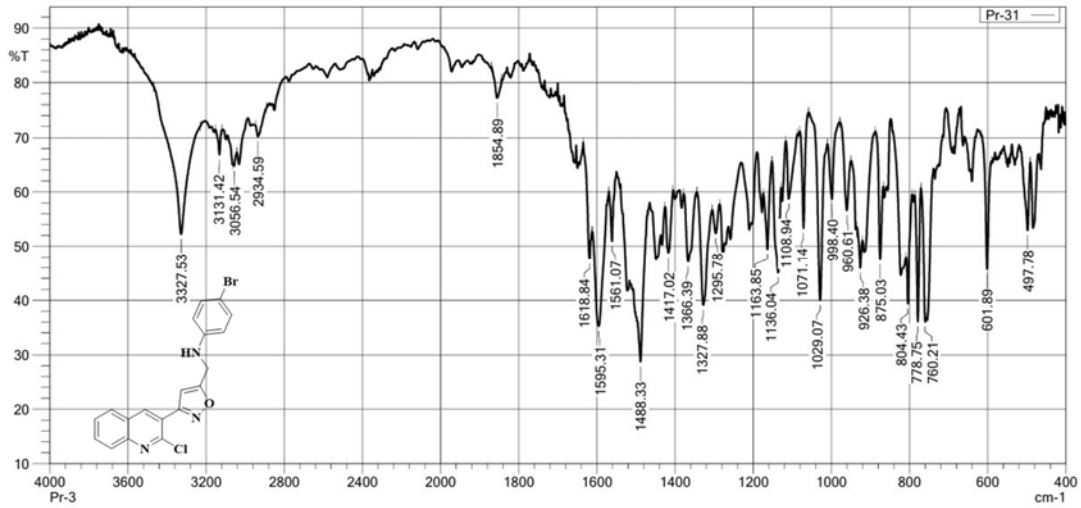

Figure 17: IR spectra of compound **6c**

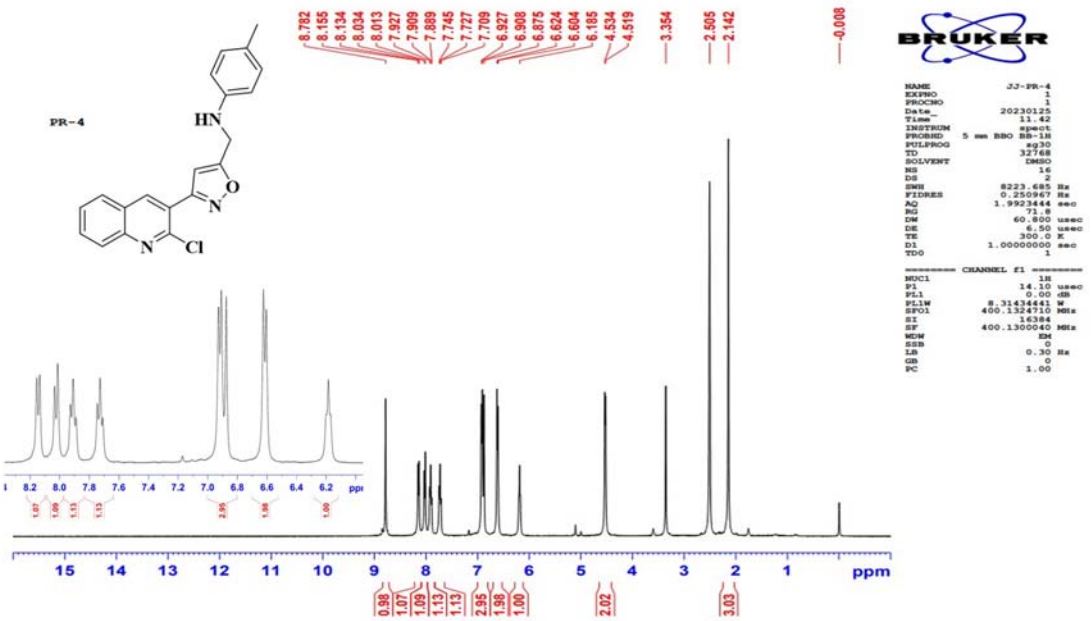

Figure 18: ^{1}H NMR of compound **6d**

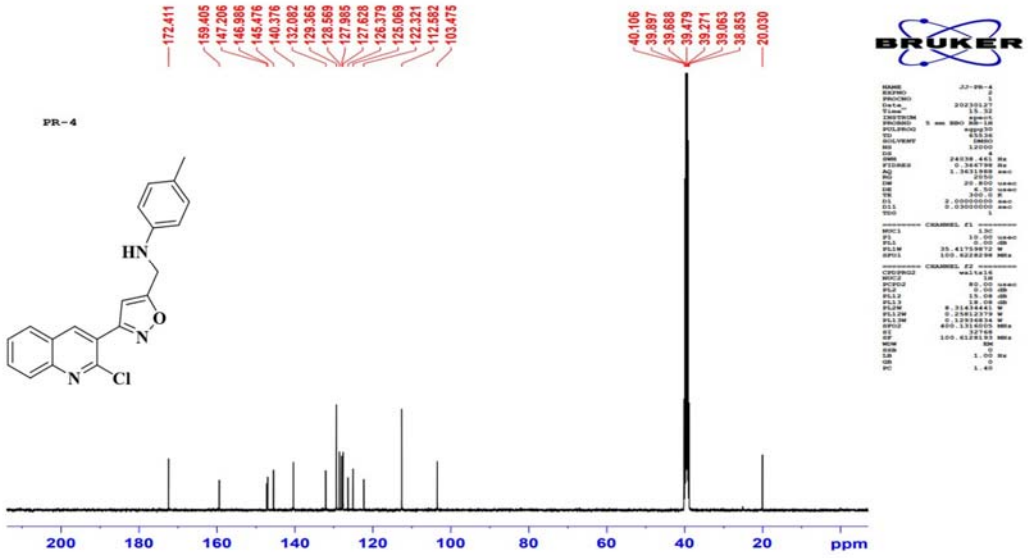

Figure 19: ^{13}C NMR of compound **6d**

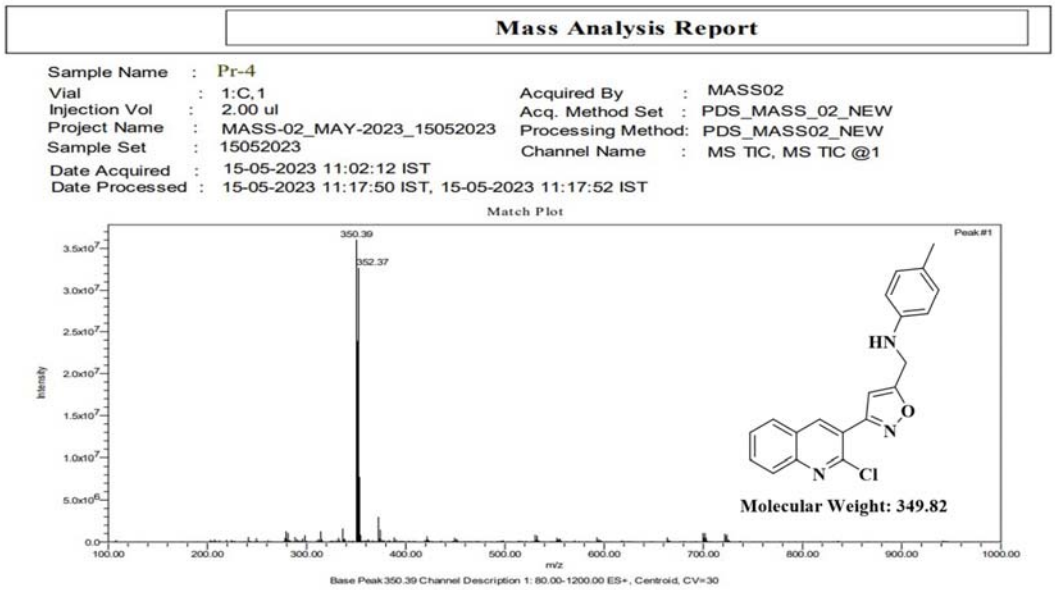

Figure 20: Mass spectra of compound **6d**

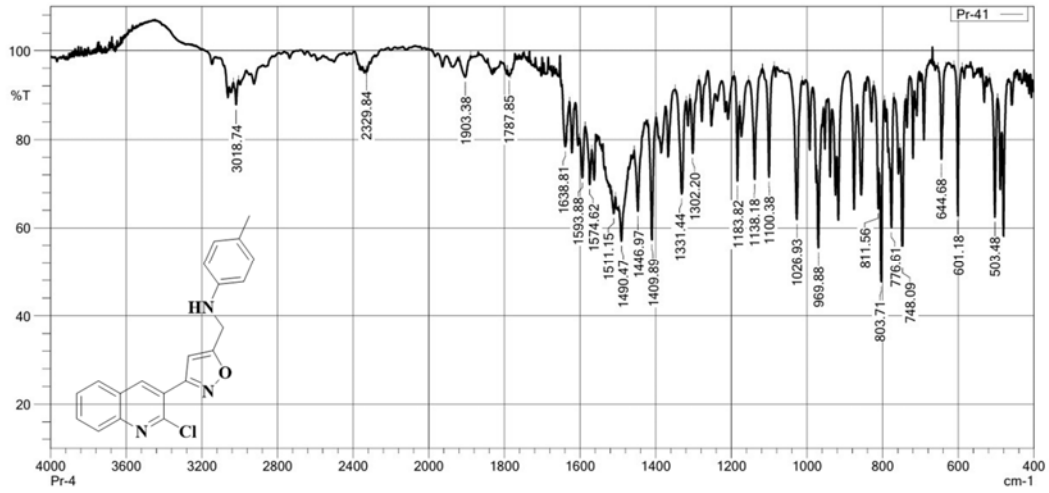

Figure 21: IR spectra of compound **6d**

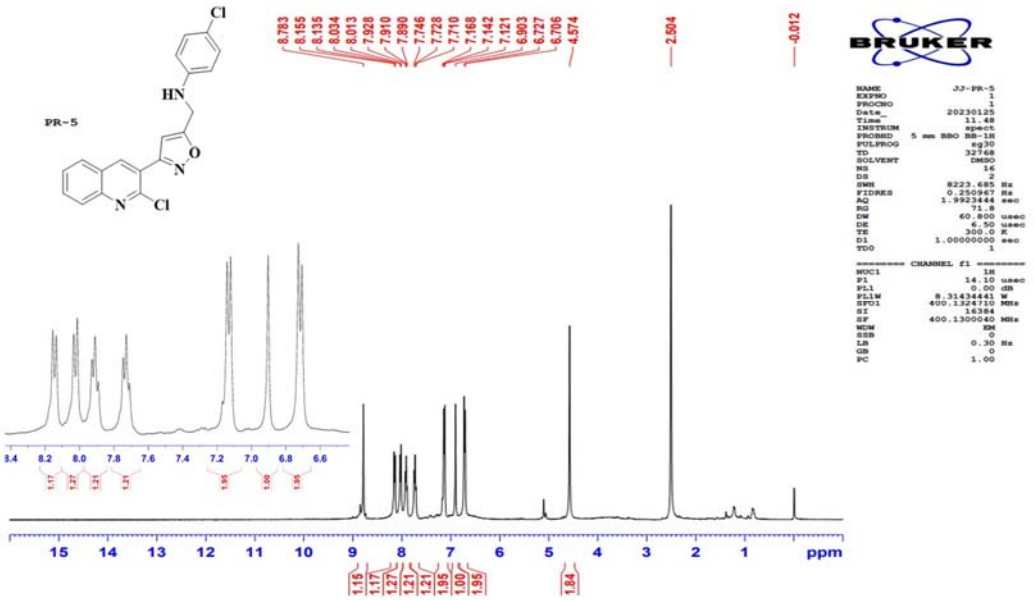

Figure 22: ^{1}H NMR of compound **6e**

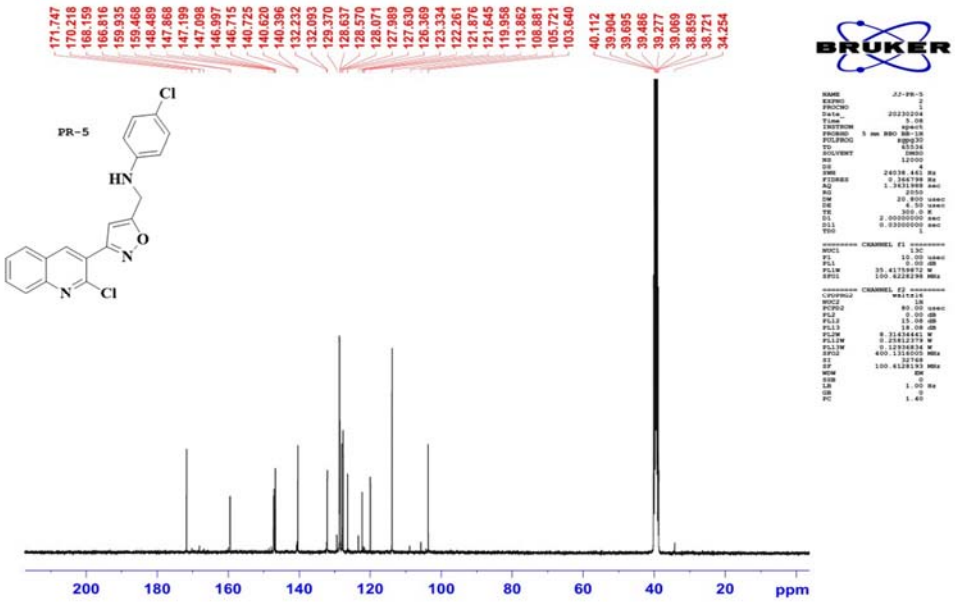

Figure 23: ^{13}C NMR of compound **6e**

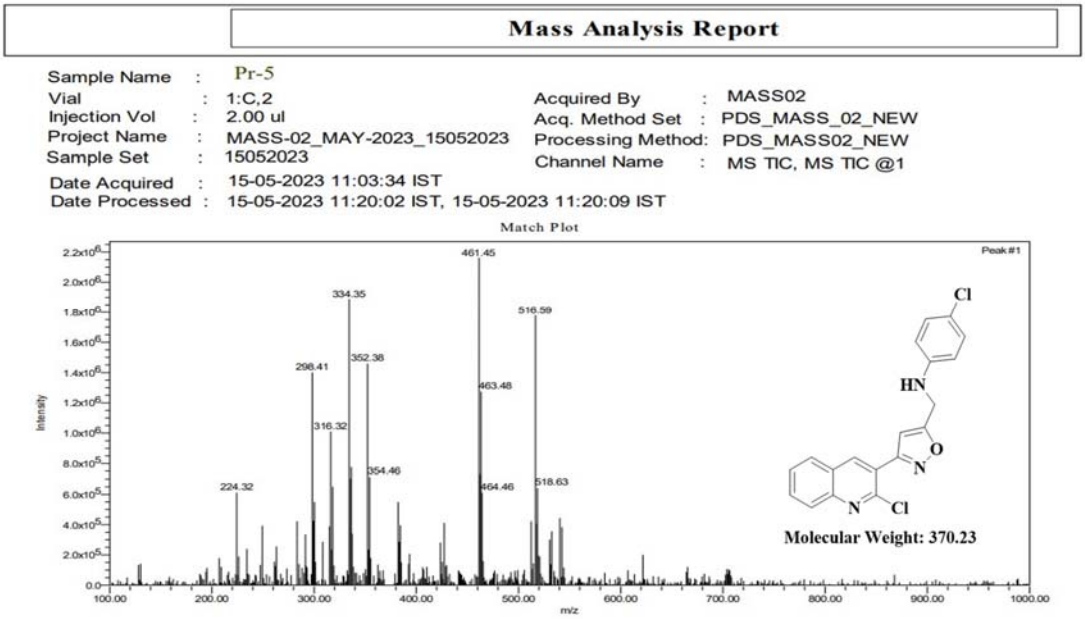

Figure 24: Mass spectra of compound **6e**

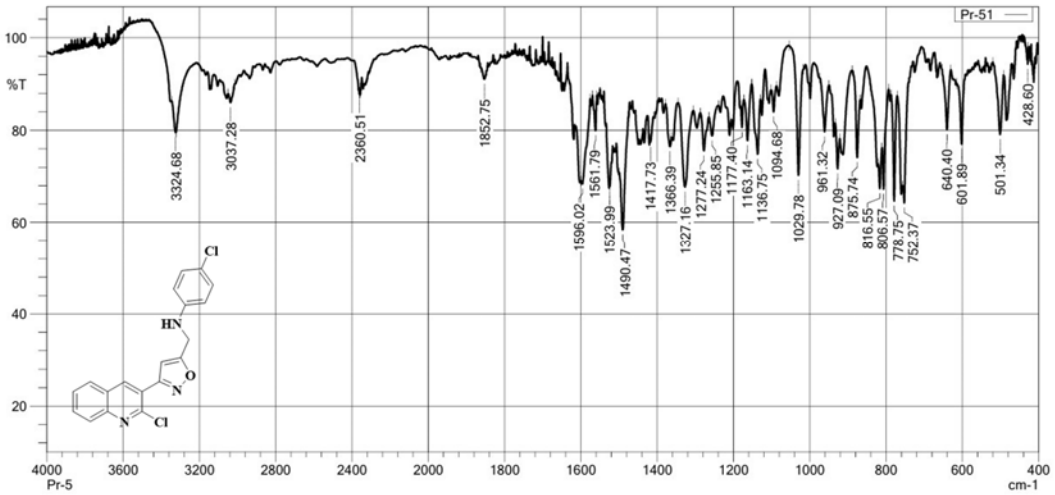

Figure 25: IR spectra of compound **6e**

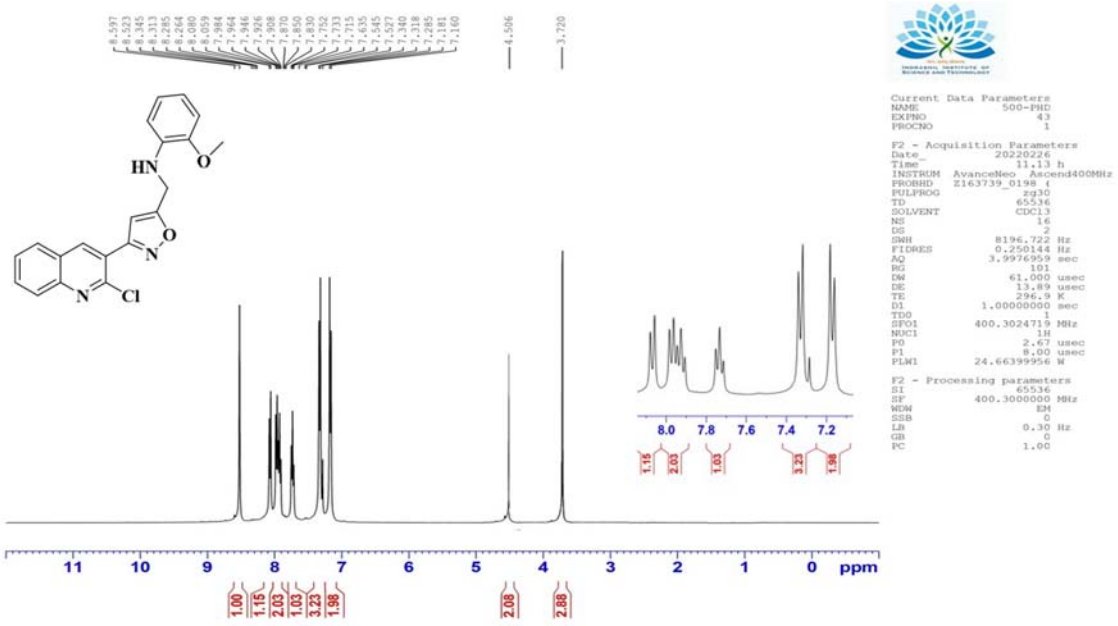

Figure 26: ^{1}H NMR of compound **6f**

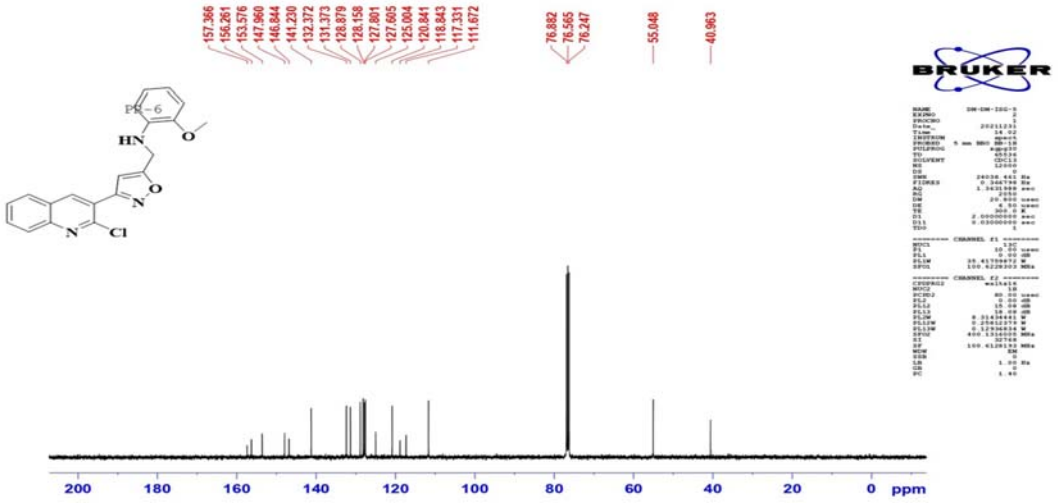

Figure 27: ^{13}C NMR of compound **6f**

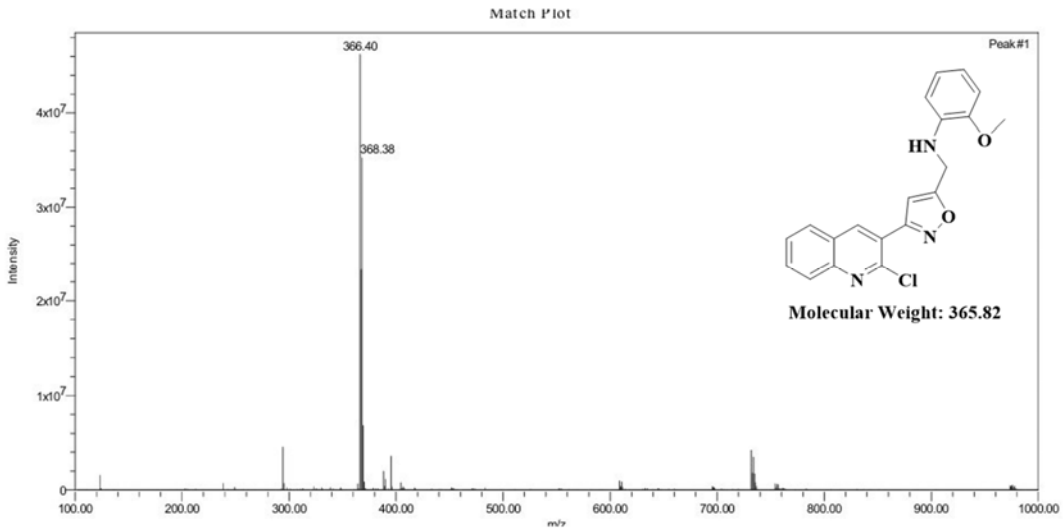

Figure 28: Mass spectra of compound **6f**

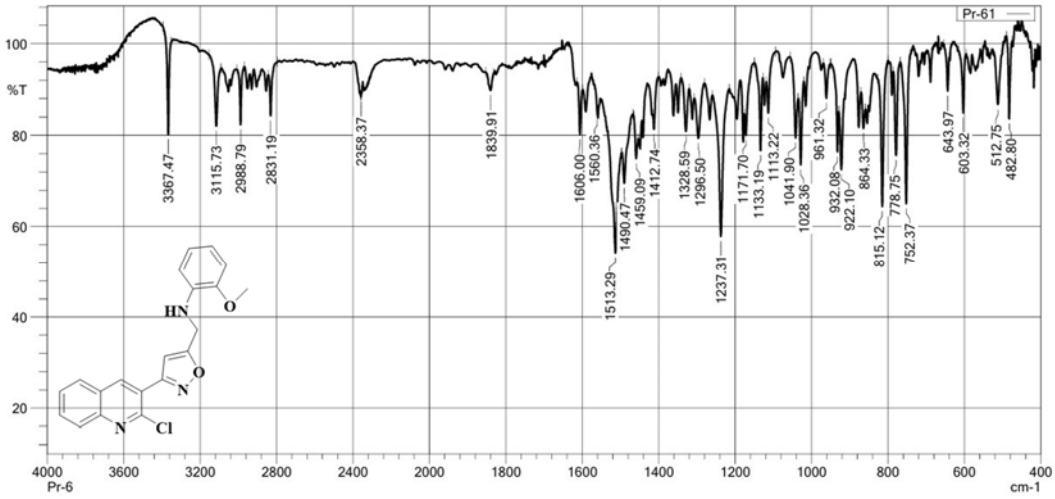

Figure 29: IR spectra of compound **6f**

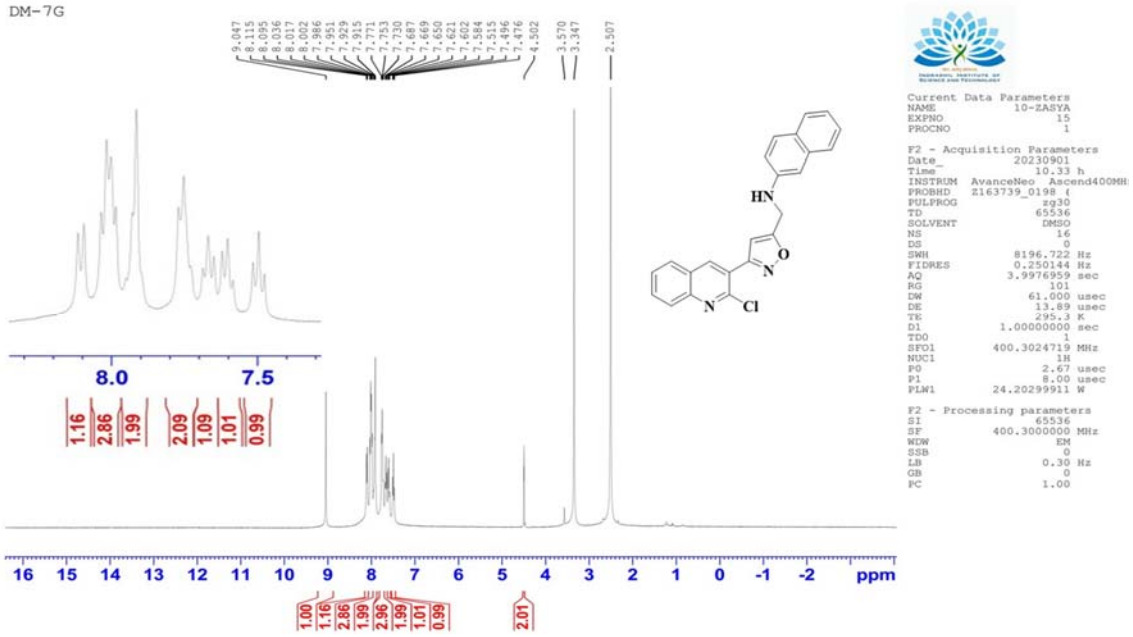

Figure 30: ^{1}H NMR of compound **6g**

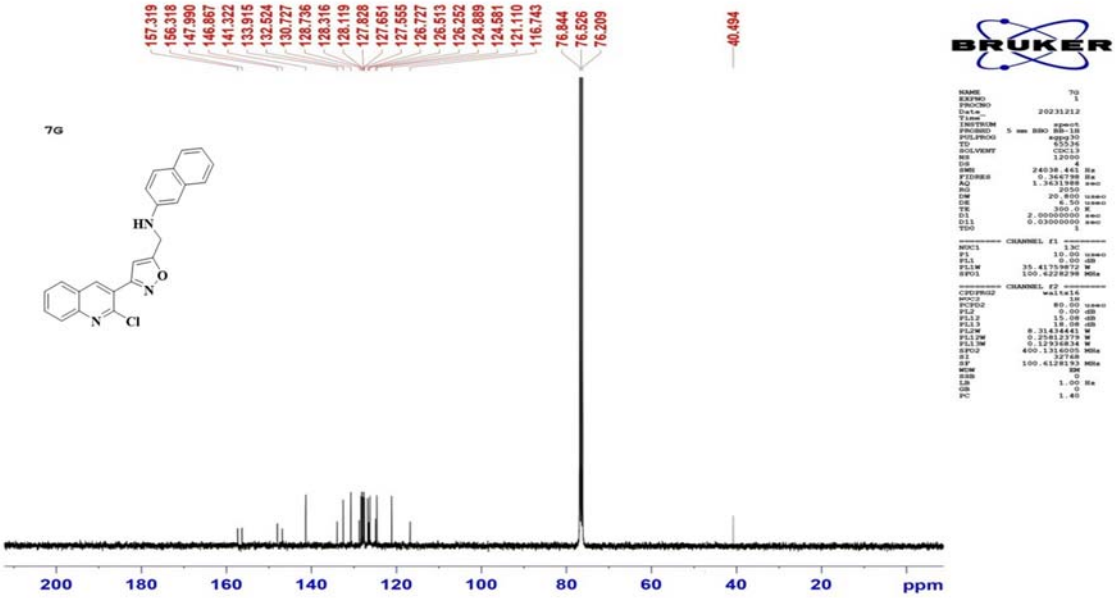

Figure 31: ^{13}C NMR of compound **6g**

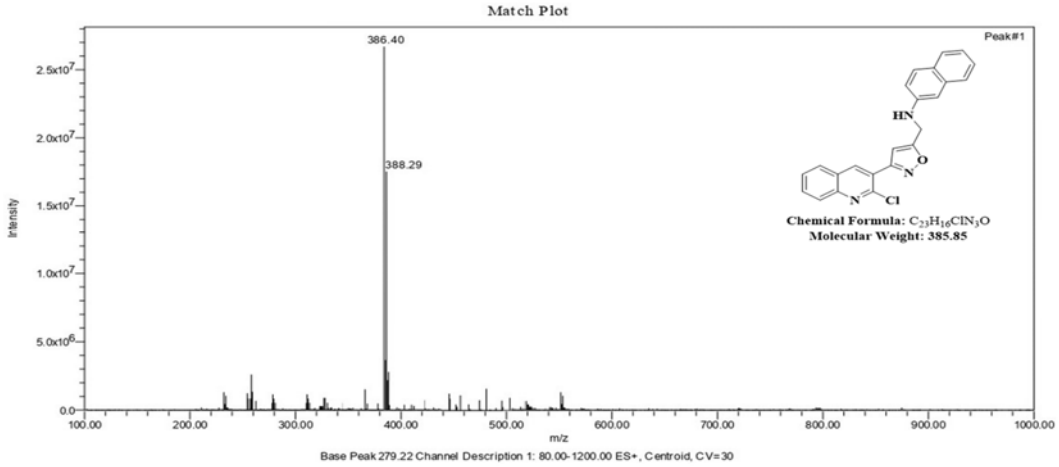

Figure 32: Mass spectra compound **6g**

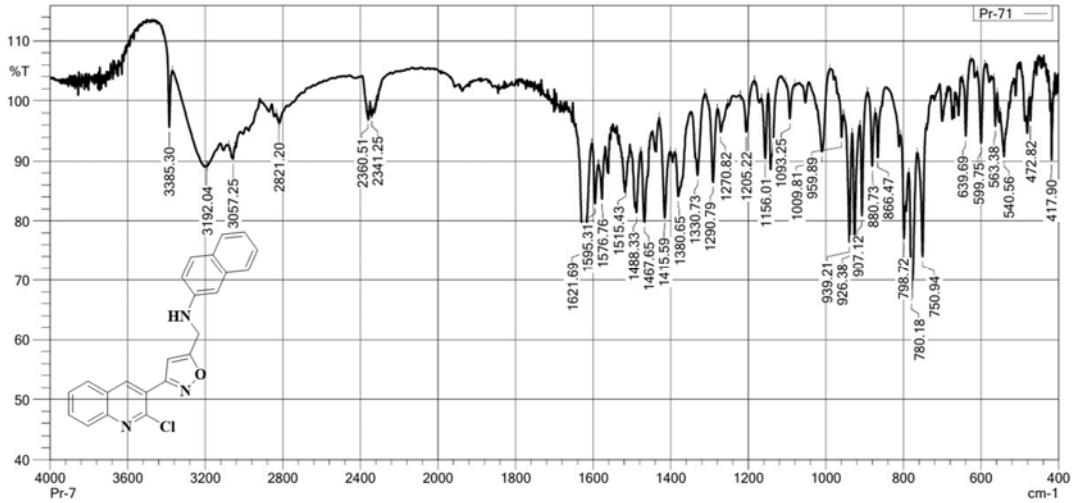

Figure 33: IR spectra of compound **6g**

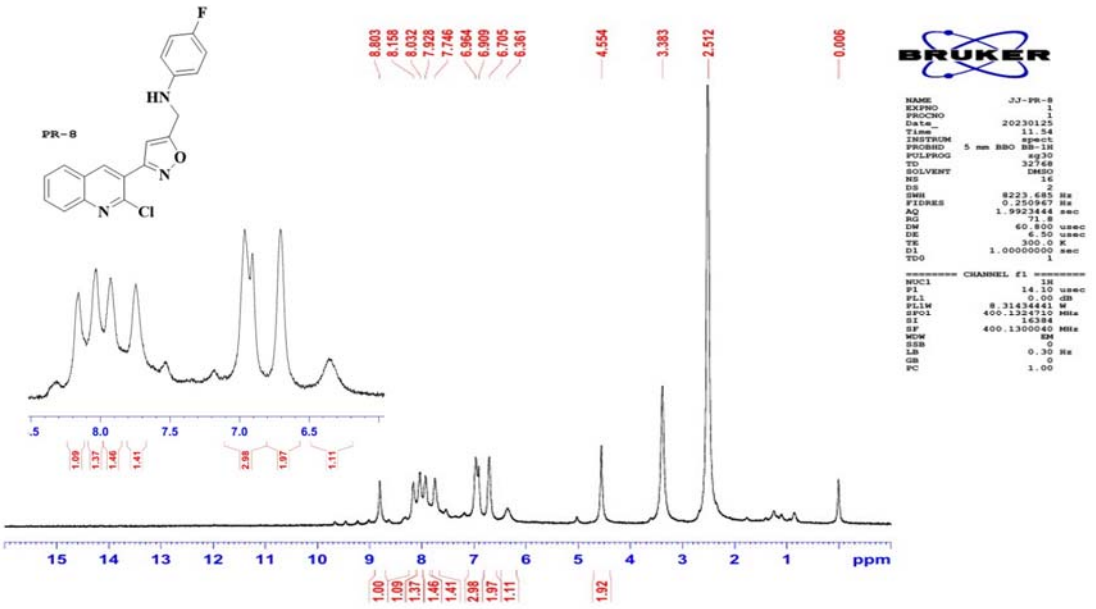

Figure 34: [1]H NMR of compound **6h**

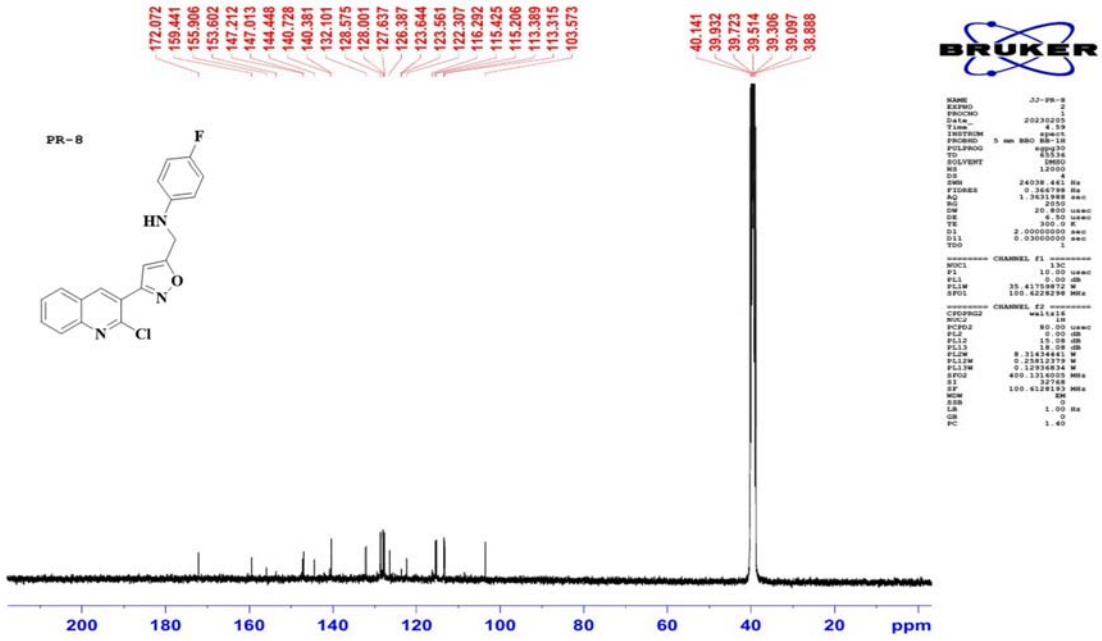

Figure 35: [13]C NMR of compound **6h**

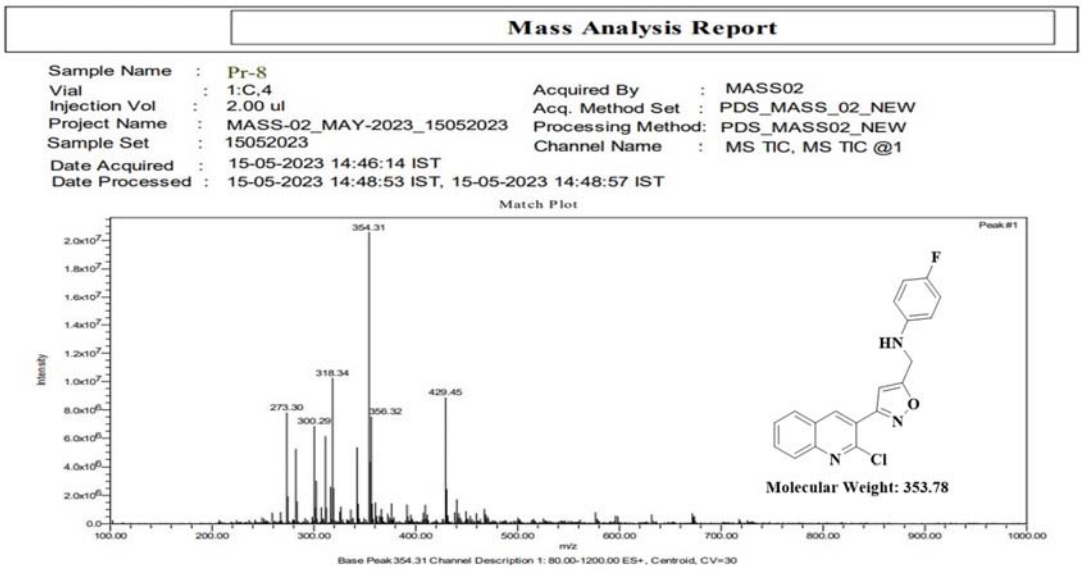

Figure 36: Mass spectra of compound **6h**

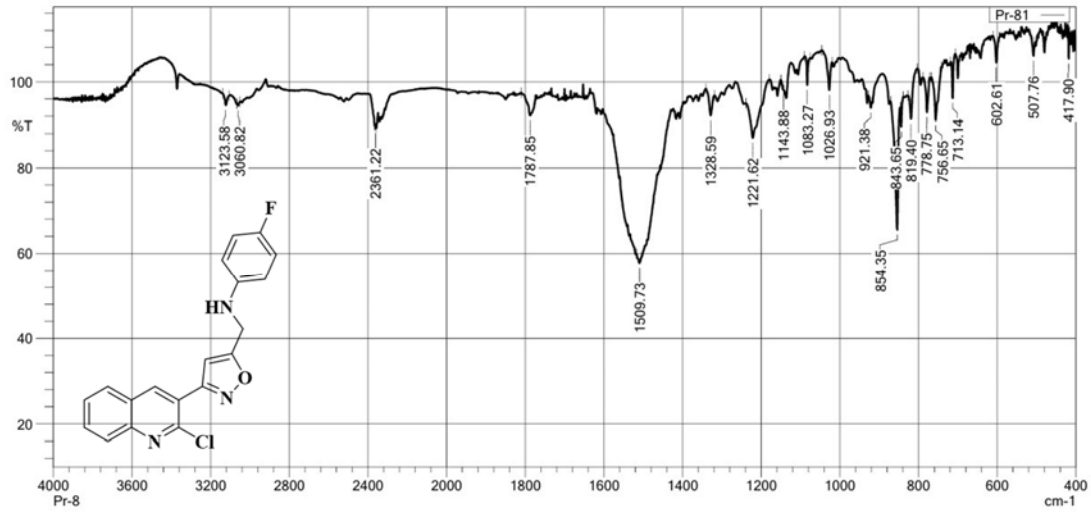

Figure 37: IR spectra of compound **6h**

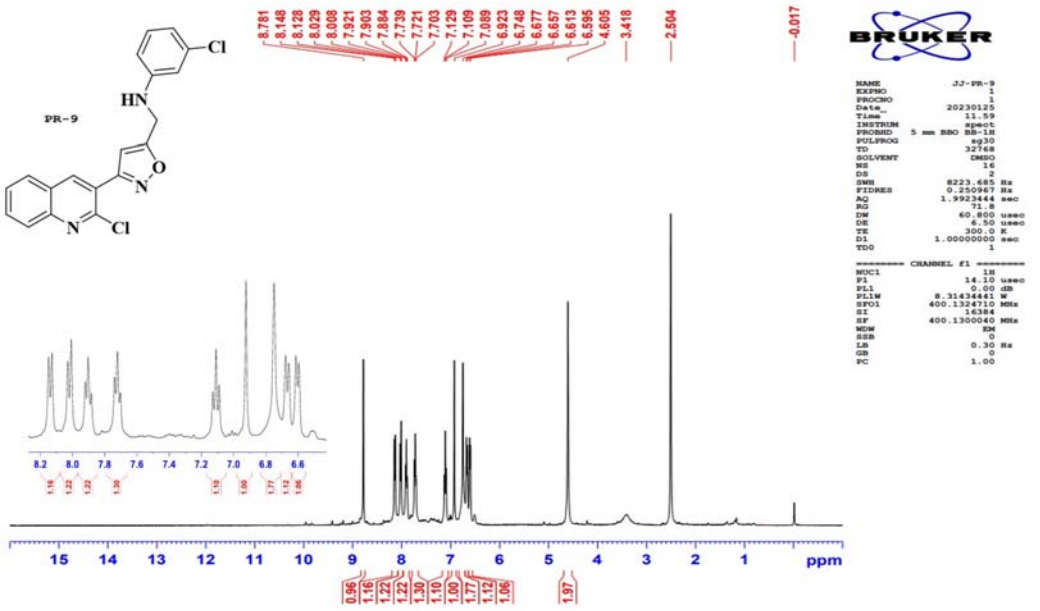

Figure 38: ^{1}H NMR of compound **6i**

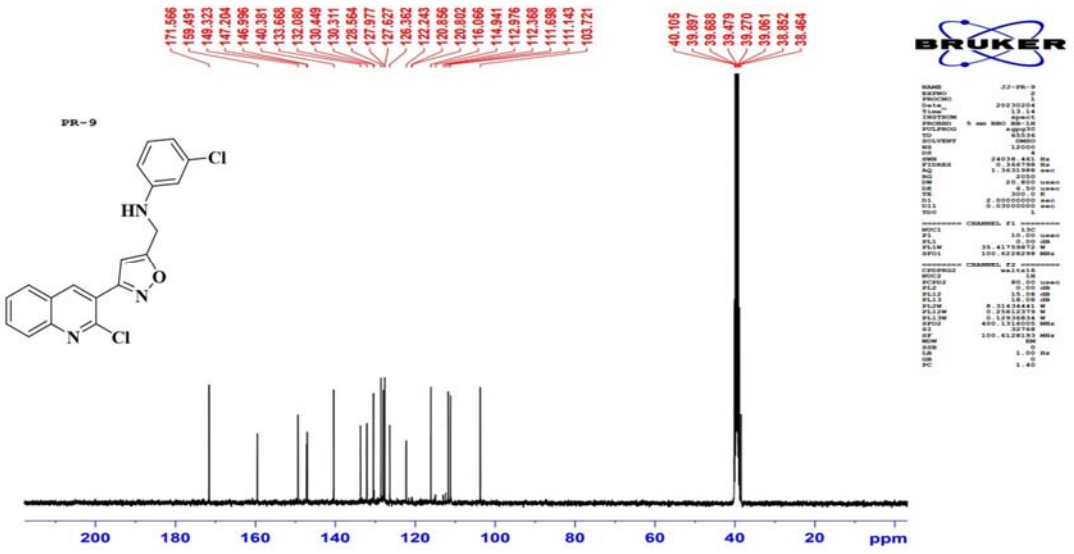

Figure 39: ^{13}C NMR of compound **6i**

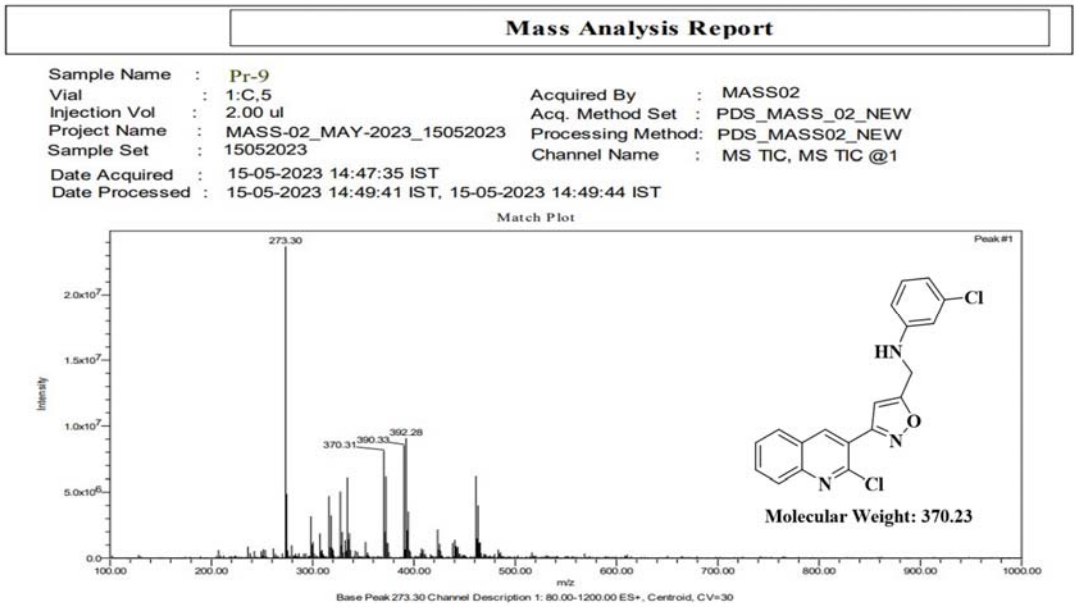

Figure 40: Mass spectra of compound **6i**

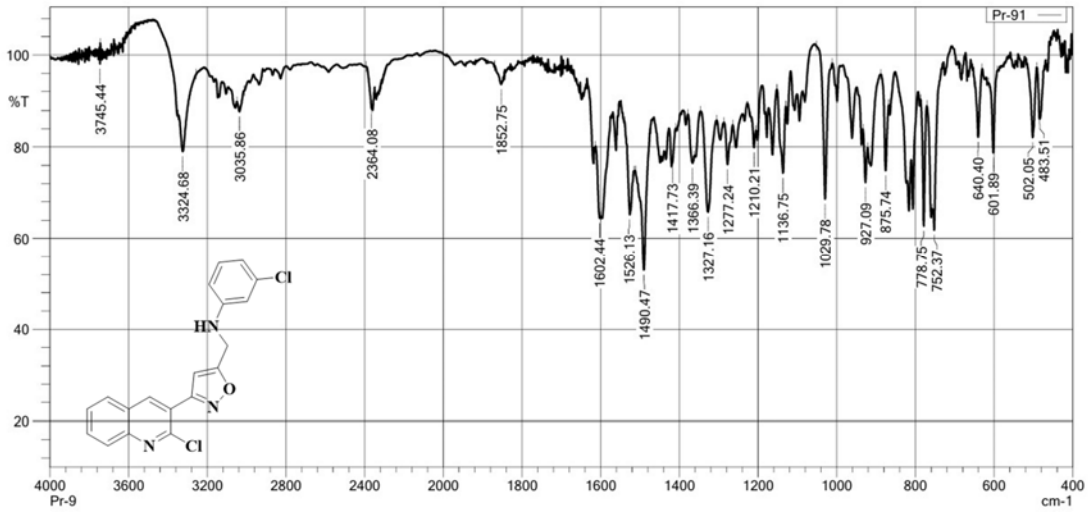

Figure 41: IR spectra of compound **6i**

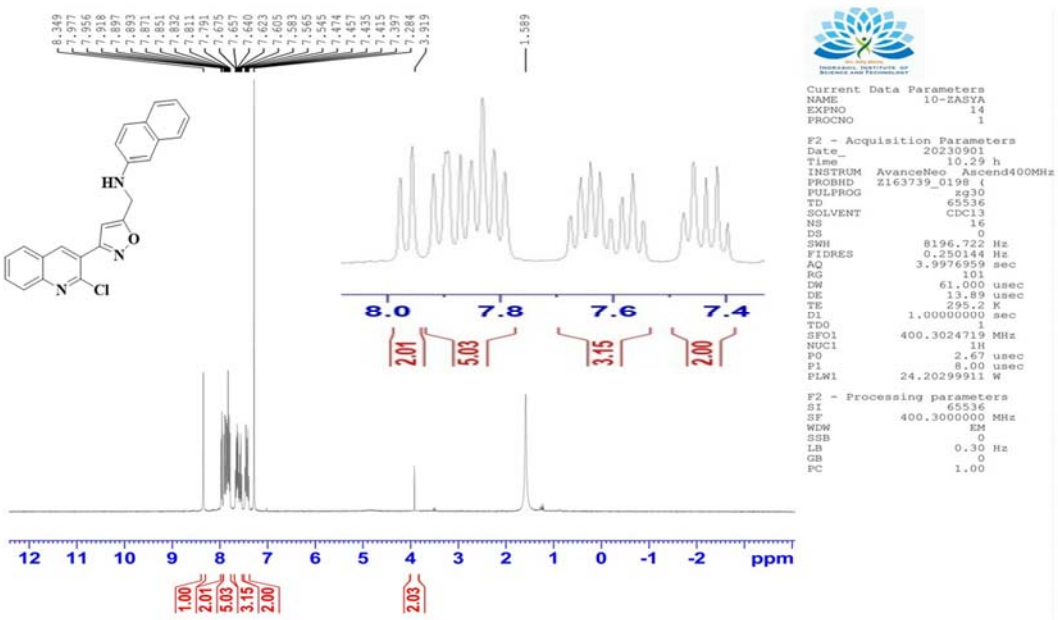

Figure 42: ^{1}H NMR of compound **6j**

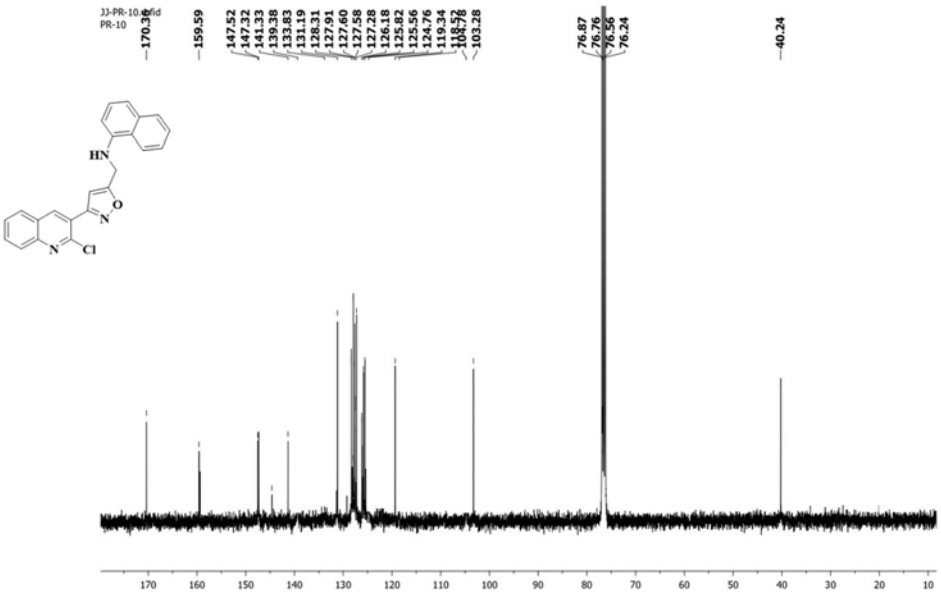

Figure 43: ^{13}C NMR of compound **6j**

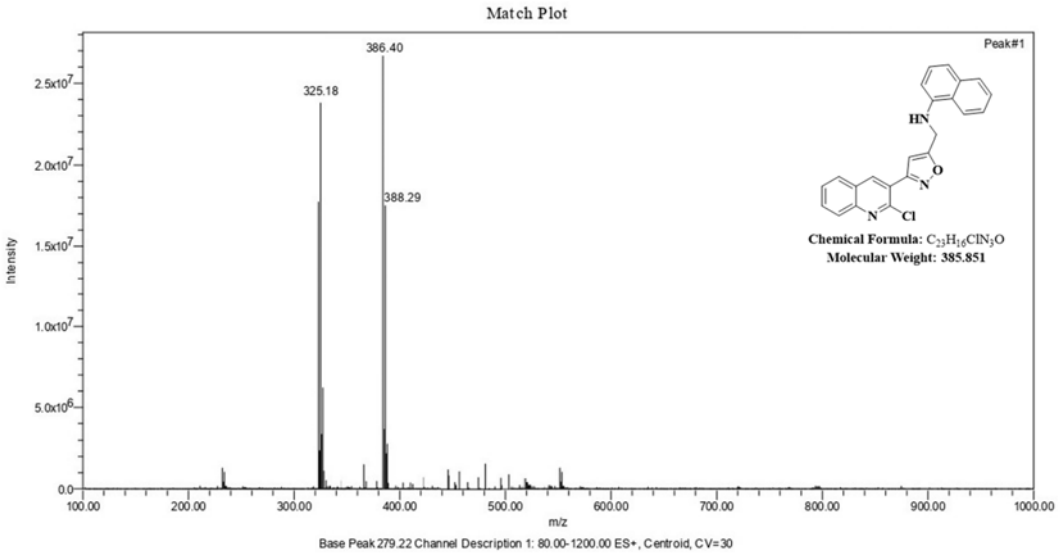

Figure 44: Mass spectra of compound **6j**

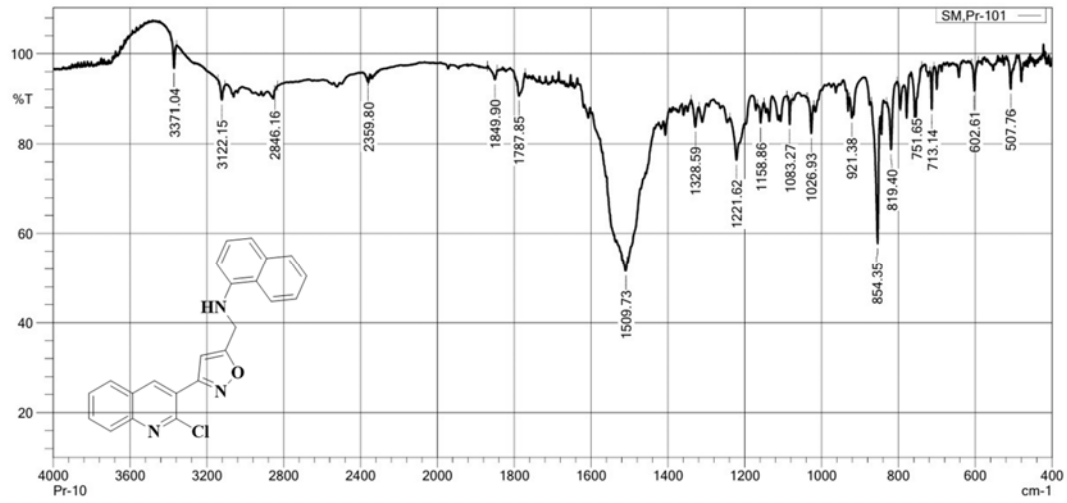

Figure 45: IR spectra of compound **6j**

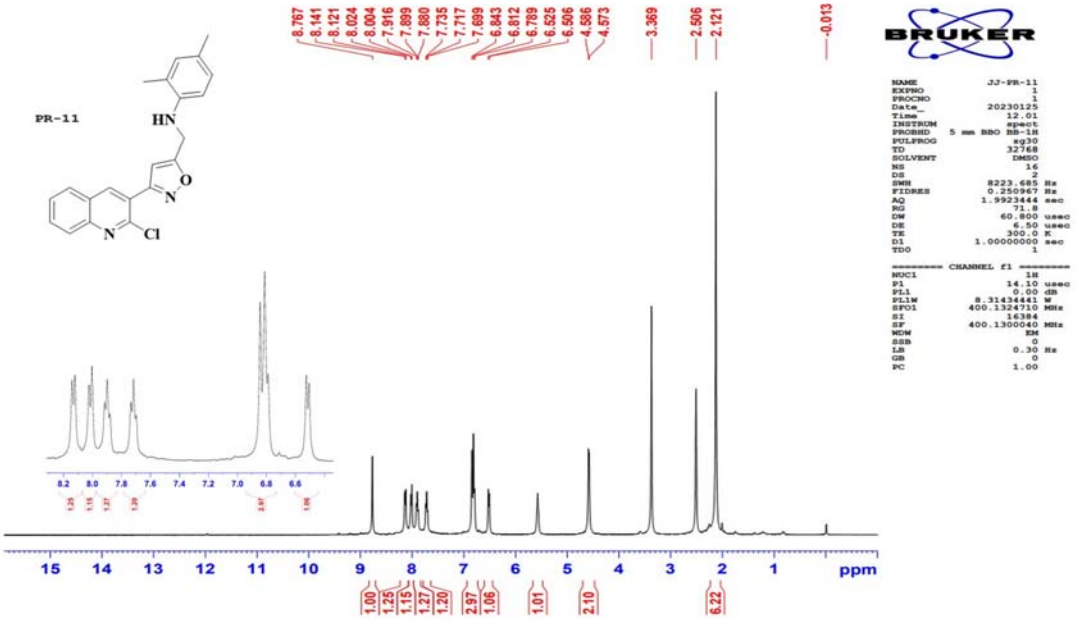

Figure 46: ^{1}H NMR of compound **6k**

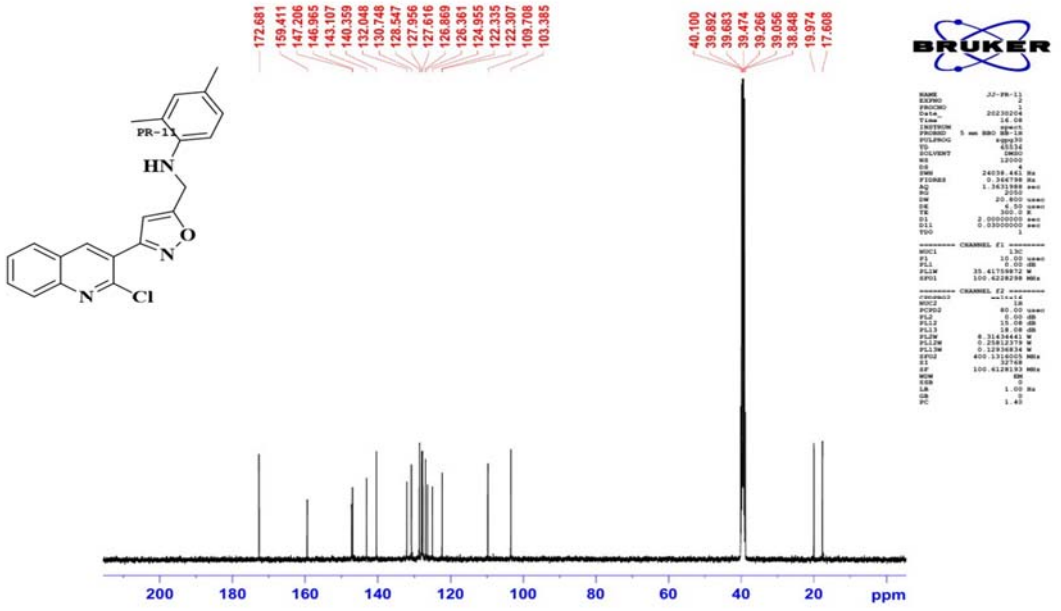

Figure 47: ^{13}C NMR of compound **6k**

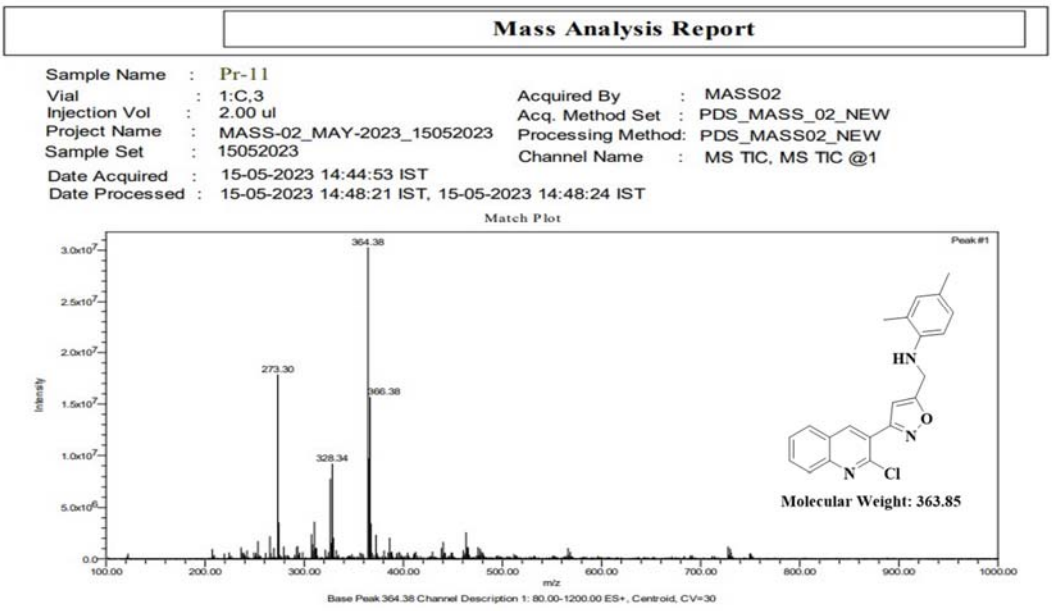

Figure 48: Mass spectra of compound **6k**

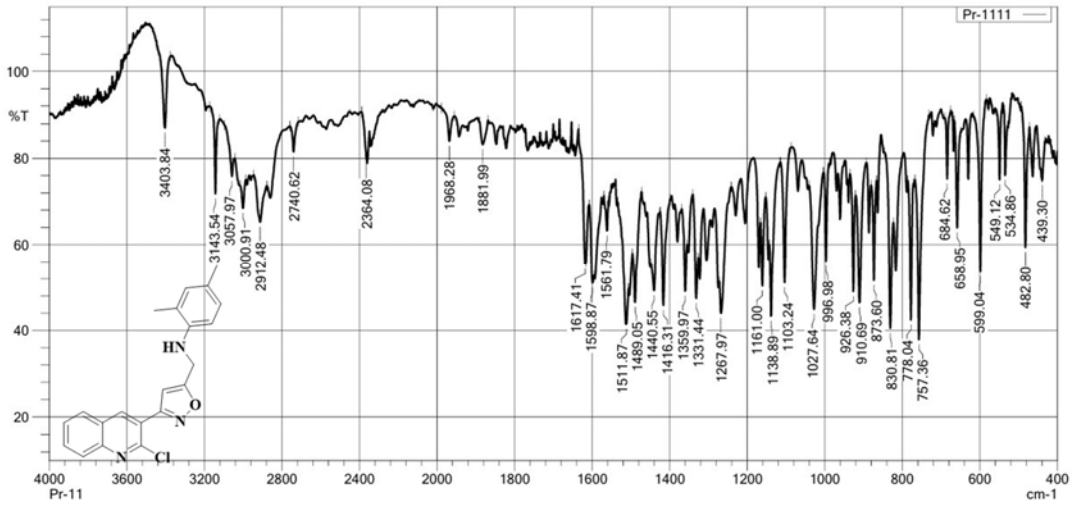

Figure 49: IR spectra of compound **6k**

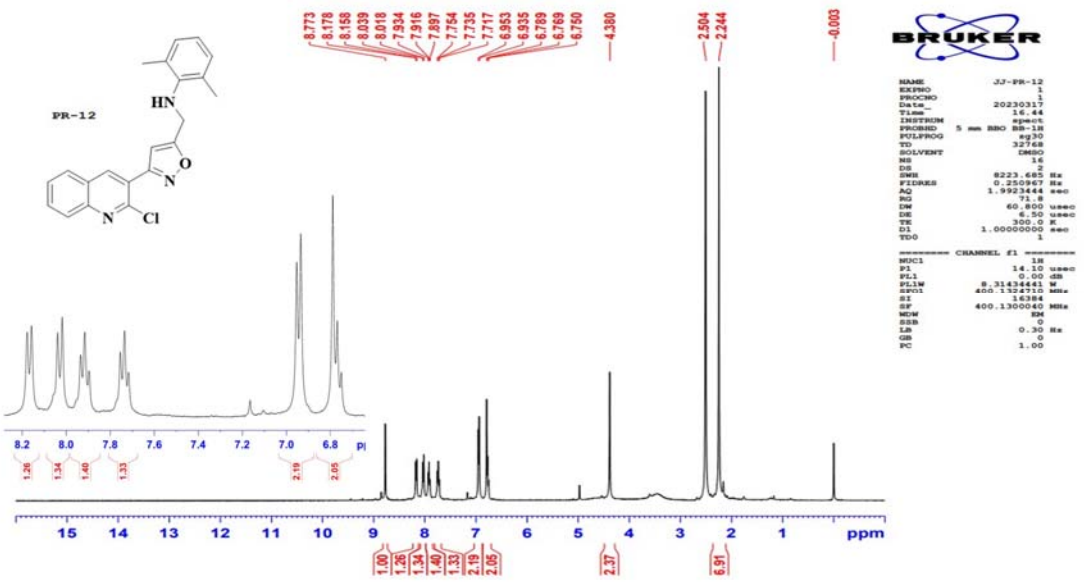

Figure 50: ^{1}H NMR of compound **6l**

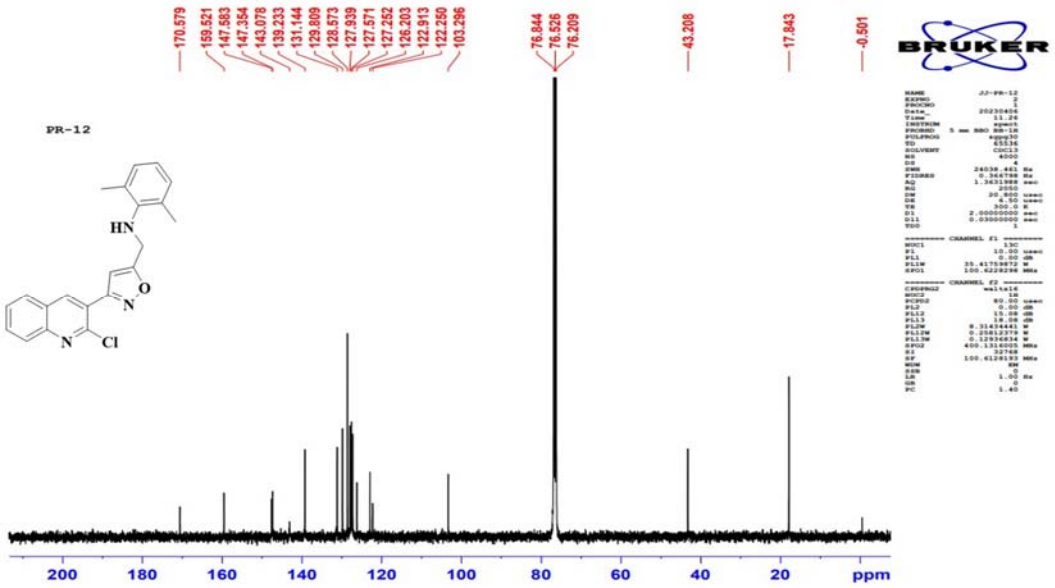

Figure 51: ^{13}C NMR of compound **6l**

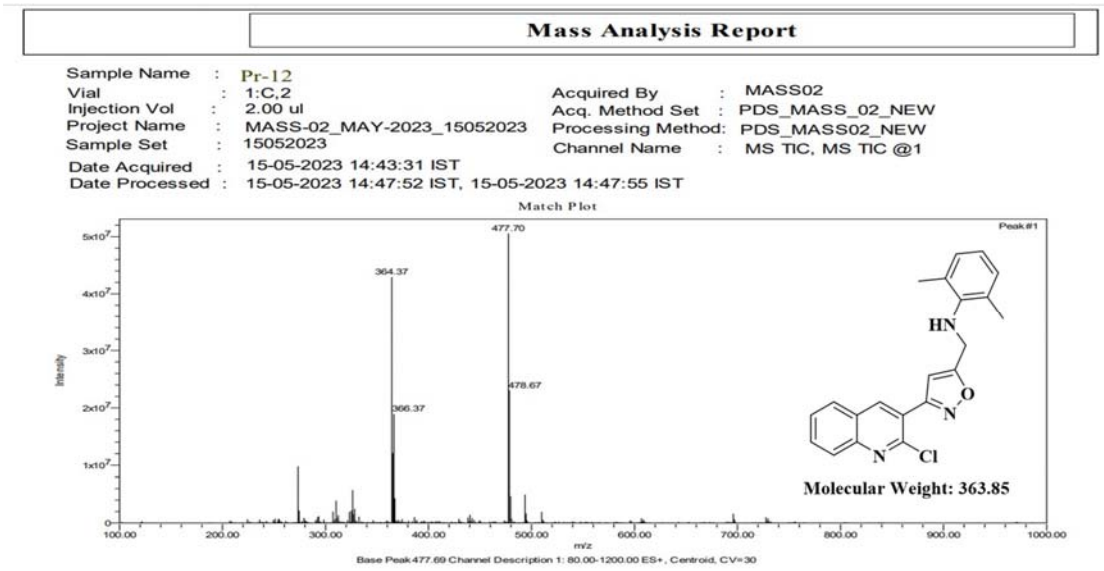

Figure 52: Mass spectra of compound **6l**

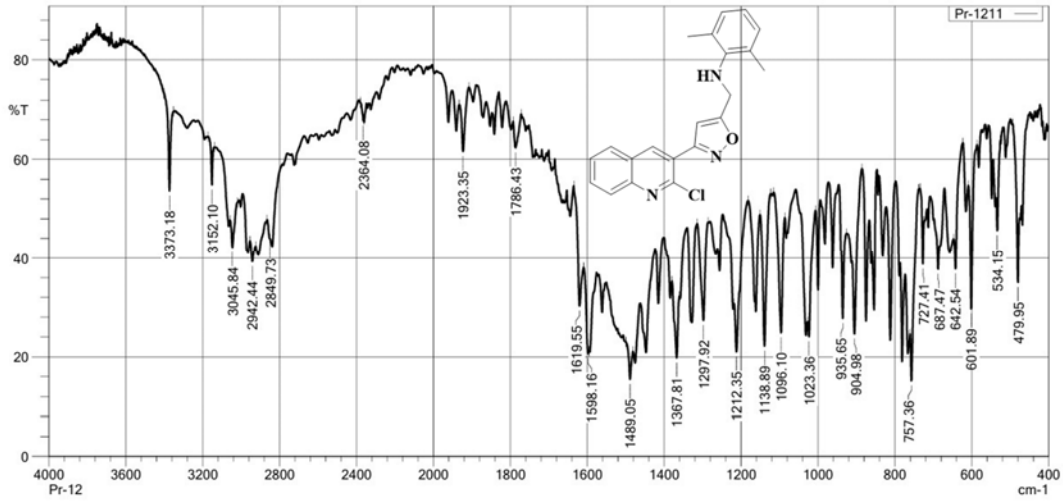

Figure 53: IR spectra of compound **6l**

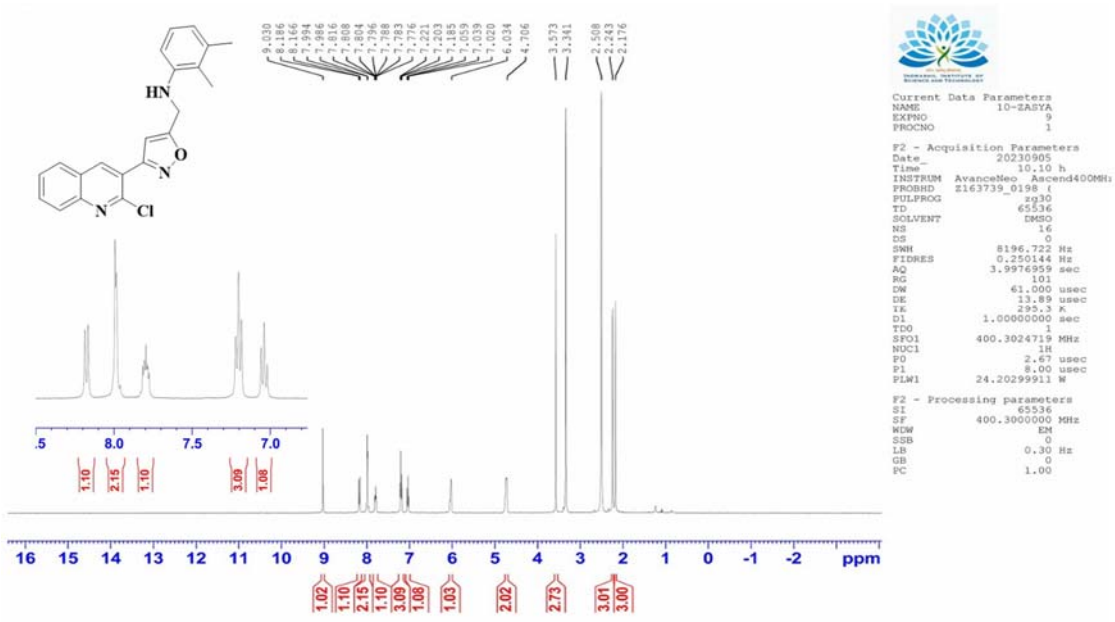

Figure 54: ^{1}H NMR of compound **6m**

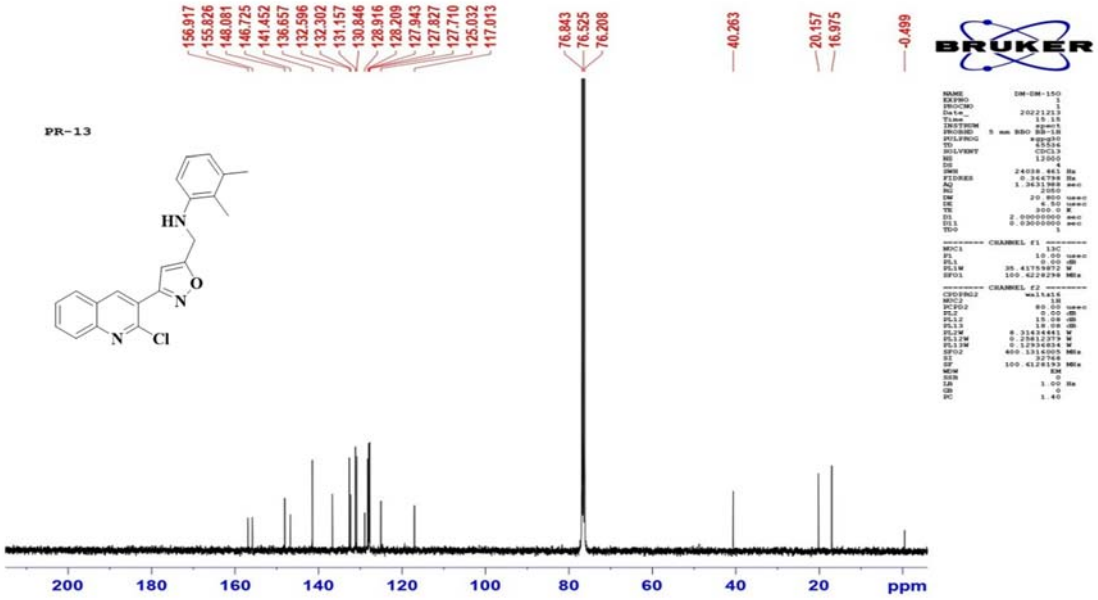

Figure 55: ^{13}C NMR of compound **6m**

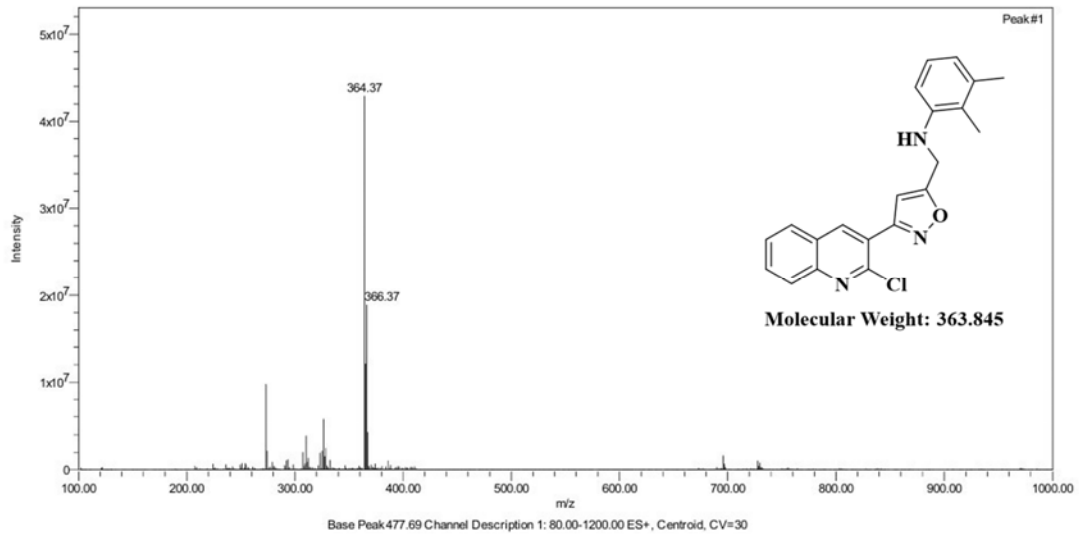

Figure 56: Mass spectra of compound **6m**

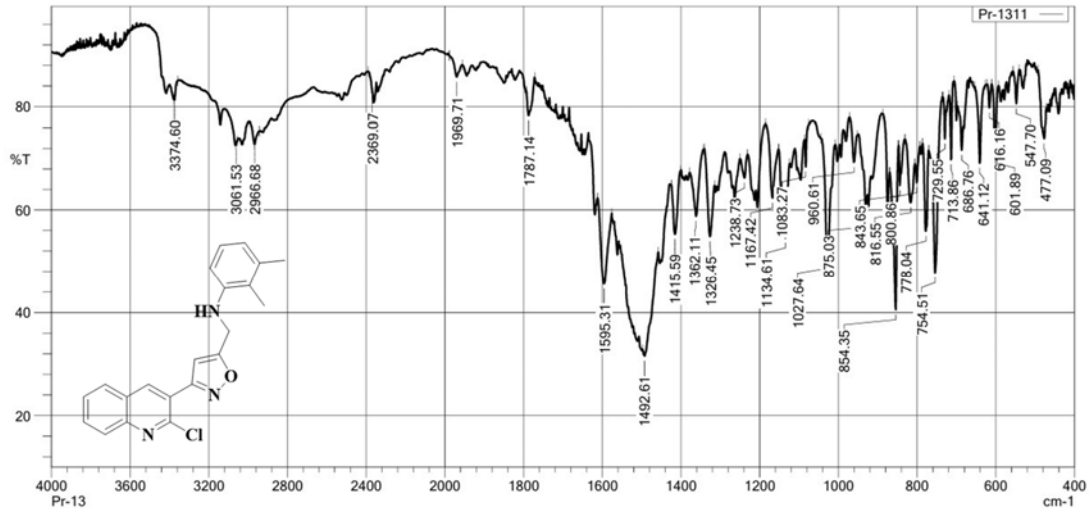

Figure 57: IR spectra of compound **6m**

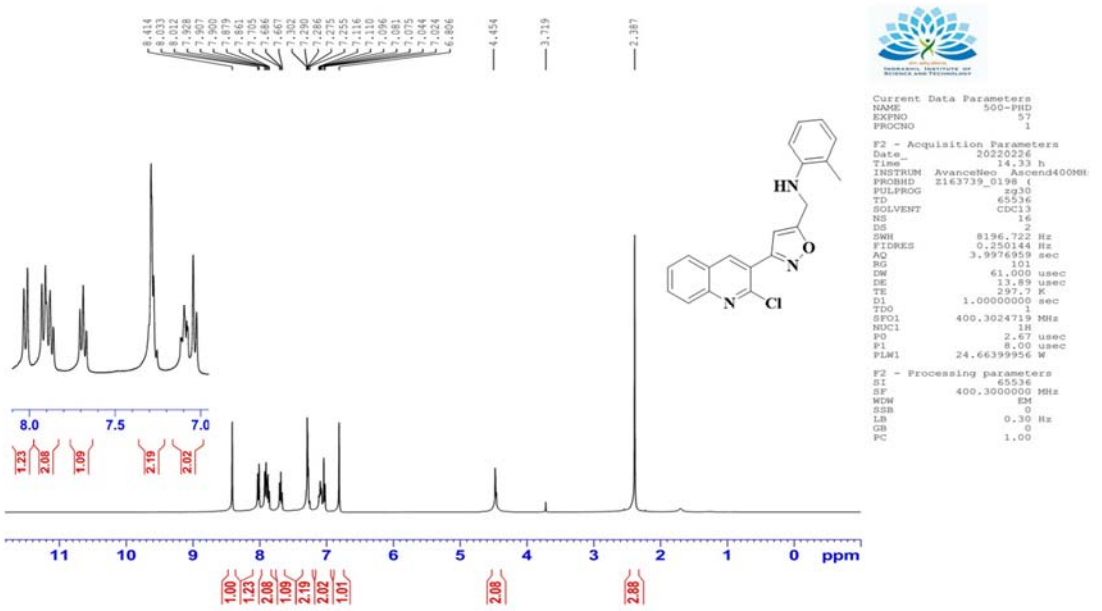

Figure 58: ^{1}H NMR of compound **6n**

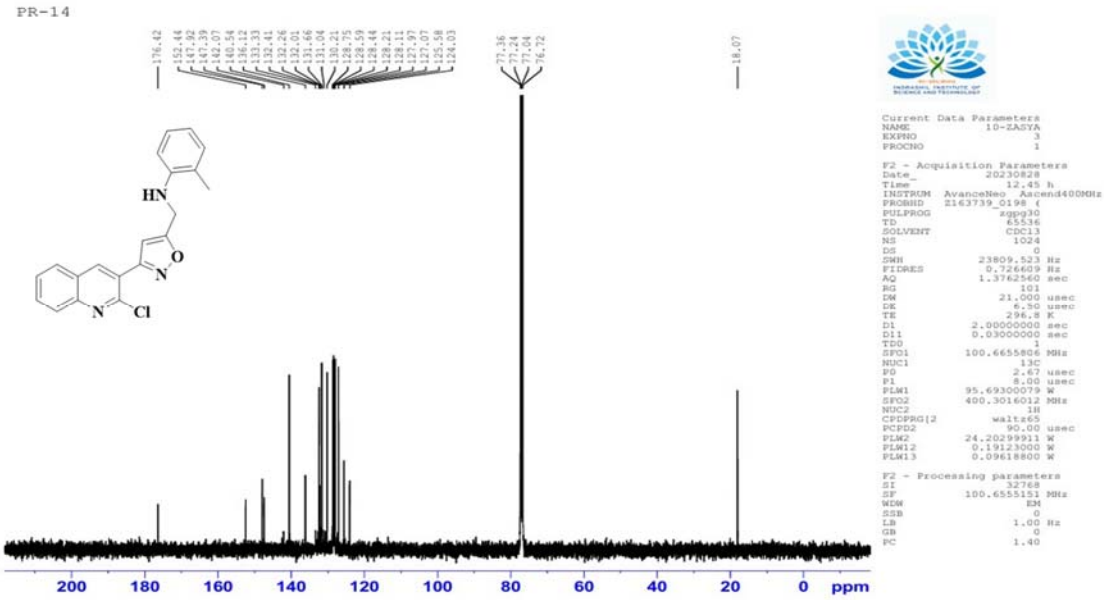

Figure 59: ^{13}C NMR of compound **6n**

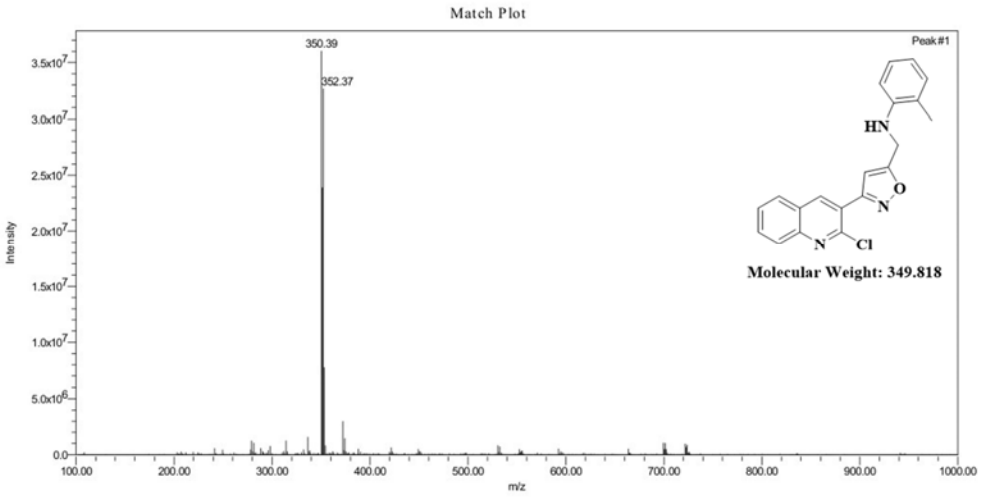

Figure 60: Mass spectra of compound **6n**

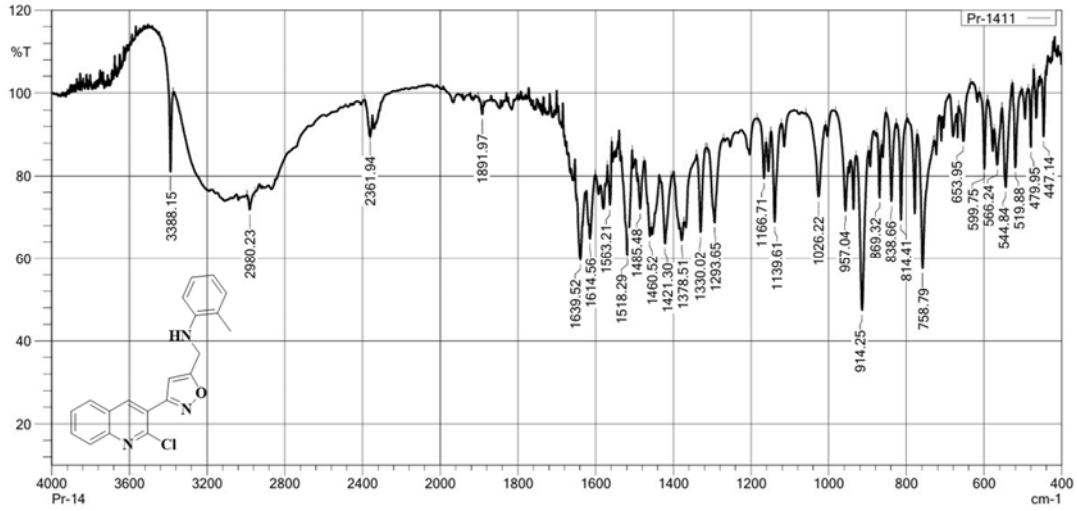

Figure 61: IR spectra of compound **6n**

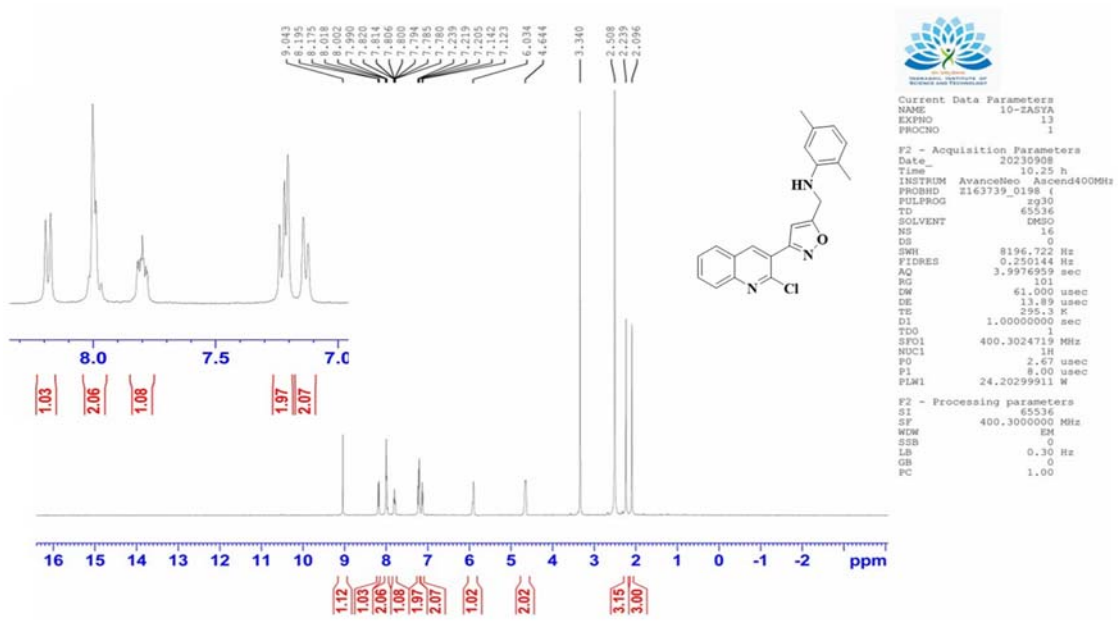

Figure 62: ^{1}H NMR of compound **6o**

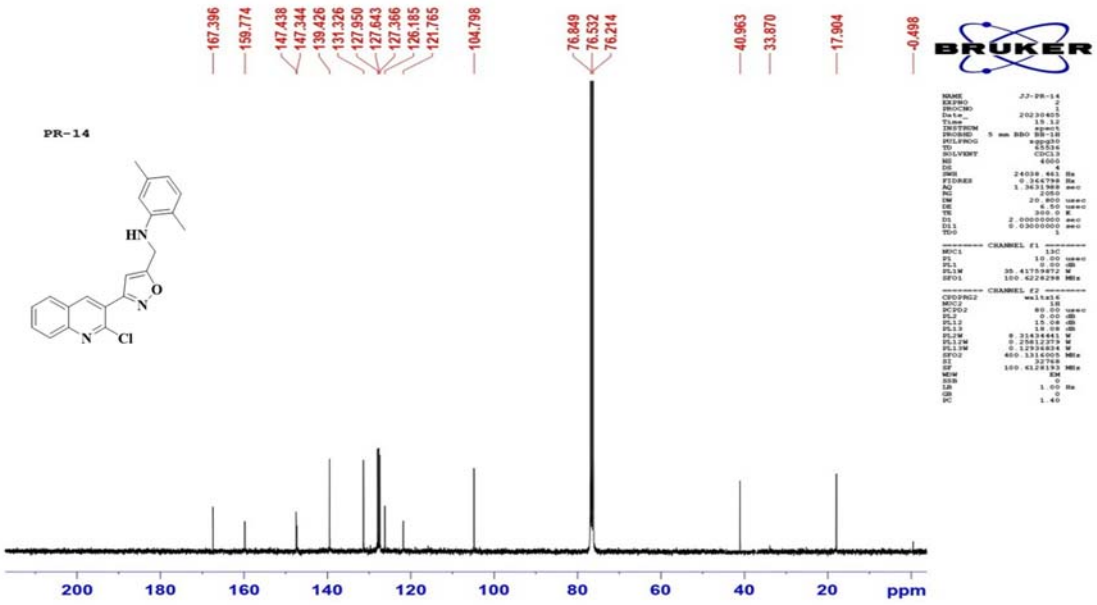

Figure 63: ^{13}C NMR of compound **6o**

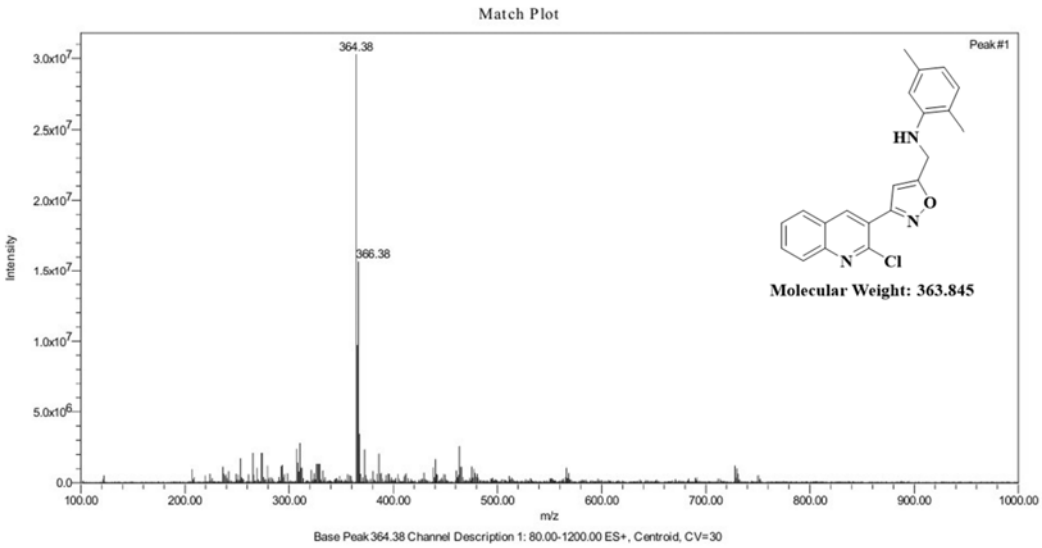

Figure 64: Mass spectra of compound **6o**

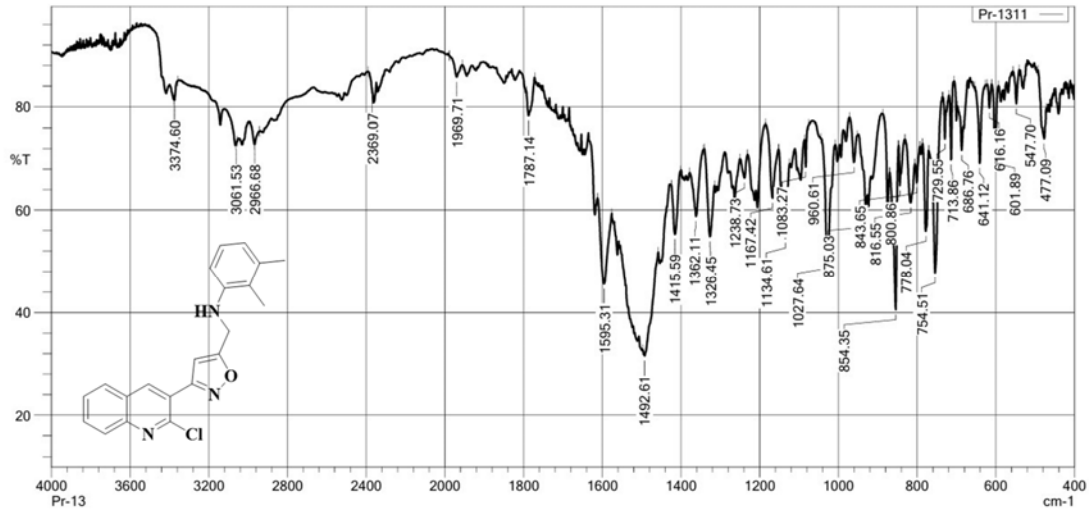

Figure 65: IR spectra of compound **6o**